Deciphering The Role of miR-506 in Ovarian Cancer Drug Sensitivity

Thesis

Roberta Nicoletti

Degree in Biological Sciences

OU personal identifier: C8590724

Deciphering the role of miR-506 in ovarian cancer drug sensitivity

Thesis presented for the Degree of Doctor of Philosophy

The Open University, Milton Keynes (UK)

Faculty of Science Technology Engineering and Mathematics (STEM)

School of Life, Health and Chemical Sciences

Date of submission: January 2018

Affiliated Research Centre:

Fondazione IRCCS Istituto Nazionale dei Tumori, Milan (Italy)

Director of studies: Dr. Delia Mezzanzanica

Internal supervisor: Dr. Marina Bagnoli

External supervisor: Prof. Iain McNeish

Contents

Declaration of authorship 5
Abstract 6
List of Figures: 8
List of Tables: 9
List of abbreviations 10
1 Introduction 13
1.1 Epithelial ovarian cancer 14
1.1.1 Clinical aspects 14
1.1.2 Histological subtypes and Origins of ovarian cancer 15
1.1.3 Treatments 19
1.1.4 Platinum agents: mode of action and resistance in EOC 20
1.1.5 Molecular driven therapeutics for EOC 22
1.2 DNA Damage Repair Mechanisms 23
1.2.1 DNA damage sensors 24
1.2.2 Mechanisms of DNA repair 24
1.3 Cell cycle and checkpoints activation in cancer 26
1.3.1 RAD17 30
1.3.2 RAD17 and cancer 32
1.3.3 DDR and cancer 32
1.3.4 DDR and targeted therapy 33
1.3.5 Combining DDR inhibitors with DNA damaging drugs 35
1.4 MicroRNAs 36
1.4.1 Biogenesis and role of miRNAs as regulator of gene expression 36
1.4.2 MicroRNA and cancer 37
1.4.3 MicroRNA and EOC 39
1.4.4 MiRNAs as early diagnostic, prognostic and predictive biomarkers in EOC 41
1.4.5 MiR-506 43
2. Aims of the Project 46
3. Materials and Methods 47
3.1 Cell biology technique 48
3.1.1 Cell Cultures 48
3.1.2 Drug used and treatments 49

3.1.3 Transient transfection 50
3.1.4 Clonogenic assay 52
3.1.5 Test of cell viability and proliferation assays 52
3.1.6 Cell cycle analysis by flow cytometry 53
3.2 Biochemical techniques 54
3.2.1 Cell lysis and assessment of protein concentration 54
3.2.2 SDS-PAGE 55
3.2.3 Western blot 55
3.2.4 Immunofluorescence 56
3.3 Cloning techniques 57
3.3.1 Design and annealing of oligonucleotides 57
3.3.2 Restriction digests of vector 58
3.3.3 Ligation of insert and vector 59
3.3.4 Transformation of competent E. coli cells and isolation of plasmid DNA 59
3.4 Molecular biology technique 60
3.4.1 RNA extraction 60
3.4.2 Total RNA and microRNA reverse transcription 61
3.4.3 Quantitative Real time PCR (qRT-PCR) 62
3.4.4 Luciferase assay 63
3.5 Bioinformatic studies: miRNA Target prediction and identification of deregulated functions with Ingenuity Pathway Analysis 64
3.6 Ovarian cancer patients selection 66
3.6.1 INT-MI/CRO OC72 case material 66
3.6.2 OC179 case material 68
3.7 Statistical analysis ..... **Error! Bookmark not defined.**
4 Results 71
4.1 Clinical impact of miR-506 expression in EOC patients 72
4.2 MiR-506 is expressed at low level in EOC cell lines 73
4.3 MiRNAs transient transfection is a suitable method for long-term biological evaluations 75
4.4 MiR-506 overexpression enhances sensitivity to platinum 76
4.5 Identification of miR-506 target genes and functional analysis of miRNAs targets by Ingenuity Pathway analysis (IPA) 79
4.6 RAD51 and RAD17 are regulated by miR-506 81

4.7 RAD17 is a direct target of miR-506 84
4.8 Clinical relevance of RAD17 in EOC patients 86
4.9 RAD17 silencing sensitises EOC cells to platinum 88
4.10 RAD17 is directly involved in miR-506-induced drug sensitisation 90
4.11 Effect of miR-506-RAD17 regulatory axis on sensitivity to PARP inhibitors 93
4.12 MiR-506 increases frequency of chromosomes breaks and causes abnormalities in mitotic progression in platinum treated cells 95
4.13 MiR-506 impacts on DNA Damage 97
4.14 MiR-506 causes a delay in platinum-induced G2 cell cycle arrest 100
4.15 RAD17 is synthetically lethal with Chk1 and Wee1 inhibitors in EOC models in vitro 104
4.16 MiR-506 reintroduction causes synthetic lethality with Chk1 and Wee1 Inhibitors resembling RAD17 silencing. 106
4.17 Combination of Chk1 or Wee1 inhibitors with platinum showed a synergistic effect in miR-506-reconstituted SKOV3 cells 108
5 Discussion 110
6 Conclusions and Future perspectives 118
List of publication 119
Acknowledgements 120

Declaration of authorship

I declare that this thesis has been written entirely by me and the work presented in is solely my original work, except where otherwise indicated.

I did not perform:

RNA extraction of case materials: OC179 performed by INT-Pascale, Naples, and OC72 performed by Genomic Facility at Istituto Nazionale dei Tumori, Milan.

MiRNA/Gene expression profiling of samples from OC72 and OC179 case materials, performed by Genomic Facility at Istituto Nazionale dei Tumori, Milan

Short Tandem Repeat (STR) profiles authentication, performed by Genomic Facility at Istituto Nazionale dei Tumori, Milan.

Sequencing for the verification of sequence insertion in cloning experiments was performed by Eurofins Genomics-genomic service (MWG Eurofins)

This thesis has not been submitted previously for a higher degree. The research was conducted at Fondazione IRCCS Istituto Nazionale dei Tumori di Milano under the supervision of Dr Delia Mezzanzanica, Dr Marina Bagnoli and Prof. Iain McNeish

Abstract

Although the incidence is quite low, epithelial ovarian cancer (EOC) is the most lethal gynaecologic malignancy. The unfavourable prognosis and the high mortality rate associated with EOC are mainly owed to late diagnosis, frequent relapse and development of chemoresistance. Indeed, most of the patients who achieve a complete response to first-line platinum-based treatment eventually relapse often developing platinum-resistant disease. Due to their master regulatory role, miRNAs are considered powerful tools to obtain representative molecular portraits of specific tumour characteristics and behaviours. My laboratory performed microRNA expression profiles on advanced stage EOC patients and a cluster of miRNAs, including miR-506, located on ChrXq27.3 was identified as down-regulated in EOC early relapsing patients. Since I observed that expression of miR-506 was associated with EOC patients' sensitivity to platinum treatment, the overall aim of this thesis was to better characterize the role of this miRNA in regulating response to chemotherapy. Among the miR-506 predicted targets, I identified several genes involved in DNA damage repair (DDR) pathway, like *RAD51*, *RAD17*, *CHEK1* and *WEE1* and I concentrated on genes not previously studied in EOC. I validated *RAD17* as a direct target of miR-506 and identified the miR-506-RAD17 axis as relevant in chemosensitising EOC cells to different treatments. I demonstrated that miR-506 expression, by targeting RAD17, was able to mediate sensitisation to platinum treatment and accordingly RAD17 silencing exerted the same effect. MiR-506 expression in EOC cells led to a reduced ability to properly sense DNA damage following platinum treatment causing mitotic defects, micronuclei formation, and

impairing the signalling cascade responsible for G2/M checkpoint activation upon DNA damage insults. This behaviour, recapitulating a BRCAness phenotype, would allow propagation of cells with unrepaired DNA damage with the subsequent sensitisation to DNA damaging drugs. Furthermore, miR-506 expression, by regulating *RAD17*, impairs ATM signalling pathway, sensitising EOC cells to PARP inhibitor olaparib. Acting in the same way, miR-506 expression was synthetic lethal with Chk1 and Wee1 checkpoint kinases inhibitors in agreement with recent data reporting RAD17 depletion to be synthetically lethal with these small molecules. Accordingly, RAD17 down-modulation phenocopied the effect of miR-506 expression. Also combination treatments of Checkpoint kinases inhibitors with platinum resulted to be synergistic. Together the findings presented in this thesis support miR-506 as a key node in regulating DDR pathway in response to drug treatments and provide the rationale for its use to select EOC patients with BRCAness phenotype for efficient personalized therapeutic treatments.

List of Figures:

Figure 1: Defining EOC origins
Figure 2: The revised dualistic model in the pathogenesis of EOC
Figure 3: DNA damage sources and mechanisms of repair
Figure 4: DNA damage-induced cell cycle checkpoints
Figure 5: Sensitizing cancer cells to DNA-damaging agents with checkpoint inhibitors
Figure 6: Schematic illustration of RAD17 protein function in the activation of DDR
Figure 7: Illustration of the possible role of RAD17 in the ATM signalling pathway
Figure 8: Synthetic lethality induced by Inhibition of PARP1 enzymatic activity
Figure 9: Biogenesis of miRNAs and their regulatory function in cells
Figure 10: Tumour suppressive role of miR-506 on different biological processes
Figure 11: Expression of miR-506 correlates with EOC patients' platinum sensitivity
Figure 12: MiR-506 expression level in cancer cell lines
Figure 13: Expression of miR-506 is maintained over time
Figure 14: Forced expression of miR-506 increased platinum sensitivity in EOC cell lines
Figure 15: Identification of miR-506 target genes and related deregulated cell functions
Figure 16: miR-506 regulates expression of RAD17 and RAD51
Figure 17: RAD17 is a direct target of miR-506
Figure 18: RAD17 is anticorrelated with miR-506 and associates with poor prognosis in EOC samples
Figure 19 Effect of RAD17 silencing on sensitivity to platinum
Figure 20: RAD17 contributes to mediate miR-506 induced chemosensitisation
Figure 21: Forced expression of miR-506 induce sensitivity to PARP inhibitors and the effect is phenocopied by RAD17 silencing
Figure 22: MiR-506 reintroduction causes abnormal mitotic figures following drug treatment
Figure 23: miR-506 reintroduction impairs response to DNA damage
Figure 24: MiR-506 reconstitution affects cell cycle progression
Figure 25: Abrogation of G2/M cell cycle checkpoint in miR-506 reconstituted cells
Figure 26: Synthetic lethal effect of RAD17 depletion with checkpoint kinases inhibitors
Figure 27: Synthetic lethality effects of miR-506 reconstitution with checkpoint kinases inhibitors
Figure 28: Inhibition on Wee1 or Chek1 in mR-506 reconstituted cells results in synergistic effect with platinum treatment.

List of Tables:

Table 1: miRNAs found to be consistently dysregulated in ovarian cancers compared to different normal counterpart.
Table 2: Ovarian cancer cell lines
Table 3: List of the antibodies used
Table 4: List of the TaqMan® probes used
Table 5: List of the TaqMan® miRNA probes used
Table 6: Clinical and pathological data of OC72 case material
Table 7: Clinical and Pathologic characteristics of OC44 case material

List of abbreviations

5-Aza-dC: 5-aza-2'-deoxycytidine
Ago2: Argonaute 2
ATM: ataxia-telangiectasia mutated
ATR: ataxia-telangiectasia and Rad3-related
ATRIP: ATR interacting protein
BCA: bicinchoninic acid
BER: DNA base excision repair
BRCA1: Breast Cancer 1
BRCA2: Breast Cancer 2
CDC25A: CHK2 phosphorylates cell division cycle 25A
CDK: cyclin dependent kinases
CDK1: cyclin-dependent kinase 1
Chk1: checkpoint kinase 1
CI: confidence interval
CI: combination index
CIC: cortical inclusion cysts
Ct: cycle threshold
DDP: Cis-diamminedichloroplatinum
DDR: DNA Damage Response
DFS: Disease free survival
DMSO: dimethyl sulfoxide
DSB: double strand breaks
dsDNA: double strand DNA
EDTA: Ethylenediaminetetraacetic acid
EGTA: ethylene glycol-bis(β-aminoethyl ether)-N:N:N':N'-tetraacetic acid
EMA: European Medical Agency
EMT: epithelial to mesenchymal transition
EOC: Epithelial ovarian cancer
ERCC1: Excision Repair Cross-Complementation Group 1
F: Fraction Affected
FBS: fetal bovine serum
FDA: Food and Drug Administration
FFPE: formalin-fixed paraffin embedded
FIGO: Federation of Obstetrics and Gynaecology
GAPDH: Glyceraldehyde 3-Phosphate Dehydrogenase
HEK: human embryonic kidney
HGSOC: High Grade Serous Ovarian Carcinomas
HR: hazard ratio
hRluc-neo: Renilla luciferase
HRR: homologous recombination repair
IF: Immunofluorescence
IOSE: immortalized ovarian surface epithelium:
IPA: Ingenuity Pathway Analysis
KAP1: KRAB-associated protein 1

KM: Kaplan-Meier
LGSOC: Low Grade Serous Ovarian Carcinomas
LOH: loss of heterozygosity
Luc2: Firefly luciferase
MDR1: multidrug-resistant protein 1
miRNA or miR: MicroRNA
MiROvaR: miRNA-based predictor of Risk of Ovarian Cancer Relapse or progression
MITO: Multicentre Italian Trial in Ovarian cancer clinical trial
MLH1: MutL Homolog 1
MMR: mismatch repair
mRD: minimal residual disease:
MRN: MRE11-RAD50-NBS1
MSH2: MutS Homolog 2
NaCl: Sodium chloride
NED: non evident disease
NER: nucleotide excision repair
NHEJ: Non-homologous end joining
NT: not treated
OS: overall survival
OSE: ovarian surface epithelium
PAGE: Polyacrylamide gel electrophoresis
PARP: poly ADP-ribose polymerase
PARPi: PARP inhibitor
PFS: progression free survival
PGK: phosphoglycerate kinase
pH3: phosphorylated histone H3
PI: Propidium Iodide
PLB: passive lysis buffer
pre-miRNA: precursor microRNA
pri-miRNA: primary microRNA
R: relapse
RISC: RNA-induced silencing complex
RLU: Relative Luminometer Units
ROS: reactive oxygen species
RPA: replication protein A
RPL13: ribosomal protein L13
RQ: relative quantification
RT: room temperature
Scr: scramble
SDS: sodium dodecyl sulfate
siRNA: small interference RNA
SSB: single strand breaks
ssDNA: single strand DNA
SSBR: single strand break repair
STIC: serous tubal intraperitoneal carcinomas
STR: short tandem repeat

TCA: trichloroacetic acid
TP: miR-target protector
TTR: time to relapse
UTR: untranslated region
VINC: vinculin
WHO: World Health Organization
α-tubulin-ac: acetylated alpha tubulin

1 Introduction

1.1 Epithelial ovarian cancer

1.1.1 Clinical aspects

Epithelial ovarian cancer (EOC) is the leading cause of death among gynaecological cancers in the developed world[1] and it is characterised by high pathological and molecular heterogeneity and with a high fatality rate[2]. The absence of early and specific symptoms and the lack of screening strategies[3] contribute to late diagnosis. As a result, most cases of EOC do not come to clinical attention with a confined mass in the ovary, but more often patients present with advanced stage III/IV disease. According to International Federation of Obstetrics and Gynaecology (FIGO) criteria, the advanced stage is characterised by a widespread intraperitoneal disease with the involvement of different pelvic structures other than ovary and intra-abdominal ascites. The standard of care for EOC is cytoreductive surgery, followed by six to eight cycles of a combination of platinum- and taxane-based chemotherapy as first-line treatment for advanced EOC[1]. Although up to 80% of patients can be placed into remission after surgery and chemotherapy, the majority of them will relapse with a median progression-free survival of 18 months and a 5-years survivorship being below 40% [2, 3]. The length of the disease-free period categorises patients as: refractory or resistant if relapse occurs during or within 6 months of the end of chemotherapy, partially sensitive when relapsing after 6 and before 12 months, sensitive when relapsing after 12 months from the end of treatment[4]. Disease relapse following front-line treatment is frequently associated with the development of chemoresistance that, together with a late detection of the disease represents the main problem to overcome in the management of EOC.

Unfortunately, no validated screening tests are available for the general population and the identification of new biomarkers for early diagnosis or disease progression, prognosis and response to therapy are of great interest to improve the management of this aggressive malignancy.

1.1.2 Histological subtypes and Origins of ovarian cancer

- **Histological subtypes**

The three main types of ovarian cancer classified by the World Health Organization (WHO) include epithelial ovarian cancers (EOC), whose origin is still an area of active investigations (commented below), malignant germ cell tumours, which develop from the cells that produce the oocyte, and sex cord stromal tumours, which develop from connective tissue cells that hold the ovary[5]. EOC is the most common type and represents 90% of malignant ovarian tumours[6]. Histological subtypes of EOC include: high grade serous, low grade serous, endometrioid, clear cell and mucinous tumours[7] as represented in Figure 1.

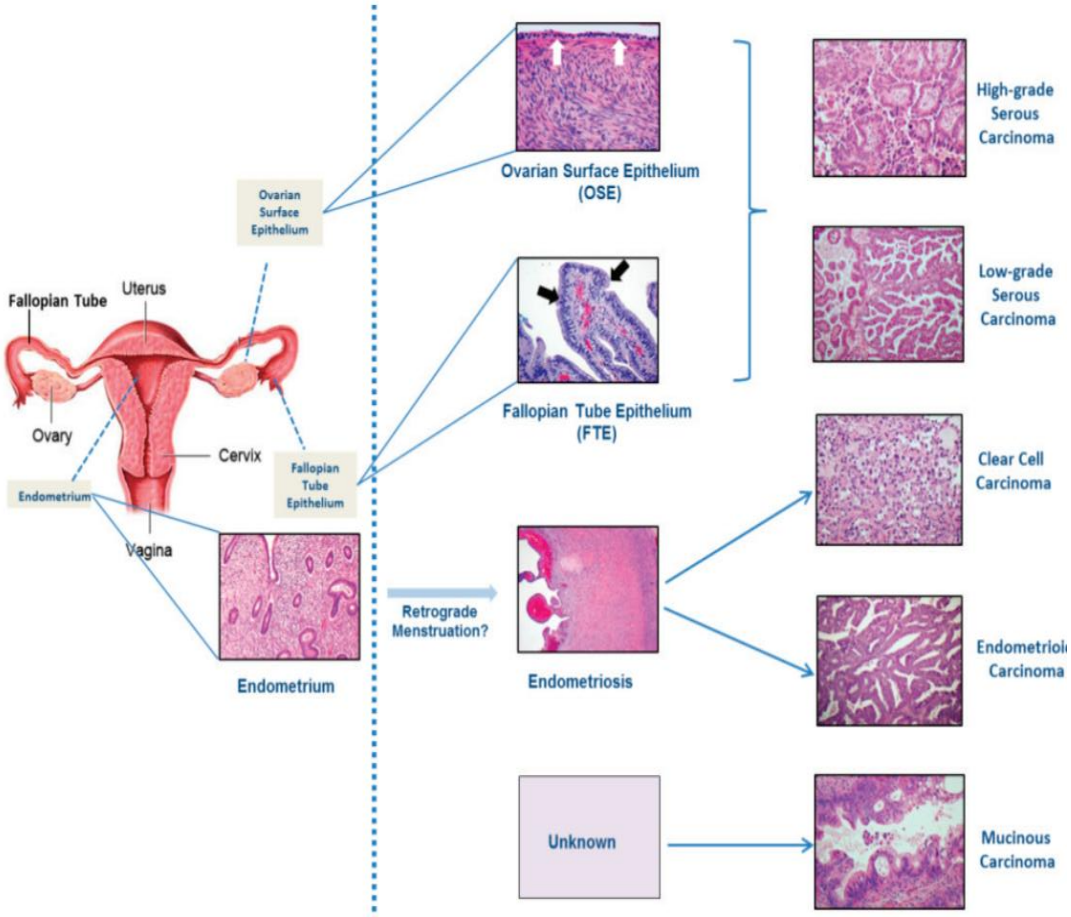

Figure 1: Defining EOC origins
Site of origin of EOC is still debated. Recent evidences suggest that HGSOC originates from the fallopian tubes, and then metastasize to the ovary. Image from Ovarian Cancers. Evolving Paradigms in Research and Care (2016).

Morphological and molecular genetic studies have elucidated our understanding of ovarian carcinogenesis. Almost 10 years ago, a new classification was proposed that, according to cell type and molecular features and on the basis of a dualistic model of carcinogenesis, divides the histological types of EOC into two categories designated as type I and type II tumours[8] (Figure 2). Type I tumours comprise Low Grade Serous Carcinomas (LGSOCs), low grade endometroid tumours, clear cells and mucinous carcinomas. Overall these tumours account for only 10% of deaths from EOC. They are generally indolent with a good prognosis when masses are

confined to one ovary (stage I) but with a poor outcome when diagnosed at advanced stage. Type I tumours are associated with frequent somatic mutations in *KRAS*, *BRAF*, *CTNNB1*, *PTEN*, *PIK3CA*, *MAP*, *ERK* and *ARID1A*, with rare mutational events occurring in *TP53*[9]. In contrast, Type II tumours present at more advanced stages and constitute approximately 75% of ovarian tumours, and are responsible for 90% of EOC deaths. Type II tumours are largely composed of High Grade Serous Carcinomas (HGSOCs), carcinosarcoma and undifferentiated carcinoma. Extensive gene expression profiling studies, mostly performed in HGSOC, substantially improved the knowledge of EOC biology and were also expected to significantly improve the management of EOC patients. Novel molecular subtypes of EOC based on gene expression profile were firstly identified by the Australian Ovarian Cancer Study[10], then the Cancer Genome Atlas (TCGA) validated the study identifying four molecular subtypes whose prognostic significance has been recently validated[11, 12]. However their clinical utility is still a challenge. HGSOCs are genetically unstable and almost all harbour a mutation in the *TP53* [13]. These studies revealed the complexity and the molecular heterogeneity of HGSOC and indeed, the performance of these survival signatures differ among independent cohorts, indicating that the use of these signatures for EOC patient management is still a challenge. Moreover different abnormalities in homologous recombination repair (HRR) (such as mutations or epigenetic alterations in *BRCA1* (Breast Cancer 1) and *BRCA2* (Breast Cancer 2), and defects in Rb protein, Cyclin E1, FOXM1 and NOTCH3 signalling pathways often occur in type II tumours[9, 12] (Figure 2).

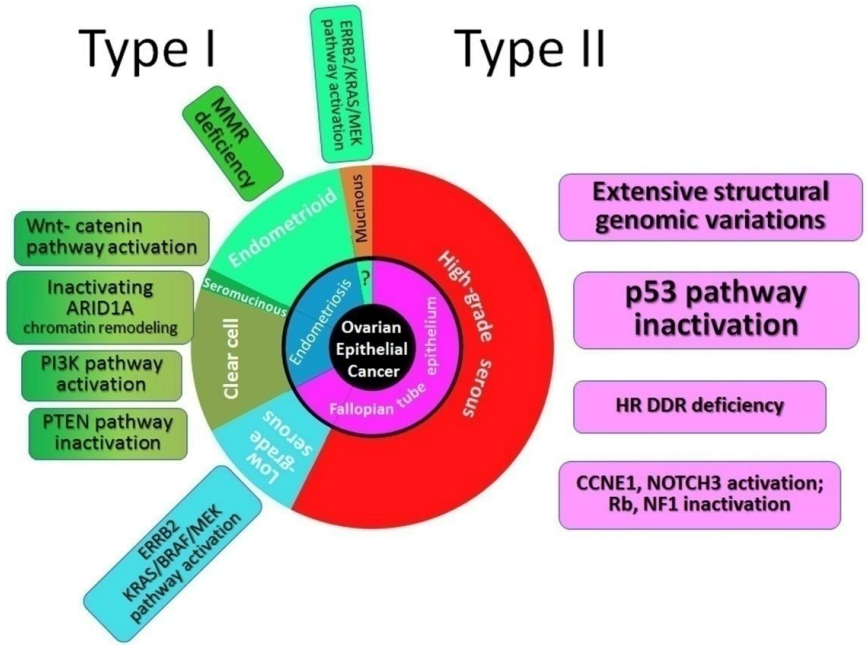

Figure 2: The revised dualistic model in the pathogenesis of EOC
Type I and Type II tumour classification with areas in individual histotypes reflecting their relative prevalence. The inner circle indicates the likely cell of origin of the different type I and type II tumours indicated in the external circle. The square boxes summarized the molecular tumour alterations of the different subtypes. HR: Homologous Recombination; DDR: DNA Damage Response. Image from Kurman and Shih[11].

- **Origins of ovarian cancer**

The traditional dogma of ovarian carcinogenesis was that EOC arises from ovarian surface epithelium (OSE) which gives rise to cortical inclusion cysts (CICs) that undergo malignant transformation[14]. The fact that EOCs are composed of cells that do not resemble cells in the ovary made OSE origin theory hard to be sustained. It is now well sustained by several lines of evidence the hypothesis that many HGSOCs arise from high grade serous tubal intraepithelial carcinomas (STICs) that shed from the fallopian tube into the ovary[15]. This paradigm shift has profound implications in

the management of this disease and has begun to affect treatment strategies. However definition of site of origin is still a matter of debate[16].

The dualistic model dividing EOC in type I and type II tumours present limitations indeed dramatic differences between the two groups are now emerging describing completely different groups of diseases and demonstrating that EOC is not a single disease but a set of different types of cancer with very different pathological and clinical features[17-19]. Thanks to the huge number of molecular and histopathological studies that have provided new insights into the origin and molecular pathogenesis of this disease, the standard model has been further revised and expanded[11]. It is of course important when studying ovarian cancer to distinguish by type taking into account also the huge quantity of molecular new data that are now available in order to improve diagnosis and treatment of this aggressive disease.

1.1.3 Treatments

The treatment of ovarian cancer is characterised by a combination of aggressive cytoreductive surgery followed by platinum based chemotherapy with new targeted therapeutic options now available for selected patients and driven by molecular characterisation of EOC (see section 1.1.5) The main purpose of the surgery is to remove the bulk of the tumour and establish the histopathological diagnosis (FIGO stage). As a result, the accurate resection of the entire visible tumour is of primary importance since residual disease remains a strong prognostic factors and optimal cytoreduction is associated with longer survival[20]. For advanced stage tumours, platinum-based chemotherapy remains the standard of care.

1.1.4 Platinum agents: mode of action and resistance in EOC

- ***Mode of action***

The mechanism of action of platinum agents relies on their ability to bind to DNA to form bulky adducts which require effective repair to prevent apoptosis. Intra-strand DNA cross-links are the most common cytotoxic lesions caused by platinum treatments[21, 22]. These platinum-induced lesions cause distortions of the DNA structure that are recognized by multiple DNA Damage Repair (DDR) pathways[23]. In particular NER (nucleotide excision repair) and MMR (mismatch repair) repair pathways are primarily activated for the resolution of platinum lesions[24, 25], then also HRR (homologous recombination repair) and ICL (interstrand crosslinks) repair are activated when lesions increase (overview of repair mechanisms in section 1.2). The cell cycle also takes a role in repair processes and if damage is limited, cells arrest in the S and G2 phase of the cell cycle to repair their damage, if the extent of lesions increases, cells are no longer able to repair the damage and are committed to death[26].

- Platinum resistance

Drug resistance is a major problem associated with the use of platinum agents. While the intrinsic model of resistance is based on the pre-existence of a small proportion of chemotherapy-resistant tumour cells that after treatment repopulate the tumour and recurrence is observed (refractory disease), acquired resistance is based on an initial platinum sensitivity of tumour cells that, following multiple cycles of platinum-based chemotherapy, may acquire resistance. In both cases,

unravelling the mechanisms of resistance to platinum agents remains a critical goal for EOC therapy.

Platinum resistance is a multifactorial event driven by different molecular mechanisms including genetic or epigenetic alterations, inaccessibility of drugs in cancer cells, increased ability to tolerate or repair DNA lesions[27]. Dysregulation of cell ability to repair DNA damage is one of the prevalent factors that lead to platinum resistance. Platinum-resistant cells acquire the ability to tolerate and repair platinum induced adducts through different mechanisms. Dysfunctions in genes involved in NER pathway such as overexpression of *ERCC1* (Excision Repair Cross-Complementation Group 1), or *ERCC2* (Excision Repair Cross-Complementation Group 2), proteins participating in NER, have been correlated with poor survival in advanced EOC and were found to be markers of resistance to platinum-based drugs[28, 29]. Components of MMR, such as MSH2 (MutS Homolog 2) and MLH1 (MutL Homolog 1), are often mutated or low expressed in platinum-resistant tumours, including EOC, where MLH1 promoter methylation predicted poor survival in relapsing patients[30-33]. Platinum induced adducts such as interstrand crosslinks, require also homologous recombination repair (HRR), an accurate type of repair with exchange of homologous DNA sequences in which BRCA1 and BRCA2 are major players. These genes are often mutated in HGSOC. Interestingly EOC patients carrying *BRCA1/2* mutations are sensitive to platinum treatment and have a better overall prognosis[34, 35]. However, in platinum-resistant tumours compensatory mutations that restore BRCA function and re-establish a correct HRR have been shown to favour acquired chemoresistance[36-38]. In addition to DNA repair

dysfunction, the internalization and degradation of copper transporter 1 and 2 (Crt1, Crt2), which mediate platinum uptake, also contributes to resistance in ovarian cancer due to reduced availability of the drug within the cell[39, 40]. Two other components of the copper family, ATP7A and ATP7B, mediate efflux of drugs and were reported to be overexpressed in platinum-resistant EOC cells[41, 42]. Interestingly Patch and colleagues performed a whole genome analysis on tumour samples from patients with primary refractory, resistant, sensitive and matched acquired resistant disease and observed heterogeneity of the genome under the selective pressure of chemotherapy. Among major findings, they observed changes in promoter methylation or reversion of mutational status of *BRCA* genes and up-regulation of multidrug-resistant protein 1 (MDR1) transporters, that mediate efflux of drugs[43], mediated by a novel fusion gene not previously reported in which the promoter of *SLC25A40* was juxtaposed with *ABCB1* which encodes for MDR1. These findings further support the acquired platinum resistance model and the idea of cells adaptation to survive.

1.1.5 Molecular driven therapeutics for EOC

Advances in routine genomic studies (next-generation sequencing, expression profiles) are now providing new insight into individual genetic abnormalities for a more personalized medicine. Beyond platinum-based therapy, ovarian tumours can be now treated with targeted therapies as an alternative strategy for selected patients. One example is the case of tumours with *BRCA* abnormalities. As previously said, patients who harbour mutations in *BRCA1* and *BRCA2* show deficiencies in HRR, one of the main mechanisms for the repair of DNA double

strand break damage. These tumours appear sensitive to poly (ADP-ribose) polymerase (PARP) inhibitors and olaparib, rucaparib and niraparib are now therapeutic options for these patients[44, 45 46 47]. Moreover tumours presenting wild type *BRCA1/2* but bearing HRR defects and therefore sharing molecular features of *BRCA* mutated tumours, may also respond to similar therapeutic approaches[44 46 47]. This concept, firstly introduced by Ashworth and collaborators more than 10 years ago and named BRCAness[48, 49], is generally associated with mutations of other genes of the same signalling pathway and may thus have important implications for the clinical management of these cancers[48, 50, 51].

Another example of approved targeted therapy for ovarian cancer is Bevacizumab, a humanized monoclonal antibody that binds to vascular endothelial growth factor A (VEGF-A), a protein that promotes the formation of new blood vessels (angiogenesis) for nutrients delivery to tumour cells. Bevacizumab, blocking angiogenesis, blocks the growth by tumour cell starvation. Bevacizumab is also able to initiate vessel normalization leading to vessel permeability for an improved tumour drug uptake and increase of partial oxygen thus reducing hypoxia[52, 53]. Bevacizumab was recently approved as first line treatment and maintenance chemotherapy. This evidence suggests the importance of better defining the molecular landscape of the different subtypes of ovarian carcinoma in order to stratify patients for tailored therapy.

1.2 DNA Damage Repair Mechanisms

DNA is the repository of genetic information and maintaining its integrity and stability is essential to life. Many type of lesions can affect DNA including

endogenous metabolic products such as reactive oxygen species (ROS), external chemical agents such as cytotoxic chemotherapeutic agents (platinum-agents) or electromagnetic radiations (ionizing radiation or UV lights). When lesions happen in one strand of DNA, single strand breaks (SSBs) occur; when both strands of DNA are involved we observe double strand breaks (DSBs). DSBs are the most dangerous among lesions[54] which if not correctly repaired can lead to genomic instability[55]. In order to avoid such genomic instability cells can use, the so called DDR (DNA Damage Response), to sense DNA damage and mediate appropriate cellular response and repair.

1.2.1 DNA damage sensors

DNA damage sensors detect the DNA lesions for initiating DDR. The Mre11–Rad50–Nbs1 (MRN) complex is a sensor of the DNA damage responsible for processing DNA ends and recruits other molecules of the DDR at damaged sites[26, 56]. The DNA lesion recognition leads to activation of Ataxia Telangiectasia Mutated (ATM) or Ataxia Telangiectasia and Rad3 Related (ATR) kinases, in particular, ATM is activated by DSBs recognition while ATR by stalled replication forks[57, 58]. Then a signal cascade is propagated with the recruitment of the other members that participate in this complex pathway for DNA damage repair and the activation of checkpoints for cell cycle regulation (overview in section 1.3).

1.2.2 Mechanisms of DNA repair

Each type of damage acts in a specific way determining a different type of damage detection and repair mechanism activation as schematically shown in Figure 3. DSBs lesions are preferentially repaired by two pathways, the homologous recombination

repair (HRR) and non-homologous end joining (NHEJ). HRR is an error free repair pathway relying on the presence of a sister chromatid as template to for accurate DNA repair and is the most used mechanism by cells for repairing DSBs and restarting stalled replication forks. The error-prone NHEJ mediates the ligation of the two ends of DNA DSBs without the need of a homologous template[59]. SSBs are repaired by differ mechanisms in which the intact complementary strand can be used as a template to repair the damaged strand. In particular base excision repair (BER) resolves damage to a single base mainly caused by oxidation or alkylation; the nucleotide excision repair (NER) is activated for the repair of helix-distorting lesions (bulky adducts such as pyrimidine dimers) and mismatch repair (MMR) is activated to corrects errors of DNA replication and recombination[56].

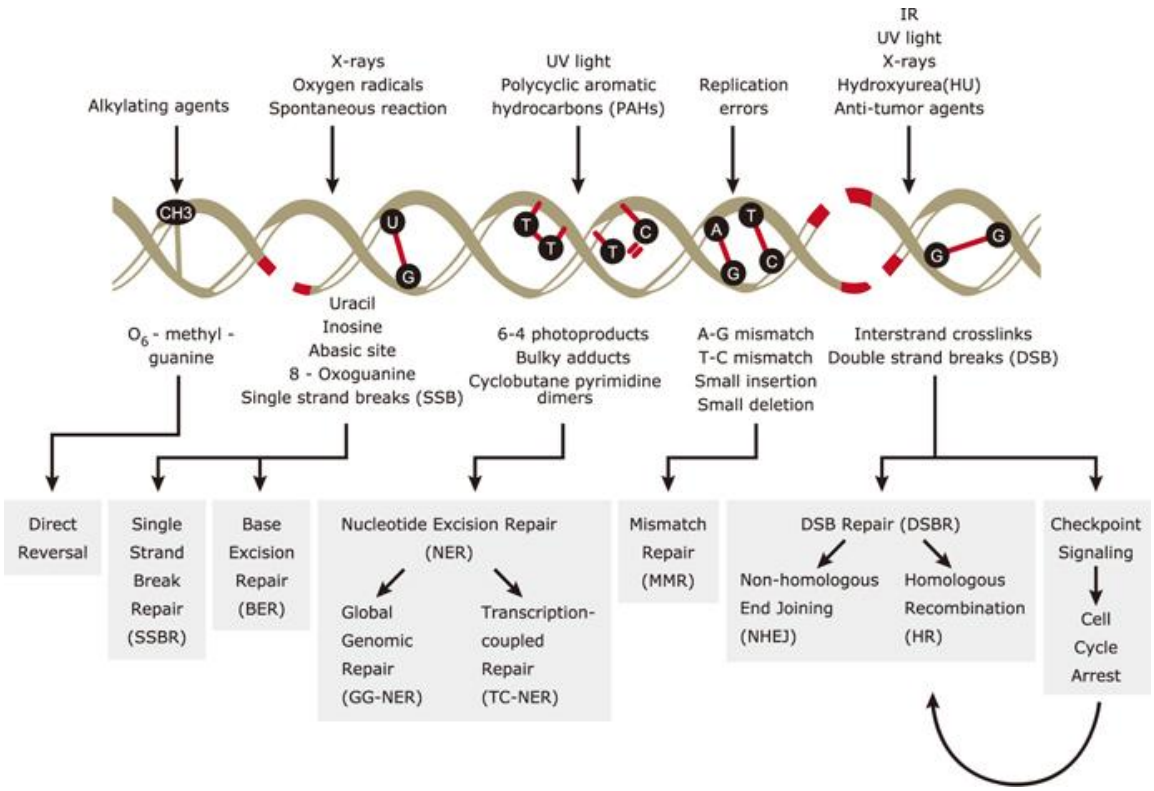

Figure 3: DNA damage sources and mechanisms of repair

Schematic overview of the different environmental factors and endogenous cellular processes responsible for DNA damage. Cells have developed different repair mechanisms in order to fix these damages such as DNA base excision repair (BER), single strand break repair (SSBR), nucleotide excision repair (NER), mismatch repair (MMR), homologous recombination (HR), and Non-homologous End Joining (NHEJ), activated by different types of damage insults. Checkpoint signalling is also activated in order to arrest cell cycle progression to facilitate DNA repair.

Image from http://www.genetex.com/Web/News/NewsList.aspx?id=322

1.3 Cell cycle and checkpoints activation in cancer

Among the events activated during DDR there is the delay or block of the cell cycle progression to give time for the cell to repair any DNA lesions prior to replication or mitosis. The cell cycle is an ordered series of events that regulate cell growth and proliferation leading to the formation of two daughter cells that receive a correctly duplicated copy of genome and organelles from the parental cell. Control mechanisms act during the cell cycle to ensure a correct duplication preventing cells

to divide under unfavourable conditions (for instance, when their DNA is damaged) and give them time to repair damage[60]. The G1 checkpoint (controlling the G1 to S transition), is the first restriction point after which cells become committed to entering the cell cycle[61]. Once the cell passes the G1 phase and enters S phase (DNA duplication phase), it becomes irreversibly committed to division. Cells have an additional checkpoint before M (mitosis) phase, called the G2 checkpoint. At this stage, the cell will check DNA integrity and DNA replication. If errors or damages are detected, the cell will pause at the G2 checkpoint to allow for repairs[62, 63]. Among Checkpoint kinases involved in DDR, ATM and ATR act as sensor proteins of the damage and consecutively phosphorylate mediator proteins, such as Chk1 (checkpoint kinase 1) and Chk2 (checkpoint kinase 2), that transduce signal. Chk1 and Chk2 block cell cycle progression through phosphorylation and inhibition of CDC25 phosphatases required for cyclin dependent kinase (CDK) activation. This results in sustained inhibitory phosphorylation of CDK1 and CDK2 leading to cell cycle arrest. Wee1 protein is also involved in the control of cell cycle progression being responsible of inhibitory phosphorylation of CDK1 and CDK2[64]. In Figure 4 are summarized the molecular events of cell cycle checkpoints activation upon damage.

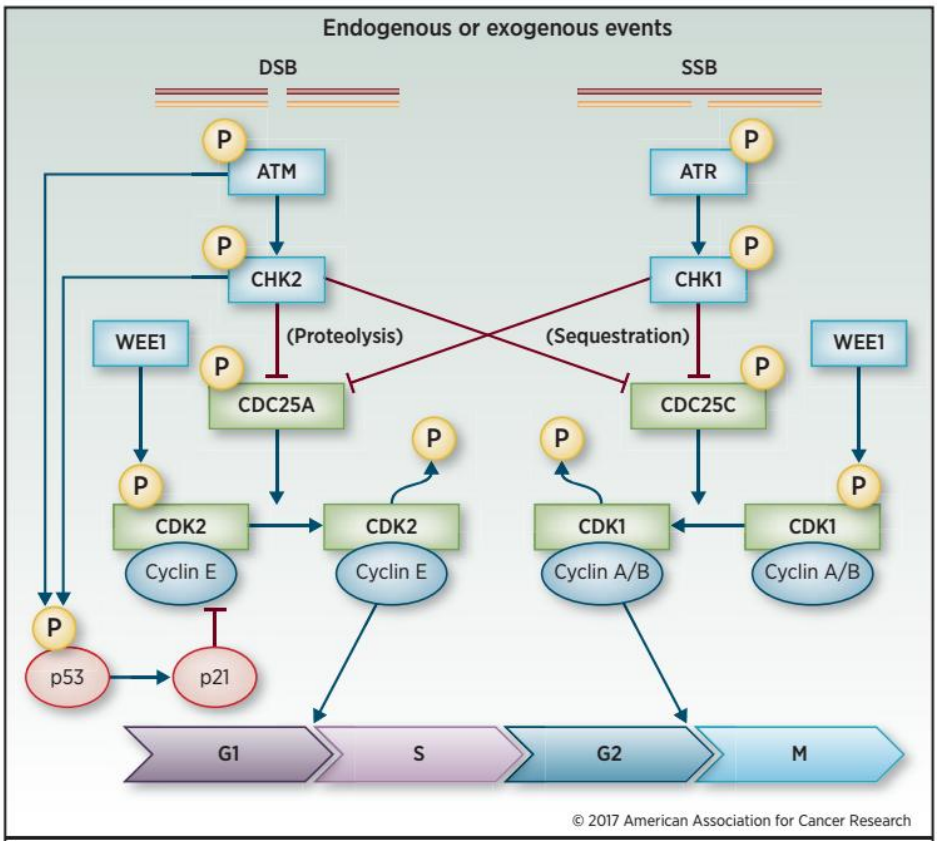

Figure 4: DNA damage-induced cell cycle checkpoints

DNA double-strand breaks (DSBs) and single strand breaks (SSBs) induce activation of ataxia-telangiectasia mutated (ATM) and ataxia-telangiectasia and Rad3-related (ATR) kinases which phosphorylates and activates the checkpoint effector kinases CHK2 and CHK1 respectively. CHK2 phosphorylates cell division cycle 25A (CDC25A), which can prevent replication of damaged DNA by activating p53 and p21, resulting in G1/S checkpoint arrest due to inhibition of CDK2-cyclin complex. CHK1 phosphorylates cell division cycle 25C (CDC25C) which dephosphorylates CDK1 resulting in CDK1-Cyclin /B complex inhibition thus inducing G2/M checkpoint arrest to allow DNA repair. In addition, G1/S and G2/M checkpoint are maintained blocked by WEE1 kinase that inhibit dephosphorylation of CDK1/2. Image from Lin AB et al[64].

p53 is a cell cycle G1 checkpoint regulator which, when impaired, forces cells to rely on other checkpoints for cell cycle regulation. Interestingly HGSOC are characterised by near universal aberration in the tumour suppressor *TP53* [13]. Focusing on p53 deficiency as the target selection criteria, it becomes evident that targeting the G2

checkpoint could represents a valuable strategy to kill cancer cells sparing normal cells protected by a p53-dependent response[65] (Figure 5). As a result, maximising the DNA damage during G1 and prevent repair in G2 should be the goal for the use of DDR targeted therapy. Indeed G2/M checkpoint abrogation, can ultimately lead to mitotic catastrophe and cell death or senescence.

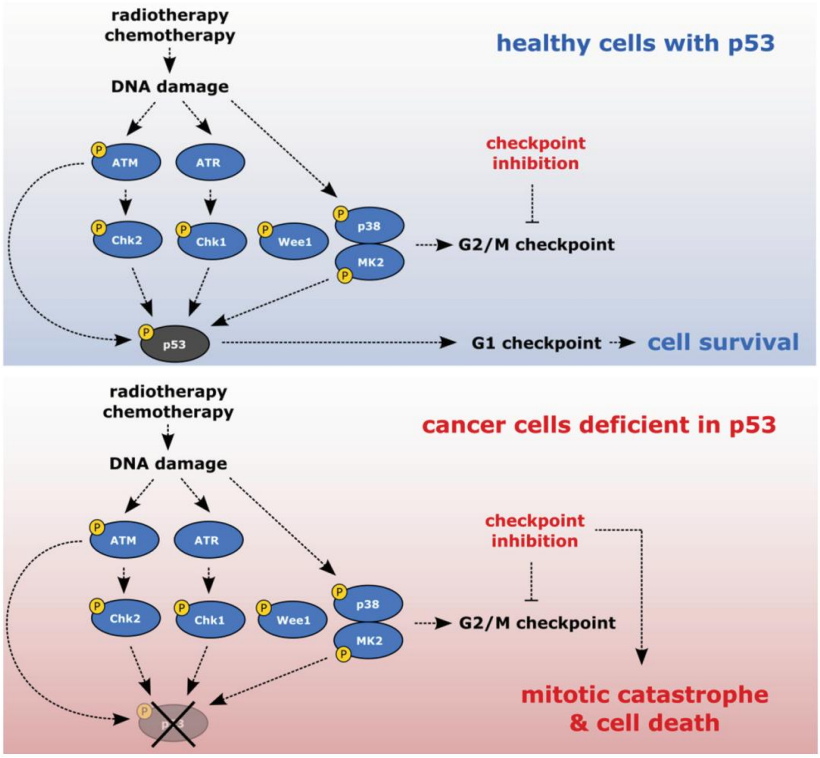

Figure 5: Sensitizing cancer cells to DNA-damaging agents with checkpoint inhibitors
Cancer cells deficient in p53 lack the G1 checkpoint and may depend more on the G2/M checkpoint to block cell cycle and repair damage. Checkpoint inhibitors in combination with DNA damaging therapy leads to the G2/M checkpoint abrogation that culminate in mitotic catastrophe and cell death. Notably, healthy cells are protected by p53-dependent response. Image from Benada J et al[65].

1.3.1 RAD17

RAD17 is a DNA damage checkpoint gene firstly identified in yeast *Schizosaccharomyces pombe* and the human homolog RAD17 has been also identified and characterised[66, 67]. It is thought to be a critical early sensor protein through which DNA damaging insults activate the ATR dependent signal cascade that lead to cell cycle arrest and DNA repair[68]. RAD17 is part of the RAD17-RFC (complex of Rfc1-5 subunits) complex which binds to single strand DNA (ssDNA) structures[69]. Acting as a clamp loader, RAD17 loads the complex Rad9-Hus1-Rad1 (9-1-1 complex) onto DNA damage sites, an event that potentially create a chromatin location site for 9-1-1- sliding clamp to interact with other elements of the checkpoint machinery and facilitates ATR-dependent phosphorylation of downstream targets to fully activate the DNA damage response[68] (Figure 6).

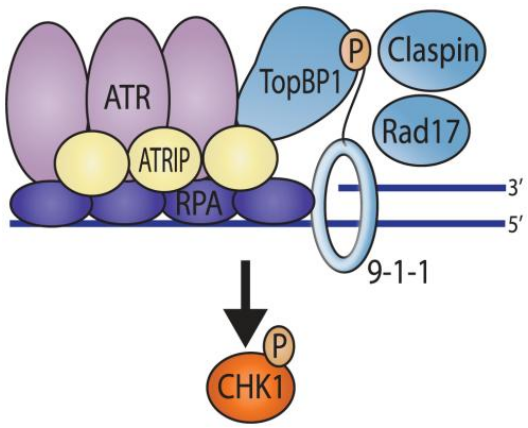

Figure 6: Schematic illustration of RAD17 protein function in the activation of DDR
When damage occurs, ssDNA at sites of damage is coated by Replication protein A (RPA) important event for the recruitment of ATR (ataxia-telangiectasia and Rad3-related) through a direct interaction with ATRIP (ATR interacting protein). At this point, the Rad17 clamp loader load the 9-1-1 (Rad9-Hus1-Rad1) checkpoint clamp onto the junction of the ss/dsDNA (single strand/double strand DNA), event that promote the recruitment of TopBP1, an ATR kinase activator, that culminate in the activation of ATR kinase and in the phosphorylation of the Chk1 (checkpoint kinase 1), facilitated by claspin, for signal transduction. Image from Mohni KN et al[70].

Beside the role of RAD17 in the ATR signalling, it has been recently shown that RAD17 is required for early ATM kinase activation and consequent ATM-mediated phosphorylation of downstream targets which promote HRR[71] . The proposed role for RAD17 is the early recruitment and maintenance at damage sites of the MRN (Mre11-Rad50-Nbs1) complex thus allowing ATM activation by phosphorylation and subsequent phosphorylation of ATM targets (Figure 7), which are the essential steps for the detection of DSBs and initiation of DNA damage signalling cascade[71].

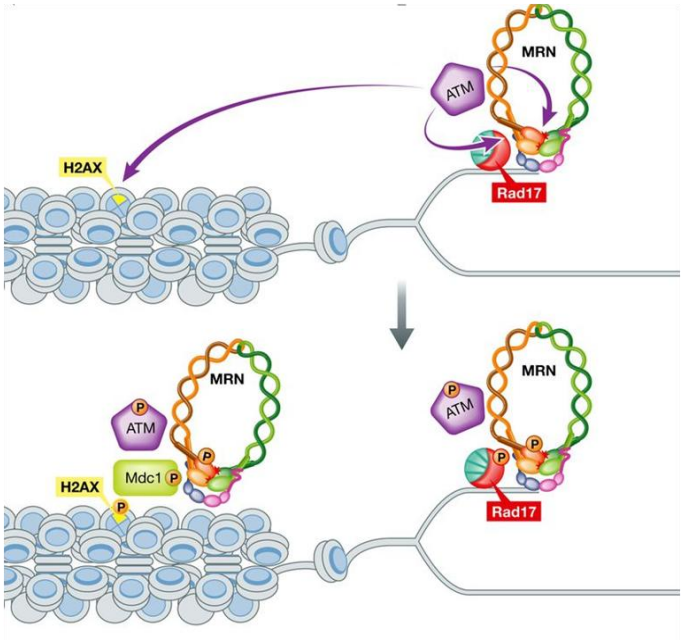

Figure 7: Illustration of the possible role of RAD17 in the ATM signalling pathway
RAD17 play a role also in the ATM pathway by helping in the recruitment and retention at the sites of DNA damage of the MRN complex (upper panel). In this way, it would promote the phosphorylation mediated by ATM of downstream targets such as γH2AX and Mdc1 amplifying the ATM-dependent DNA damage signalling cascade leading to homologous recombination repair. Image adapted from Paull TT and Lee JH[72].

1.3.2 RAD17 and cancer

The dysregulation of RAD17 was found to be associated with different types of tumours[73-76]; moreover *RAD17* is located on chromosome 5q13.2, a region known to be deleted in a variety of human cancers[77-79]. For example, Ming Zhao et al identified loss of RAD17 expression, often due to genomic deletion, to be associated with genome instability in head and neck cancer[73]. On the other hand, an overexpression status of the RAD17 protein was detected in colon carcinoma compared to normal tissues by Bao S and colleagues[74]. Overexpression of the *RAD17* gene was also identified to be associated with lymph node metastasis in breast and non-small cell lung cancers[75, 76]. Fredebohm and colleagues conducted a synthetic lethal RNAi screen and identified depletion of *RAD17* to be linked with an increased sensitivity of pancreatic cells to gemcitabine[80]. Interestingly Shen and colleague identified RAD17 Knockdown as synthetically lethal with Checkpoint kinases inhibition in HeLa and LN428 cell lines[81]. Since its role in activating the DNA damage response and its altered expression in cancer cells, RAD17 represents a suitable target to be regulated in order to potentially obtain sensitisation to chemotherapy and DDR targeted therapy.

1.3.3 DDR and cancer

The DNA damage response is a complex signalling network, essential for maintaining the genomic integrity of the cell, and its disruption is one of the hallmarks of cancer[82]. Indeed proteins involved in DDR are frequently mutated or abnormally expressed in cancer cells[83]. Compared to normal cells, cancer cells often display defects in one or more DDR pathways leading to a higher dependency on

the remaining repair pathways[26]. One example is mutation in the *TP53*, the guardian of the genome, which is a common feature of late stage tumours and is responsible for tumour susceptibility[13, 84]. Upregulation of DDR factors such as Chk1, Chk2, RAD50 or NBS1 has been reported in several cancer types, while mutation or reduced expression of protein such as ATM RAD51 or BRCA1 has been also observed as reviewed by Hosoya and colleagues[85]. In particular in ovarian cancer mutations in *BRCA1* and *BRCA2*, critical effectors proteins of the HR pathway are associated with tumorigenesis. Also mutations in ATM or RAD51 genes were found to correlate with hereditary ovarian cancer and increased risk of disease[86, 87].

1.3.4 DDR and targeted therapy

Cancer cells display a major susceptibility to DNA-damaging agents compared to normal cells due to their DDR and DNA repair-deficiency. This feature of cancer cells can be used as a therapeutic opportunity by targeting protein components of the DDR system[88, 89]. For this reason, several DDR targeted therapies have been developed in the last 10 years in order to achieve what is defined as synthetic lethality. This approach is based on the concept that targeting two or more cancer relevant genes lead to cell death, whereas perturbation of only one does not. Such a mechanism provides significant patient benefit, enabling normal cells with a functional DDR to remain unaffected reducing general toxicity[90]. The best example of targeting DDR in a synthetic lethal way is probably the use of PARP inhibitors for *BRCA1/2* mutated cancer cells[91, 92]. PARP1 is an enzyme that detects and binds to DNA SSBs initiating DNA repair by a variety of mechanisms such as BER and NER[93, 94]. Inhibition of PARP1 enzymatic activity causes the failure of SSBs lesions to be

repaired, resulting in their accumulation and conversion to deleterious DSBs that require HRR to be repaired and therefore functional BRCA1/2. Indeed, BRCA1/2 play a critical role in HRR facilitating the recruitment of RAD51 at ssDNA sites, a key molecule for homologous strand exchange in HRR pathway. Inactivating mutations of *BRCA1/2* in cancer cells therefore cause severe defects in HRR and simultaneous inactivation of PARP1 enzymatic activity renders impossible the DNA repair thus causing cell death[95, 96] (Figure 8). Of note, the PARP inhibitor olaparib, was recently approved by Food and Drug Administration (FDA) and European Medical Agency (EMA) as maintenance monotherapy for recurrant, platinum sensitive ovarian cancer patients bearing germline *BRCA1/2* mutations[97, 98] and represents one of the best examples to date of personalized therapy for ovarian cancer[99,100, 101].

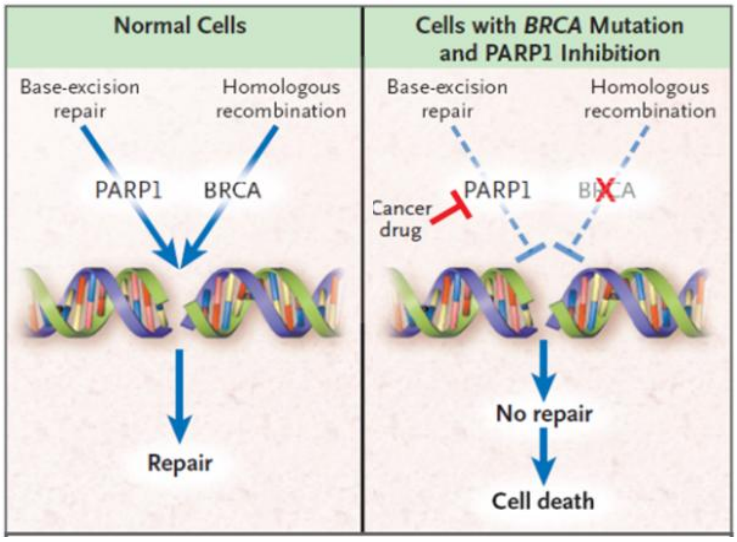

Figure 8: Synthetic lethality induced by Inhibition of PARP1 enzymatic activity.
In normal cells, DNA damage is repaired by different DDR pathways, such as base-excision repair mediated by PARP1 activity, and homologous recombination mediated by BRCA proteins function (left panel). In cancer cells with mutation in *BRCA1* or *BRCA2*, homologous recombination is non-functional and when PARP1 is inhibited, both base-excision repair and homologous recombination pathway are no more available and cells are committed to death (right panel). Image adapted from Iglehart JD et al[102].

Besides homologous recombination, also targeting replication stress, another hallmark of cancer[103], can be of great value. Replication stress, typically occurring during DNA replication, is characterised by generation of stalled replication forks and induction of a DDR in order to stabilize them to prevent replication forks collapse and generation of cytotoxic DNA DSBs[104]. Both ATR-Chk1 pathway and Wee1-CDK1/2 pathway are important regulators of replication stress thus representing attractive DDR targets[105, 106]. Several inhibitors of these molecules are currently being investigated in clinical trials such as inhibitors of ATR (AZD6738, VX970), Chk1 (LY2606368, MK8776) and Wee1 (AZD1775) also in the context of EOC[107].

1.3.5 Combining DDR inhibitors with DNA damaging drugs

Platinum agents (cisplatin, carboplatin), alkylating agents (temozolomide) and inhibitors of topoisomerase (topotecan, irinotecan, doxorubicin) are commonly used DNA damaging drugs and interesting data on combination with DDR inhibitors has been presented in preclinical[83, 108, 109] and clinical studies[110] thus representing important opportunities for cancer therapy. Importantly it has been observed that combinatorial strategies can re-sensitise resistant tumours as in the case of platinum resistant lung cancer patients which displayed a re-sensitisation to platinum treatment when exposed to the Wee1 inhibitor AZD1775 [110]. Moreover DDR-DDR agent combinations are being tested and several clinical trials are underway[107] as in the case of the combination of PARP inhibitor and Wee1 inhibitor (Clinicaltrials.gov ID NCT02272790). However, successful combination of DDR

inhibitors or DDR inhibitors and DNA damaging drugs will depend on the right association of cancer genetic background with the specific DDR dependency.

1.4 MicroRNAs

1.4.1 Biogenesis and role of miRNAs as regulator of gene expression

MicroRNAs (miRNAs) are a class of endogenously expressed non-coding RNA, with a length of 19–25 nucleotides, discovered over two decades ago, now recognized as one of the major regulators of gene expression[111]. Thousands of different miRNAs have been identified in animals and plants, and more than 2500 in humans as documented in the Sanger miRBase sequence database (http://www.mirbase.org). A large number of miRNAs are conserved in closely related species and many have homologs in distant species, suggesting that their function could also be conserved throughout evolution[112]. RNA polymerase II transcribes microRNA molecules from genomic DNA into a primary microRNA molecule (pri-miRNA). Pri-miRNA molecules that contain a stem-loop structure are recognized by the RNAse III DROSHA and its partner protein DGCR8, which cuts the double-stranded RNA into ~70-nucleotide precursor microRNA (pre-miRNA) in the nucleus. Pre-miRNA molecules are exported to the cytoplasm by exportin-5 and are processed by DICER, an RNAse III, into two unique single-stranded mature microRNA molecules representing each side of the stem loop structure. Mature microRNA molecules are loaded onto the Argonaute-containing RNA-induced silencing complex (RISC). Within this structure, mature microRNA molecules function to repress gene expression by complementary binding of the 3' untranslated region (UTR) of the target gene to the miRNA seed sequence, constituted by nucleotides 2–8 of the mature miRNA molecule, leading to

transcript degradation or translation inhibition depending on the level of complementarity[113] (Figure 9).

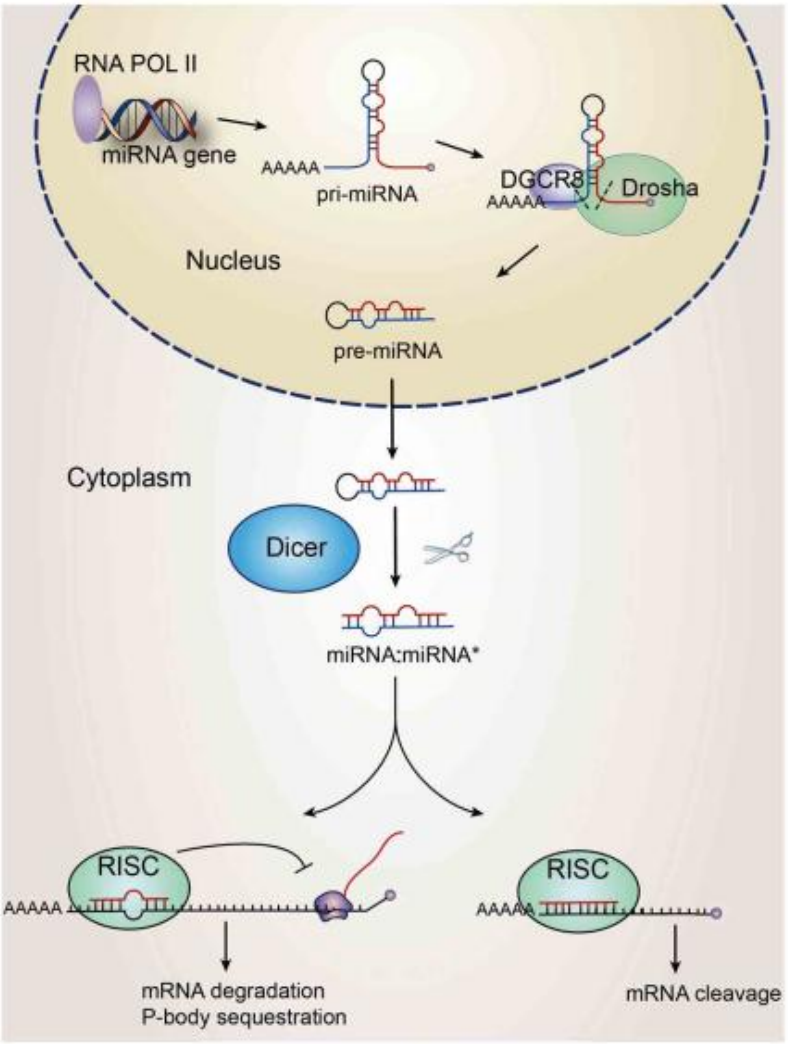

Figure 9: **Biogenesis of miRNAs and their regulatory function in cells** Image from Barca-Mayo O and Lu QR[114].

1.4.2 MicroRNA and cancer

Each miRNA has multiple target genes and regulate different physiologically important processes in the body, such as cell proliferation, differentiation, metabolism, regulation of immune response and cell cycle resulting very important in maintaining the integrity of a cell. Moreover the same target gene can be

influenced by multiple miRNAs, so it is not surprising that abnormalities in their expression are implicated in the pathogenesis of several diseases including cancer[115-117]. Global alteration in miRNA expression patterns was identified in cancer cells compared to normal tissues linking miRNA deregulation to tumorigenesis[118]. Deregulated miRNA expression can be partially attributed to genomic alterations in miRNA loci and in miRNA copy number variations. Indeed miRNAs often maps in particular genomic regions prone to alteration in cancer as fragile sites or region with high frequency of LOH (loss of heterozigosity), deletion and amplification events contributing to their deregulation[116, 119]. First evidences of these genomic alterations were for example the loss of miR-15a/16 cluster region at chromosome 13q14 in B-cell leukemia[120] or the amplification of miR-17–92 cluster gene in B-cell lymphomas and lung cancer[121, 122].

Upregulations and downregulations of different miRNAs have been identified as critical for various aspects of tumorigenesis, from transformation to metastatic events and dissemination and chemoresistance mechanisms of many cancers. Several studies correlated miRNA expression with different tumour types and their expression is often exclusively of specific tissue type. MiRNAs acting as key regulators of gene expression can be classified as tumour suppressor miRNAs or oncomiRNAs based on their function in regulating tumour phenotype[116, 123]. For this reason miRNA expression profiles provides an additional layer of information compared to the mRNA profiles, thus increasing the accuracy for tumour diagnosis and improving prediction of therapeutic responses and overall survival (OS) of cancer patients.

1.4.3 MicroRNA and EOC

Most of publications focusing on miRNAs in EOC have been published in the last 5 years indicating the increasing interest in defining their role in this malignancy. The possibility to better define miRNA-driven mechanisms regulating EOC phenotype represents an exciting opportunity in EOC cancer therapeutics. Several miRNA profiling studies discovered aberrant expression of miRNAs associated with EOC tumorigenesis and progression, providing improved diagnostic, prognostic and therapeutic approaches[124-126]. A general downregulation trend of miRNA expression in EOC compared to normal counterpart has been observed by different authors and similar set of dysregulated miRNAs were identified. In a study performed by Iorio and Croce[127] using ovarian cancer tissues and cell lines compared to normal counterpart (normal ovarian tissues sample), 25 out of 29 dysregulated microRNAs were found to be downmodulated, and 4 microRNAs were found to be upmodulated. The overall miRNA expression was able to differentiate normal versus tumour samples. Zhang and collaborators[128] found a similar trend of significantly differentially expressed microRNAs with 31 out of 35 miRNAs downregulated in EOC cell lines compared to IOSE (immortalized ovarian surface epithelium) cells. Furthermore a trend of downregulation of differentially expressed miRNA was observed in late compared to early stages and in high compared to low-grade EOC[128]. In addition, miRNAs differentially expressed in omental secondary lesion compared to primary tumour were found to be responsible of increased cancer cells' survival and drug tolerance[129] suggesting the important role of miRNAs both in

the disease progression and response to therapy. Data in the table list the principal dysregulated miRNAs in ovarian cancer (Table 1).

Table 1: miRNAs found to be consistently dysregulated in ovarian cancers compared to different normal counterpart (adapted from Zhang S et al[77]).

Alteration	miRNAs	Counterpart	Effect	Mechanism of Deregulation	Targets
Down-regulated	Let-7a/b/d/f	OSE, IOSE, ovary, fallopian tube from fimbriated end	tumour suppressor	promoter methylation, copy number variations	*KLK10*, HMAG2
	miR-22	OSE	tumour suppressor		*ARRB1*, CLIP2, EVI1,FRAT2, EDC3
	miR-31	OSE	tumor suppressor	copy number variation	*E2F2, STK40*, CEBPA
	miR-34a/b/c	IOSE, ovary, fallopian tube from fimbriated end	tumour suppressor	promoter methylation, copy number variations and TP53 mutations	*MET, CDK4*
	miR-125b	OSE, IOSE, ovary, fallopian tube from fimbriated end	putative tumour suppressor		BCL3,VEGF,HIF-1α,HER3
	miR-127-3p	OSE, NOSE, ovary, serum	related to drug-resistant	imprinting, copy number variations, promoter methylation	
	miR-152	OSE, IOSE, fallopian tube from fimbriated end	putative tumour suppressor	promoter methylation	
	miR-155	IOSE, blood, serum	putative tumour suppressor		
	miR-181a-3p	OSE, ovary, blood		copy number variations, promoter methylation	
	miR-382	HOSE		copy number variations, promoter methylation	
Up-regulated	miR-15a/16	OSE, fallopian tube from fimbriated end		promoter methylation	*Bmi-1*
	miR-20a	OSE, fallopian tube from fimbriated end	oncogenic miRNA		*APP*
	miR-23a/b	ovary		copy number variations, promoter methylation	
	miR-30a/b/c	OSE, IOSE, fallopian tube from fimbriated end	related to drug-resistant	copy number variations	*AVEN*, GALNT1
	miR-92	OSE, fallopian tube from fimbriated end	putative oncogenic miRNA		
	miR-93	ovary	putative oncogenic miRNA	copy number variations, promoter methylation	
	miR-106a	OSE, fallopian tube from fimbriated end	putative oncogenic miRNA		
	miR-146b	OSE, IOSE, fallopian tube from fimbriated end	putative oncogenic miRNA	copy number variations	
	miR-182	OSE, IOSE, ovary, fallopian tube from fimbriated end	putative oncogenic miRNA	copy number variations, promoter methylation	*PDCD4*
	miR-200	OSE, ovary, fallopian tube from fimbriated end	putative oncogenic miRNA	copy number variations	*ZEB, c-Myc*,TUBBIII,FN1, NTRK2,QKI
	miR-203	OSE, ovary, fallopian tube from fimbriated end		promoter methylation	
	miR205	OSE, ovary, fallopian tube from fimbriated end	putative oncogenic miRNA	promoter methylation	
	miR-223	OSE	putative oncogenic miRNA		*SEPTIN6*, MMP9, USF2

1.4.4 MiRNAs as early diagnostic, prognostic and predictive biomarkers in EOC

The lack of reliable biomarkers for EOC early diagnosis, prognosis or for monitoring drug response during chemotherapy, and the lack of reliable patients' stratification strategies before starting treatment, represent gaps to be covered in order to improve success in treating EOC. It is now emerging that microRNAs are good candidates to be taken into account to achieve this goal. They maintain stability also in formalin fixed tissues, which represent the commonest source of samples for biomarkers analysis, and are also abundantly present in body fluids such as blood, where they can circulate and regulate the gene expression of recipient cells[130, 131]. Many studies showed that the blood miRNAs of patients affected by various diseases is altered compared to that of healthy subjects[132-134]. MiRNAs in the blood stream are resistant to degradation by RNAse enzymes and are high stable[135, 136], since they are complexed with proteins such as Ago2 (Argonaute 2) or are transported by vesicles such as exosomes[137]. For all these reasons, circulating miRNAs represent minimally invasive promising category of early diagnostic markers also for EOC[138]. Dysregulated expression of microRNAs at tissue level as potential prognostic and predictive markers has been also deeply investigated in recent years. MiR-200 family members, known epithelial to mesenchymal transition (EMT) regulators, are deregulated in ovarian cancer as reported by several authors[127, 139] and their expression correlate with progression-free survival (PFS) and OS in EOC patients. In particular, in stage I EOC low expression level of miR-200c was shown to be an independent prognostic factor of poor survival and a biomarker of disease relapse by Marchini and collaborators[140]. Let-7b, was reported to be an

unfavourable prognostic biomarker in HGSOC and was able to stratify patients in distinct risk groups with different survival rate[141]. Calura et al performed a study on 203 early stage snap-frozen EOC samples, collected at surgery, showing that a miRNA signature, combined with a gene expression profile, was able to provide a prognostic cell pathway, composed of 16 miRNAs and 10 genes, that was associated with OS and progression free survival PFS[142]. Another important prognostic model was developed and validated by my research group analyzing the miRNA expression profile of 894 EOC samples, the largest EOC collection so far available, with the aim of identifying a miRNA signature associated with progression and relapse. A signature based on 35 miRNAs, MiROvaR (miRNA-based predictor of Risk of Ovarian Cancer Relapse or progression), was developed[143]. This signature was able to predict the risk of progression or early relapse in EOC, allowing patient stratification into low- and high-risk groups, with a difference in the median progression-free survival of 20 months between the high-risk and low-risk groups. MiROvaR maintained its prognostic independency when adjusted for stage and residual disease, the two most important clinical prognostic factors in EOC. Among microRNAs that most contributed to MiROvaR and found to be downregulated in the group with high risk of relapse there were the miR-200 family and the miR-506 family. Interestingly we previously reported the miR-506 family to be downregulated in early relapsing advanced stage EOC patients[144] and we contributed with other groups to show that miR-506 is involved in EMT process[145], tumour proliferation[146] and chemotherapy response[147]. Overall, these studies strengthen the role and the ability of miRNAs in stratifying patients into risk classes. Furthermore both Calura's and Bagnoli's

studies[142, 143] showed that the prognostic role associated with their miRNA signatures is independent from histological subtype, further supporting the use of miRNAs as prognostic biomarkers in EOC.

1.4.5 MiR-506

We previously identified a cluster of eight miRNAs mapping on the chromosome X in the q27.3 region (ChrXq27.3 cluster) whose down-regulation is independently associated with early relapse in advanced stage high grade EOC patients[144]. MiR-506 belongs to this cluster and it represents the most investigated among the family and probably the driver miRNA of the cluster, being a key node in regulating EMT in EOC. MiR-506 functional and biological characterization revealed its involvement in regulation of both cell plasticity and drug response to chemotherapy[145, 148]. Furthermore, many different studies so far demonstrated the tumour suppressor role of miR-506 across different tumour types[149-152] through regulation of different target genes involved in several biological processes such as cell growth, migration and invasion, apoptosis and chemoresistance (Figure 10).

Interestingly miR-506 and the other microRNAs of the ChrXq27.3 cluster are all included in the MiROvaR predictor identified by my research group further supporting its important role in EOC and our interest in better define its contribution to this aggressive disease.

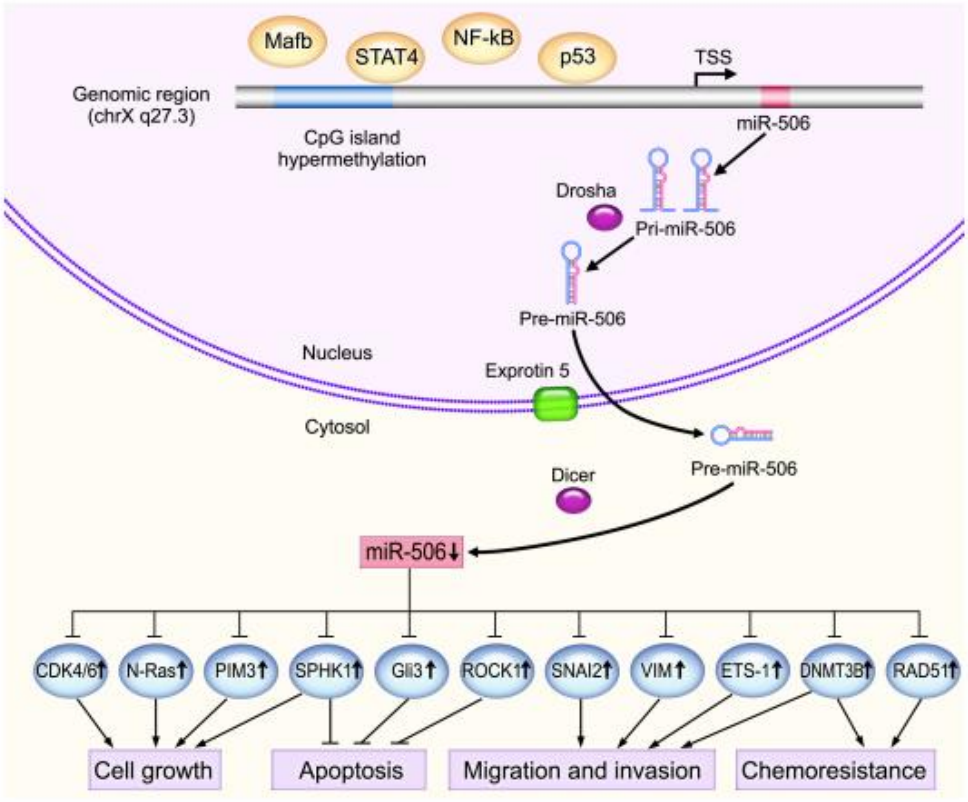

Figure 10: Tumour suppressive role of miR-506 on different biological processes
Mir-506 is often downregulated in various types of cancer and putative binding sites of transcription factors have been identified upstream of miR-506 gene. Acting as a tumour suppressor miRNA, it regulates important genes involved in different cellular processes, such as *ROCK1*, *N-RAS*, *VIM*, *RAD51*, *CDK4/6*. Image from Li Jet al 2016[153].

-MiR-506 in ovarian cancer

Many studies have shown the important role of miR-506 in regulating important cellular processes in ovarian cancer. We reported that miR-506 reintroduction was able to inhibit cell proliferation and increase cell sensitivity to platinum treatment in EOC cell lines[144]. Yang D and collaborators showed that miR-506 through direct targeting of SNAI2, a transcriptional repressor of the epithelial phenotype marker E-cadherin, inhibited cell migration and invasion, induced E-cadherin expression and was able to abolish a TGF-β induced mesenchymal phenotype in EOC cellular models[148]. Moreover miR-506 suppresses other components of the EMT network,

Vimentin and N-cadherin, two important mesenchymal markers, thus inducing a reversion versus a more epithelial and less aggressive phenotype[145]. An anti-proliferative effect of miR-506 was shown by the same authors on EOC cells due to the suppressive effects on the CDK4/6-FOXM1 signalling pathway, usually activated in serous EOC. By a direct targeting of CDK4 and CDK6, cyclin-dependent kinases involved in cell cycle progression, miR-506 promoted cell senescence[146].

Due to the increasing evidences of the involvement of EMT in EOC chemoresistance[154-156], we contributed with Liu G and colleagues to unravel the role of miR-506 in chemoresponse showing that miR-506 is associated with a better response to therapy and longer PFS ad OS in high grade ovarian cancer. MiR-506, through direct targeting of RAD51, involved in double strand DNA (dsDNA) repair through HRR process, is able to sensitise cells to platinum and PARPi olaparib [147]. All these findings support the important role of miR-506 as tumour suppressor in ovarian carcinoma.

2. Aims of the Project

Despite optimal surgery and chemotherapy, the majority of EOC patients experience relapse of the disease. Thus a major challenge in EOC remains prediction of chemoresistant relapse and definition of mechanisms of chemoresistance. MiRNAs are considered important tools through which to obtain a molecular portrait of EOC chemoresistance and represent possible therapeutic targets to be used in the clinic. We previously identified the ChrXq27.3 miRNA cluster as downregulated in early relapsing advanced stage EOC patients and we defined miR-506, belonging to the ChrXq27.3 miRNA cluster, as potentially relevant as regulator of EOC cellular plasticity and response to therapy.

Thus this thesis aimed to dissect the miR-506-driven molecular mechanisms involved in regulating response to chemotherapy by:

1. Investigating the potential role of miR-506 in the response to chemotherapeutic treatments and identifying possible miR-506 targeted genes involved in chemo-response;

2. Define the miR-506-driven molecular mechanisms at the basis of chemo-response.

3. Materials and Methods

3.1 Cell biology technique

3.1.1 Cell Cultures

Human ovarian carcinoma cell lines

Several EOC cell lines, resembling tumour heterogeneity, and their characteristics are listed in Table 2.

Table 2: Ovarian cancer cell lines

Cell lines	Histology	TP53 mutational status	Source
OAW42	SEROUS	WT	Dr. Ullrich, Max-Plank Institute of Biochemistry, Martinsried, Germany
SKOV3	ENDOMETRIOID/CLEAR CELL	NULL	ATCC
A2774	ENDOMETRIOID	MUT	ATCC
IGROV1	MIXED	MUT	Dr. J. Bernard, Institute G. Roussy, Villejuif, France.
OVCAR3	HIGH GRADE SEROUS	MUT	ATCC
OVCAR5	SEROUS	NULL	Dr.R. Camalier, NCI, Frederick, MD
OVSAHO	HIGH GRADE SEROUS	MUT	Dr. Baldassarre, CRO Aviano,Italy
COV362	HIGH GRADE SEROUS	MUT	Dr. Baldassarre, CRO Aviano,Italy
A2780	ENDOMETRIOID/CLEAR CELL	WT	ECACC

WT: wild type; **MUT:** mutated. **ATCC:** American Type Culture Collection; **ECACC:** European Collection of Cell Culture. Histological types are reported as described [157]

Besides the EOC cell lines the following were used: HEK293T (ATCC), a human cell line isolated from human embryonic kidneys (HEK) was used for luciferase assays. A431 (epidermoid carcinoma), H460 (non small cell lung cancer), PC3, DUI45, LNCAP (prostate cancer), MDA-MB-468, MCF-10 (breast cancer), and HCT-116 (colon cancer) cancer cell lines were used for RNA extraction and real time PCR experiments. All human cell lines used in this thesis were cultured at 37°C with 5%

CO2 and maintained in RPMI 1640 (Lonza) supplemented with 10% heat-inactivated fetal bovine serum (FBS) (Gibco®, life technologies) and 2 mM L-glutamine (Sigma-Aldrich, St. Louis, MO, USA) except for OAW42 which was maintained in MEM (Gibco®, life technologies) supplemented with 10% heat-inactivated FBS 2mM L-glutamine and 1% non-essential amino acids (100X stock; Euroclone, Italy), HEK293T in DMEM (Gibco®, life technologies), supplemented with 10% heat-inactivated FBS and 1% glutamine and OVCAR3 which was maintained in RPMI supplemented with 20% heat-inactivated FBS 2mM L-glutamine and 1% sodium pyruvate.

Cells were confirmed to be mycoplasma-free using MycoAlertPlus detection kit (Lonza) and subjected to short tandem repeat (STR) DNA profiling in accordance with the ATCC guidelines, and the genetic profiles were compared with those of publicly available databases to verify their authenticity. Analysis was performed by our Genomic Facility at INT, Milan.

3.1.2 Drug used and treatments

Cis-diamminedichloroplatinum (DDP) (Teva Pharmaceuticals Industries Ltd) (3.3 mM) was used at doses ranging from 0.1 to 100 μM depending on the cell line used.

The PARP inhibitor (PARPi) olaparib (selleckchem.com) was reconstituted in dimethyl sulfoxide (DMSO) to a concentration of 10 mM and stored at -20°C. It was used at doses ranging from 0.5 to 10 μM depending on the cell line used.

The Chk1 inhibitor LY2603618 (selleckchem.com) was reconstituted in DMSO to a concentration of 10 mM and stored at -20°C. It was used at doses ranging from 50 to 300 nM depending on the cell line used.

The Wee1 inhibitor AZD1775 (Biovision Inc. Milpitas, CA; USA) was reconstituted in DMSO to a concentration of 100 mM and stored at -20° C. It was used at doses ranging from 0.25 to 200 nM depending on the cell line used.

For short term cell survival assays cells were plated in 96 wells at the concentration of 2500-5000 cells per well depending on the cell type. Then platinum titration curves were obtained by treating cells (n=6 wells per treatment) for 7h, and effects observed after 72h. Control cells were treated with appropriated medium.

For clonogenic assays cells were plated in 6 wells at the concentration of 1000 cells per well. Drug titration curves were obtained by treating cells (n=3 well per treatment) with different drugs for 10-14 days. Control cells were treated with appropriated medium.

3.1.3 Transient transfection

Transfection experiments in this thesis include:

- miRNA transfections, into the cells to examine their biological effects on cell function;
- miR-target protector (TP) transfection, to protect a single miRNA target gene;
- siRNA transfections, to reduce mRNA and protein levels of a target gene;
- plasmid transfections, for luciferase assay.

All the transfections were performed with liposome-mediated methodology using Lipofectamine® 2000 (Thermo Fisher Scientific) and Opti-MEM (Gibco®, life technologies), a specific medium with reduced serum, or serum-free media. Transfection was performed with suspended cells with Lipofectamine® 2000 used at

a ratio of 1:1 with exogenous nucleic acid and, after 15' incubation at room temperature (RT) to allow lipidic incorporation of exogenous nucleic acid, the transfection mix was added to the cells and incubated at 37°C, in a 5% CO2 incubator for 4.5 hours. Transfection mix was then removed by centrifugation and complete medium added. Cells were seeded and allowed to grow at 37°C, in a 5% CO2 incubator for the appropriate amount of time before the subsequent treatment.

MiRNAs transfection was performed with 60 nM per 10^5 cells of mirVANA miRNA mimic and negative scramble miR (Thermo Fisher Scientific). To evaluate transfection efficiency, a real-time PCR for transfected miRNA was carried out at 48/72h post transfection.

SiRNA transfection was performed with 60 nM per 10^5 cells of siRNA molecules (siGENOME Smart Pool small interfering RNA) or non targeting siRNA used as control (Dharmacon Inc, Horizon Discovery Group plc). SiRNA mediated knock-down of target gene and protein was checked 48h/72h after transfection by qRT-PCR and western blot analysis, respectively.

-Co-transfections

In case of simultaneous transfection of miRNAs and DNA, cells were first transfected with miRNAs following the protocol described above and 24h later transfected with DNA (pmirGLO vector plasmid at the concentration of 0.5 µg per 10^5 cells) used for luciferase assays. In the case of simultaneous transfection of miRNAs and miScript Target Protectors (QIAGEN), a co-transfection was performed using 60 nM of both

for 4.5 hours. Successful transfection of miRNAs and TP in the cells were checked at both protein and mRNA level by western blot and qRT-PCR assays respectively.

3.1.4 Clonogenic assay

Clonogenic assay is an *in vitro* cell survival assay used to measure response to chemotherapeutic agents. After transfection/silencing according to the type of experiment, cells were seeded in six-well plates in triplicate at the concentration of 1000 cells per well. Cells were then exposed to drug treatments, and the ability of a single cell to grow into a colony was evaluated after 10-14 days. Colonies were gently washed with PBS 1X, fixed with ice-cold methanol (stored at -20°C) for 10 min on ice, stained with 0.5% Crystal violet solution (Sigma-Aldrich, St. Louis, MO, USA) for 10 min at RT and washed with ddH2O for colony visualization. Colonies with more than 50 cells were counted using an optical microscope.

3.1.5 Test of cell viability and proliferation assays

-Trypan blue exclusion assay

Cell viability was assessed by trypan blue exclusion staining. Cell suspension was mixed in a 1:1 ratio with trypan blue (Sigma-Aldrich, St. Louis, MO, USA) and counted with an optical microscope using a boyden chamber. An automated cell count was also performed using a Countess® Automated Cell Counter (Invitrogen) mixing 10 µL of sample with 10 µL of trypan blue stain (0.4%), and pipetting 10 µL of the suspension mix into a disposable Countess® chamber slide.

-CellTiter-Glo® Luminescent Cell Viability Assay

The effect on cell growth was assessed using a CellTiter-Glo® Luminescent cell viability assay (Promega Corporation, Madison, USA), that measure ATP generated by metabolically active cells, following manufacturer's instruction. Briefly, 2500/5000 cells per well, depending on the cell line used, were plated in sterile 96-wells in complete medium. At the end of the 100 µL of CellTiter-Glo® reagent was added to cells left in 100 µL of medium for cell lysis. After 10 min incubation at room temperature, the luminescence was recorded in a luminometer (TecanUltra, Tecan trading AG, Switzerland). The luminescence signals for treated cells were normalized by the luminescence signal obtained from control cells according to specific experimental design.

3.1.6 Cell cycle analysis by flow cytometry

Cell cycle analysis by flow cytometry is a method that allow researcher to distinguish cells in different phases of the cell cycle according to their DNA content. Propidium Iodide (PI) is a fluorescent dye that stains DNA quantitatively and the relative DNA amount of cells in the different phases (G0, G1, S, G2 and M) can be determined. Cells were collected, washed with PBS 1X and fixed in 700 µL of 70% cold ethanol for at least 30 min at 4°C. Fixed cell were then centrifuged at 2000 rpm for 5 min and washed once with PBS 1X, in order to remove ethanol. Pellet was then resuspended in 100 µL of PBS 1X-Ribonuclease-A (Sigma-Aldrich, St. Louis, MO, USA) 100 ug/ml and incubated at RT for 10 to 30 min to degrade RNA molecules. DNA was stained with PI 50 ug/ml for 10 min before analysis. Cell cycle was determined

using a BD LSRII Fortessa instruments (BD Biosciences, Franklin Lakes, NJ) and results analysed using FlowJo software (Tree Star Inc, Ashland, OR).

3.2 Biochemical techniques

3.2.1 Cell lysis and assessment of protein concentration

Cells were left to grow until desired confluence, then washed once in ice-cold PBS/sodium orthovanadate (0.1 mM), lysed with appropriate volume of lysis buffer (10 mM Tris-HCl pH8.0, 1 EDTA 0.5 mM, EGTA 0.1%, SDS 0.1%, Deoxycholic acid 140 mM, NaCl 1%, Triton X-100, H2O, proteases/phosphatases inhibitor cocktails (1 tab in 10 mL of lysis buffer) (Roche, Italy) at 4°C for 30 min, and then centrifuged at 13000 rpm for 5 min at 4°C. Whole cell lysates were normalized for protein concentration using bicinchoninic acid (BCA) protein assay reagent according to the manufacturer's instructions (Pierce, USA). BSA (1 mg/ml) was used to prepare protein standards. Absorbance at 562 nm was measured using a spectrophotometer. Protein concentration was determined against the BSA standard curve. Alternatively cells were washed once with ice-cold PBS/sodium orthovanadate (0.1 mM) (Sigma-Aldrich, St. Louis, MO, USA) and then lysed with NuPAGE™ LDS Sample Buffer (1X) (Thermo Fisher Scientific, Waltham, MA, USA) diluted in dH2O plus β-Mercaptoetanol 0.1% (Sigma-Aldrich, St. Louis, MO, USA), that provides the optimal conditions for reduction of protein disulfide bonds and denaturation. Samples were analysed immediately or stored at -20°C for future analysis. Before loading into polyacrylamide gel, samples were boiled at 95°C for 5 min.

3.2.2 SDS-PAGE

SDS-PAGE (Polyacrylamide gel electrophoresis) was performed using the NuPAGE™ electrophoresis system (Thermo Fisher Scientific) with pre-casted NuPAGE™ Novex gels. Based on the molecular weight of proteins to be separated, different types of pre-casted gels were used: 3-8% polyacrilamide Tris-Acetate gels and 4-12% polyacrylamide Bis-tris gels. Run was performed at 100 V with specific buffers (Tris-Acetate for 3-8% gels and 3-N-morpholino propanesulfonic acid (MOPS) for 4-12% gels). Novex™ Sharp or SeeBlue™ Plus2 Pre-stained Protein Standards (Thermo Fisher Scientific), were used as protein molecular weight marker; 500 µL of NuPAGE™ antioxidant (Thermo Fisher Scientific) were added to the running buffer in order to protect disulfide bonds from oxidation.

3.2.3 Western blot

After SDS-PAGE, proteins were transferred to nitrocellulose membrane using iBlot2^{TM} Dry Blotting System (Invitrogen) consisting of the iBlot2^{TM} Gel Transfer Device and associated iBlot™ 2 Transfer Stacks that have integrated the nitrocellulose transfer membranes. Transfer of protein was carried out in 7 min at 20-25 Volts. After transfer the membrane was stained with Ponceau Red (Sigma-Aldrich, St. Louis, MO, USA) to verify efficiency of transfer, then rehydrated with Tris-buffered saline with Tween 20 (TBS-T) buffer [20 mM Tris, 150 mM NaCl, pH 7.6, 0.1% Tween 20] and saturated with milk (skim milk powder, Merck Millipore) to prevent non-specific interactions between the membrane and the detecting antibodies. Membranes were incubated overnight at 4°C with 5 ml of the appropriate antibody diluted in TBS-T or non-fat dry milk as specified by antibody

datasheet. After hybridization with primary antibody, membranes were washed three times with TBS-T for 5 min and incubated for 30'-60' RT with the peroxidase- or biotin- conjugated secondary antibodies (GE healthcare) from rabbit (1:200 dilution), mouse (1:1000 dilution) or goat (1:1000 dilution) depending on the source of the primary antibody. Signal was revealed using a ChemiDoc XRS system and the ECL chemoluminescence system (BIO-RAD, Hercules, CA, USA). Quantity One® software (BIO-RAD, Hercules, CA, USA) was used for quantification of band intensities. Membranes were then treated with a stripping solution (Restore™ western blot stripping buffer (Thermo Fisher Scientific) for 15 min at 37°C to allow further hybridizations with other antibodies. Antibodies used are listed in Table 3.

Table 3: List of the antibodies used

Antibody	Clone and catalog N	Supplier
VINCULIN	E1E9V 13901	Cell Signaling TECHNOLOGY®, Danvers, MA,USA
β-ACTIN	A2066	Sigma-Aldrich, St Louis MO, USA
RAD17	R8654	Sigma-Aldrich
RAD51	H-92: sc-8349	Santa Cruz, CA, USA
CHK1	2G1D5 2360	Cell Signaling TECHNOLOGY®, Danvers, MA,USA
pCHK1(S296)	D309F 90178	Cell Signaling TECHNOLOGY®, Danvers, MA,USA
γ-H2AX	A300-081A-M	Bethyl Laboratories, Inc, Montgomery, TX, USA
ATM	Y170 ab32420	Abcam, Cambridge, UK
pATM(S1981)	D25E5 13050	Cell Signaling TECHNOLOGY®, Danvers, MA,USA
CDK1/CDC2	POH1 9116	Cell Signaling TECHNOLOGY®, Danvers, MA,USA
pCDK1/CDC2(Y15)	10A11 4539	Cell Signaling TECHNOLOGY®, Danvers, MA,USA
WEE1	D10D2 13084	Cell Signaling TECHNOLOGY®, Danvers, MA,USA
pWEE1(S645)	D47G5 4910	Cell Signaling TECHNOLOGY®, Danvers, MA,USA
p-HISTONE H3(S10)	9701	Cell Signaling TECHNOLOGY®, Danvers, MA,USA
CYCLIN B1	D5C10 12231	Cell Signaling TECHNOLOGY®, Danvers, MA,USA

3.2.4 Immunofluorescence

Immunofluorescence (IF) is used to visualize target molecules by labelling them with fluorescent dyes. Cells were seeded on sterilized glass coverslips in 24 well plates or in appropriate 8-well glass chamber slides (Nunc, Thermo Fisher Scientific). Cells

were then fixed with 4% paraformaldehyde for 20 min, permeabilized with PBS 1X with Triton X-100 at 0,5% for 10 min and saturated with PBS 1X with BSA 2% for 30 min. Cells were then incubated with appropriated concentration of the primary antibody diluted in PBS 1X with 1X BSA for 1h at RT, washed three time with PBS 1X with BSA 1% to removed antibody excess and stained with the appropriate secondary antibody Alexa Fluor® (Invitrogen/Molecular Probes®) diluted in PBS 1X and BSA 1% for 1h at RT in the dark (for Alexa Fluor® 488 (green), 1:500 dilution, for Alexa Fluor® 546 (red), 1:1000 dilution). After washing three times with PBS 1X and BSA 1% coverslips were mounted on glass microscope slides with Prolong Gold Antifade with DAPI to stain nuclei (Thermo Fisher Scientific). IF were evaluated with a Nikon TE2000-S microscope with a 40X PlanFluor objective (Nikon). Images were acquired with ACT-1 software (Nikon).

3.3 Cloning techniques

3.3.1 Design and annealing of oligonucleotides

The 3' UTR of *RAD17* cloning was performed according to protocol from pmirGLO Dual-Luciferase miRNA Target Expression Vector (Promega Corporation, Madison, USA) which allow the cloning of putative miRNA binding site of a gene into the vector. The sequence of the 3'UTR of *RAD17* was obtained from UCSC Genome Browser (http://genome.ucsc.edu/index.html). Oligonucleotides pairs were synthesised by IDT (Integrated DNA Technologies, Coralville, Iowa, USA) in order to contain the desired miR-506 target region (seed sequence):

forward: 5'-AAATAGCGGCCGCTAC**GAGTGTAAACTGTGTGCCTTA**TTTACT-3'

reverse: 5'-CTAGAGTAAA**T<u>AAGGCAC</u>ACAGTTTACACTC**GTAGCGGCCGCTATTT-3'

(the 3'UTR cloned in bold and the seed region in bold and underscored). Oligonucleotides were modified to include DraI and XbaI restriction sites at the 5' and 3'end respectively of each oligonucleotide. Oligonucleotides were diluted to 1 µg/µL in sterile water, and then 2 µL of each dilution were combined to 46 µL of Oligo Annealing Buffer (Promega Corporation, Madison, USA) following the manufacturer's instruction. Annealing procedure was performed at 90°C for 3 min, then 37°C for 15 min following manufacturer's instructions.

3.3.2 Restriction digests of vector

In order to obtain a pmirGLO vector with the overhangs complementary to the annealed oligonucleotide overhangs, 20 µg pmirGLO vector (Promega Corporation, Madison, USA) was digested in a two-step digestion overnight at 37°C in a 100 µL reaction containing 4 µL (80 units) of XbaI or DraI enzymes (New England Biolabs) and 10 µL of the appropriate buffers (buffer 2 and 4 respectively, New England Biolabs), with the remaining volume made up of DNA and nuclease-free water. BSA was required for DraI enzyme. Purification was performed with the Wizard® Plus Minipreps DNA Purification System kit (Promega Corporation, Madison, USA). To verify plasmid linearization and length 500 ng purified digested vectors were run on ethidium-bromide-stained 1% agarose gel electrophoresis alongside non-digested controls. Bands-signal was revealed using a Bio-Rad Gel Doc XR System (BIO-RAD, Hercules, CA, USA) and images were acquired using Quantity One® software.

3.3.3 Ligation of insert and vector

Annealed oligonucleatides were diluted to a final concentration of 4 ng/µL and then 8 ng were ligated to 100 ng of linearized vector in a 21 µL reaction containing 1 µL quick ligase (New England Biolabs), 10 µL of 2X quick ligase reaction buffer and DNA-free water to reach final volume. The ligation reaction was carried out by incubating samples RT for 5 min and immediately purified using the Wizard® Plus Minipreps DNA Purification System kit (Promega Corporation, Madison, USA).

3.3.4 Transformation of competent E. coli cells and isolation of plasmid DNA

To carry out transformation 50 µL electrocompetent E. coli TG1 cells were defrosted on ice prior to addition of 2 µL of purified ligation reaction. Cells were electroporated with MicroPulser™ electroporator (BIO-RAD, Hercules, CA, USA) then 10 µL or 100 µL of cells were spread onto a Petri dish of Tryptone Yeast-extract (TYE) broth medium [15 g bacteriological agar type A, 10 g tryptone USP, 5 g yeast extract (Diagnostic International Distribution SPA), 8 g NaCl: add ddH2O to 1 liter], containing 100 µg/ml of ampicillin sodium salt (Sigma-Aldrich, St. Louis, MO, USA) and glucose 1%, then incubated overnight at 37°C. Colonies were isolated and picked the following day to be screened by PCR to verify the presence of the insert. Screening PCR was carried out in 50 µL reactions with: 1 µL of forward and 1 µL of reverse primers (forward: 5'-TCCGCGAGATTCTCATTA-3'; reverse: 5'-TCAGCTTCCTTTCGGGCT-3') annealing on the vector at the sides of the insert, 10 µL of 5X Green GoTaq® Reaction Buffer, 2 µL of PCR nucleotide mix, 0.25 µL of Taq enzyme 5u/µL (GoTaq® G2, Promega Corporation, Madison, USA) and 35.75 µL of sterile water. PCR was carried out with an initial stage of 95°C for 10 min followed

by 35 cycles of 95°C for 1 min, 49°C for 1 min and 72°C for 10 min, with a final step of 72°C for 1 min. PCR products were run on a 3% agarose gel in order to verify the presence of the insert, then the correct orientation and sequence of the insert was verified by sequencing, using the above primers, performed by Eurofins Genomics-genomic service (MWG Eurofins). The bacterial colony carrying the plasmid with the right insert was grown overnight at 37°C and 250 rpm in 60 ml of 2xTY medium [16gr tryptone USP, 10gr yeast extract (Diagnostic International Distribution SPA), 5gr NaCl: add ddH2O to 1 liter], supplemented with 100 µg/ml of ampicillin sodium salt and glucose 1% to allow plasmid replication. The day after the recombinant plasmid was extracted from bacterial cell culture using QIAfilter Plasmid Midi Kit (QIAGEN), resuspended in Tris-EDTA buffer pH 8.0 and quantified with NanoDrop™ 2000c (Thermo Fisher Scientific) and 500 ng were run on a 1% agarose gel to verify plasmid integrity.

3.4 Molecular biology technique

3.4.1 RNA extraction

Total RNA was extracted with NucleoSpin® miRNA kit (Macherey-Nagel, GmbH & Co, Düren, Germany) following the manufacturer's instruction. Briefly cells were harvested with trypsin and washed with PBS 1X, then centrifuged at 1500 rpm and stored as a pellet at -20°C until RNA extraction. At the moment of extraction, cell pellets were resuspended with 800 µL of TRIzol Reagent (Thermo Fisher Scientific), then 160 µL of chloroform were added and samples vortexed. Then samples were centrifuged at 12000 x *g* for 15 min at 4°C and aqueous phase recovered and loaded into columns. Samples were then washed with different buffers and RNA eluted in

30 µL of RNase-free water. RNA was then quantified using a spectrophotometer NanoDrop™ 2000c.

3.4.2 Total RNA and microRNA reverse transcription

RNA extracted from cells was reverse transcribed to cDNA to analyse genes and miRNAs expression via quantitative real time PCR.

For total RNA reverse transcription 2 µg of total RNA were reverse transcribed to cDNA with High-Capacity cDNA Reverse Transcription Kit (Applied Biosystems™, Foster City, CA, USA) using random hexamer primers following the manufacturer's instruction. Reverse transcription of RNA was conducted in 100 µL reactions containing: 10X RT buffer (10 µL), 100 mM 25X dNTP Mix (4 µL), 50 µM Random Primers (10 µL), 0.5 U/µL RNAse inhibitor (0.8 µL), 50 U/µL multiscribe™ reverse transcriptase (5 µL), 100 ng/mL RNA (10 µL) and nuclease-free water (21 µL). Cycling conditions used were as follows: 25°C for 10 min, 37°C for 120 min, 85°C for 5 min. cDNA was stored at -20°C.

For miRNA reverse transscription 10 ng of total RNA was reverse transcribed to cDNA with TaqMan® MicroRNA Reverse Transcription Kit (Applied Biosystems™, Foster City, CA, USA) using specific stem-loop reverse transcription primers following the manufacturer's instruction. Reverse transcription of miRNA was conducted in 15 µL reactions containing: 100 mM dNTPs (0.15 µL), 10X RT buffer (1.5 µL), 20 U/µL RNase inhibitor (0.19 µL), 50 U/µL multiscribe reverse transcriptase (1 µL), nuclease-free water (4.16 µL), primer (3 µL), and 5 µL of total RNA diluted to 2 ng/µL. The cycling conditions used were as follows: 16°C for 30 min, 42°C for 30 min, 85°C for 5 min. cDNA was stored at -20°C.

3.4.3 Quantitative Real time PCR (qRT-PCR)

Real time PCR was used to quantify relative expression levels of genes or miRNAs of interest monitoring their amplification during the PCR in real time. I used TaqMan® assays based on TaqMan chemistry. The probe is labelled with a reporter fluorophore at the 5' end and a non-fluorescent quencher at the 3' end. When intact the quencher suppresses fluorescent emission by the reporter. In the presence of target sequence the probe anneals and is then cleaved upon amplification of the target sequence by the forward and reverse primers, contained in the TaqMan® assay. This produces separation of the quencher from the reporter and a fluorescent signal can be detected. Data is acquired whilst PCR is in the exponential phase and is measured when the reporter dye emission reaches a threshold, known as the cycle threshold (Ct). Results were normalised to housekeeping genes whose expression is known to remain stable, to correct for any errors in RNA content. Results are relative quantifications (RQ). The $2^{-\Delta\Delta Ct}$ or the $2^{-\Delta Ct}$ methods were used, when normalised to a reference gene or to the experimental control respectively, as specified for each experiment. qRT-PCR was performed using TaqMan® gene expression assays (Table 4) or TaqMan® MicroRNA Assays (Table 5). Twenty µL reactions were prepared for each sample containing: 2X TaqMan®Universal MasterMix II (10 µL), probe (1 µL), RNAse free water (8 µL) and 1 µL cDNA. Samples were run in technical triplicates on a 96 well plate. qRT-PCR was run in a ABI Prism 7900HT sequence detection system (Applied Biosystems™ Foster City, CA, USA) using the following cycling conditions: 50°C for 20 sec, 95°C for 10 min, 40 cycles of 95°C for 15 sec then 60°C for 60 sec. Glyceraldehyde 3-phosphate

dehydrogenase (GAPDH), and ribosomal protein L13A (RPL13A) were used as stably expressed housekeepers for gene expression, while RNU44 and RNU48 for miRNA expression.

Table 4: List of the TaqMan® probes used

Gene	TaqMan Assay ID	gene ID
GAPDH	Hs03929097_g1	2597
RPL13A	Hs01926559_g1	23521
RAD17	Hs00607830_m1	5884
RAD51	Hs00153418_m1	5888

Table 5: List of the TaqMan® miRNA probes used

miRNA	TaqMan Assay ID	MIRBASE ID
RNU44	001094	
RNU48	001006	
hsa-miR-506-3p	001050	MIMAT0002878

3.4.4 Luciferase assay

Luciferase reporter assay is the most commonly used strategy to verify the direct interaction of a miRNA with a candidate target. It is based on the insertion of the miRNA target site (seed sequence) downstream of the Luciferase gene in a dual luciferase reporter vector, then the activities of the two luciferases are measured sequentially from a single sample. The wild-type miR-506 binding sites (portion including the seed sequence) of *RAD17* were cloned downstream of Firefly luciferase gene in pmirGLO Dual-Luciferase miRNA Target Expression Vector

(Promega Corporation, Madison, WI). This vector contains Firefly luciferase (luc2) as primary reporter to monitor miRNA regulation and Renilla luciferase (hRluc-neo) as a control reporter for transfection normalization and selection. For the Dual-Luciferase® Reporter Assay (Promega Corporation, Madison, WI), subconfluent HEK293T cells in 24-well plates were transfected with a triplicate repeat of pmirGLO reporter plasmid (0.5 µg) wild-type 3'-UTR construct alone or with miR-506 mimic or miR-ctrl (60 nM), and Lipofectamine® 2000 (1:1 ratio) (Invitrogen). Forty-eight hours after transfection, Dual-Luciferase® Reporter Assay was performed and Firefly and Renilla luciferase luminescence signals were determined following manufacturer's instructions. Briefly cells were lysed with passive lysis buffer (PLB Buffer) and the culture plates rocked at RT for 15 min. Three µL of lysate were added to 100 µL of luciferase assay reagent (LARII) per tube and firefly measurement was performed using TD-20/20 luminometer (TURNER DESIGNS). Then 100 µL of Stop & Glo® reagent was added and the Renilla bioluminescence measured. Ratio of Firefly:Renilla was determined.

3.5 Bioinformatic studies: miRNA Target prediction and identification of deregulated functions with Ingenuity Pathway Analysis

Identification of miRNA binding sites within the 3'UTR of target genes (seed sequence), allows to obtain information on putative miR:mRNA interactions, thanks to the use of algorithms based on different factors for the more appropriate target prediction. Human miRNA target predictions were obtained from:

- TargetScan 6.2 (http://www.targetscan.org/);
- microRNA.org (http://www.microrna.org/microrna/home.do) database;

- Diana-microT-CDS (http://www.microrna.gr/microT-CDS.);
- PITA (https://genie.weizmann.ac.il/pubs/mir07/mir07_prediction.html).

In particular TargetScan6.2, version released in June 2012, focus on the prediction of protein coding gene to be a target of a miRNA if the 3' UTR of the target harbours a conserved 7mer or 8mer motifs that can bind to the seed region. Diana-microT-CDS and Pita, analogously to TargetScan, use the 5' end of the miRNA to identify targets but with minor differences among length of the seed. Conservation across species and target sites free energy are considered. In order to identify commonly predicted mRNA targets, intersection of lists of mRNA targets, obtained from the different algorithms, was performed. I used VENNY 2.0 software, an interactive web-based tool that allow to compare up to four lists of elements and returns to the user Venn diagrams (http://bioinfogp.cnb.csic.es/tools/venny/index2.0.2.html).

IPA (Ingenuity Pathway Analysis) is a powerful analysis tool that helps researchers in analyzing data in order to evaluate molecular and chemical interactions, cellular pathways and disease processes within a system. IPA returns to the user networks that help to understand how genes in a given dataset appear to work together at the molecular level.

3.6 Ovarian cancer patients selection

3.6.1 INT-MI/CRO OC72 case material

Seventy-two high-grade, advanced stage (III-IV) fresh frozen EOC samples collected at time of primary surgery were retrospectively selected from patients with optimal debulking (residual disease <1 cm) followed by standard chemotherapeutic treatment with platinum and taxanes. In detail, 20 patients underwent primary surgery at the Fondazione IRCCS Istituto Nazionale dei Tumori (INT), Milan, Italy, while 52 patients at the IRCCS Centro Riferimento Oncologico (CRO) Aviano, Italy, after signing the informed consent. All samples were reviewed by a pathologist and only tumors with at least 70% of cellularity were included. All biological material was subjected to molecular analysis, gene expression and miRNA expression profiles by the Genomic Facility at INT and associated to complete clinical informations and follow up data.

The time to recurrence after platinum treatment determines platinum sensitivity. EOC patients were defined as *resistant*, *partially sensitive* and *sensitive* if relapse occurred respectively within 6 months, between 6 and 12 months and after 12 months from the end of first line platinum therapy.

This current classification is based on the clinical observation that when patients who responded to first line treatment were re-treated with platinum analogs, the response was better the longer the interval from the last platinum dose was. This classification is now used as stratification criteria in clinical trials

The complete data of the clinical case material are shown in Table 6. Samples were profiled for miRNA expression using Illumina v2 miRNA Chip (1145 miRNA assays)

and subsequently profiled for gene expression using Agilent SurePrint G3 Human gene expression 8x60K.

Table 6: Clinical and pathological data of OC72 case material

		OC72 (n = 72)	
		N°	%
Age, years			
median, range		54; 30-71	
Histology			
Serous		53	***74***
Undifferentiated		8	***11***
Clear Cells		1	***1***
Endometroid		4	***6***
Others + Mixed		5	***7***
NA		1	***1***
Stage (FIGO)			
III		69	***96***
IV		3	***4***
Grade			
2 moderately differentiated		16	***22***
3, poorly differentiated		53	***74***
Undifferentiated		1	***1***
NA		2	***3***
Amount of residual disease			
NED		31	***43***
<1 cm, mRD		41	***57***
Relapsing patients			
R*<6 months	-refractory and resistant	20	***28***
6<R*<12 months	-partially sensitive	15	***21***
R*>12 months	- sensitive	37	***51***

R*= relapse from the end of therapy; NED: non evident disease; mRD: minimal residual disease.

3.6.2 OC179 case material

One hundred-seventy-nine (OC179) samples (chemo naive tumours obtained at primary surgery) from formalin-fixed paraffin embedded (FFPE) was retrospectively collected from Multicentre Italian Trial in Ovarian cancer clinical trial 2 (MITO2)[158]. All samples were reviewed by a pathologist and only tumors with at least 70% of cellularity were included. RNA was extracted at INT-Pascale Naples for miRNA expression profile and for forty-four samples (OC44) out of 179 RNA aliquots were available for qRT-PCR miRNA expression validation. Clinical and pathological characteristics of OC44 are listed in Table 7.

Table 7: Clinical and Pathologic characteristics of OC44 case material

	OC179 (n = 44)	
	N°	%
Age, years		
median, range	58; 38-74	
Histology		
Serous	36	***82***
Undifferentiated	1	***2***
Clear Cells	1	***2***
Endometroid	4	***9***
Others + Mixed	2	***5***
Stage (FIGO)		
IIc	1	***2***
III	34	***77***
IV	9	***20***
Grade		
1 well differentiated	1	***2***
2 moderately differentiated	3	***7***
3, poorly differentiated	37	***84***
Undifferentiated	1	***2***
NA	2	***5***
Treatment		
Carboplatin + Paclitaxel	23	**52**
Carboplatin + PLD	21	**48**
Amount of residual disease		
NED	8	***18***
<1 cm	7	***16***
>1 cm	28	***64***

PLD: Pegylated Liposomal Doxorubicin; NED: non evident disease.

3.7 Statistical analysis

Statistical analyses were performed using GraphPad Prism 5 and 6 (GraphPad Software). This software was used to make graphs after analysis. Statistical significance of differences was determined using one-way ANOVA, two-way ANOVA or two-tailed Student's t-test as specified for each analysis. Significance was indicated as * when $p<0.05$; ** when $p<0.01$; *** when $p<0.001$.

Quantification of western blot bands was performed by Quantity One software.

KM-plotter (http://kmplot.com/analysis/) and OvMark (http://glados.ucd.ie/OvMark/index.html) online tools were used to assess the effect of the *RAD17* on ovarian cancer prognosis.

CompuSyn software (CompuSyn, Inc), based on the Chou-Talalay's CI method for determining synergism or antagonism automatically, was used to calculate combination index (CI) in drug combination experiments.

4 Results

AIM 1: Investigating the potential role of miR-506 in the response to chemotherapeutic treatments and identifying possible miR-506 targeted genes involved in chemo-response

4.1 Clinical impact of miR-506 expression in EOC patients

My research group previously published that the down-modulation of ChrXq27.3 miRNA cluster (miR-506 family) was independently associated with early relapse in advanced stage EOC patients and that miR-506 ectopic expression in EOC cells increased their sensitivity to chemotherapeutic agents[144]. Taking advantage of the miRNA expression profiles analyses performed by my research group on independent EOC case materials, I explored the possible association between miR-506 expression levels and response to platinum-based therapy. As shown in Figure 11 panel A, high miR-506 expression in OC72 case material was significantly associated with platinum sensitivity supporting the data observed *in vitro* following its transfection in EOC cells[144]. As shown in Figure 11 panel B I have been able to validate, by real time quantitative PCR (qRT-PCR), the clinical association of miR-506 expression with platinum sensitivity in further 44 EOC samples derived from a case material associated to the MITO2 clinical trial[143, 158, 159].

These observations led me to hypothesize for miR-506 a key role in EOC response to drug treatment and I therefore search for the appropriated cellular models for further biological assays.

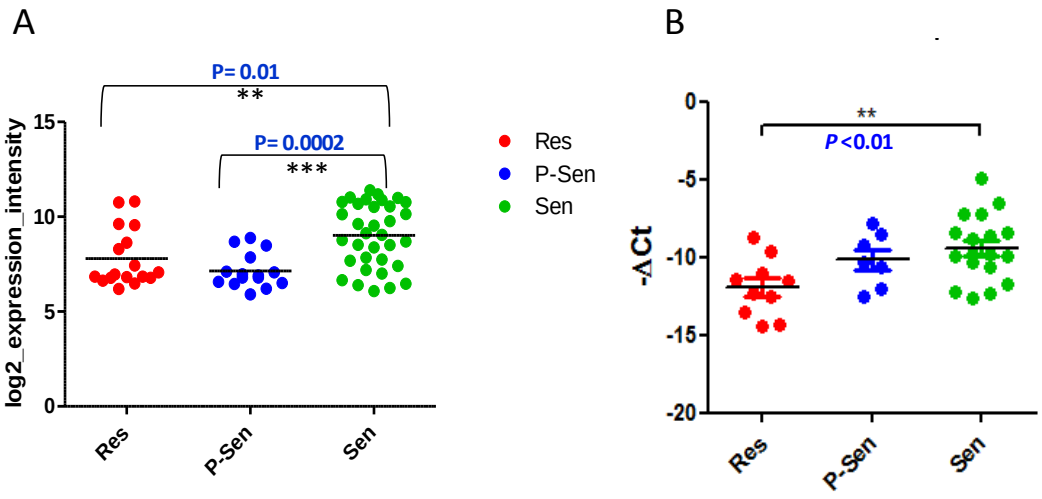

Figure 11: Expression of miR-506 correlates with EOC patients' platinum sensitivity
A) MiR-506 expression assessed by microarray analysis in OC72 case material. MiR-506 Log2 expression intensity plotted B) qRT-PCR validation of miR-506 expression in 44 retrospectively collected EOC patients from the MITO2 clinical trial. RNU48 and RNU44 were used for normalization in qRT-PCR experiment. -ΔCt values plotted. Patient
s were categorized in both datasets for response to platinum treatment as: resistant (PFS < 6 months), partially sensitive (PFS from 6 to 12 months), sensitive (PFS > 12 months). *P* value from one-way analysis of variance with Tukey's multiple comparison as post-test (** p<0.01; ***p<0.001).

4.2 MiR-506 is expressed at low level in EOC cell lines

In order to identify EOC models with different expression levels of miR-506 to be used for gain or loss of function experiments, I screened for miR-506 expression level a panel of EOC cell lines available at my laboratory by qRT-PCR analysis. As internal controls I used RNA samples obtained from EOC patients included in previous study of my research group[144] and known to have high (1H, 2H) or low (3L, 4L) miR-506 expression. As shown in Figure 12 (left panel) all EOC cell lines displayed lower expression level of miR-506 compared to positive controls 1H and 2H. To make sure that the downregulation of miR-506 in EOC cell models was not a phenomenon related to the ovarian cancer histotype, I extended the analysis to a

number of cancer cell lines of different histotypes: epidermoid carcinoma (A431), large cell lung cancer (H460), prostate cancer (PC3, DUI45, LNCAP), breast carcinoma (MDA-MB-468, MCF-10) and colon cancer (HCT). Similarly to what observed in EOC cell lines, qRT-PCR analysis showed again very low expression levels of miR-506 compared to positive controls (Figure 12, right panel). These results are in line with data from other publications reporting miR-506 low expression levels in cancer cell lines[160-162]. These observations led me therefore to use my *in vitro* EOC models essentially for gain of function experiments aimed to achieve higher expression of miR-506. The p53 null platinum resistant SKOV3 and the p53wt platinum sensitive OAW42 cell lines were selected for the majority of further biological assays.

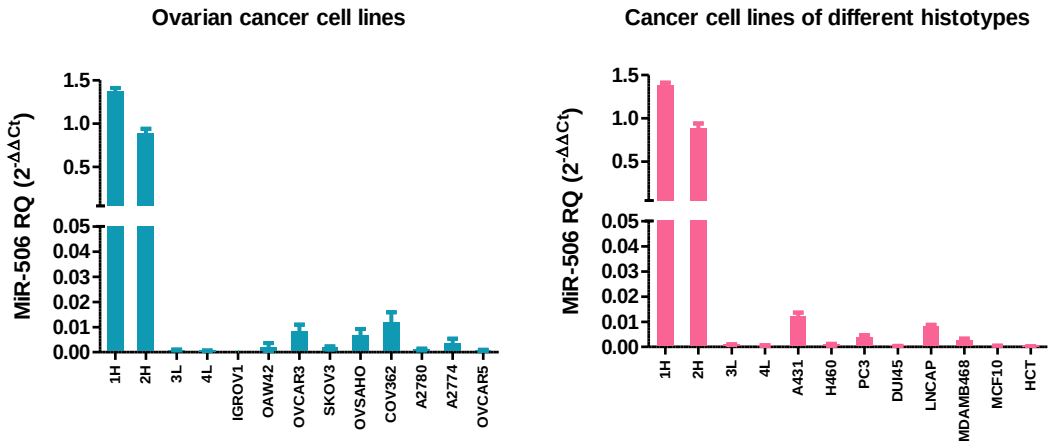

Figure 12: MiR-506 expression level in cancer cell lines

MiR-506 was tested in a panel of EOC cell lines (left panel), as well as in a panel of cancer cell lines other than ovary (right panel), using qRT-PCR method. RNU48 and RNU44 were used for normalization. Values are expressed as relative quantification value (RQ, $2^{-\Delta\Delta Ct}$). Expression levels of miR-506 were compared to those of positives (1H and 2H) and negatives (3L and 4L) controls from patients analysed for miRNA expression level and identified as miR-506 high- or low-expressing patients in previous study of my research group[144] . Data are mean ± SD.

4.3 MiRNAs transient transfection is a suitable method for long-term biological evaluations

To perform gain of function experiments I transiently transfected miR-506 or scrambled miRNAs in my *in vitro* EOC cellular models. In order to assess the extent of miRNA expression over time, following transient transfection, SKOV3 cell line was evaluated by qRT-PCR for expression of transfected miRNAs at different time points. I obtained a consistent induction of miR-506 expression 48 hours after transfection (Figure 13), in accordance with the transfection protocol which indicates this time point as the best in order to observe maximal transfection efficiency. Moreover, I was able to observe that the high expression of miR-506 remained essentially unchanged up to 96 hours after transfection (Figure 13). These results indicate that miR-506 expression upon transient transfection is persistent enough to observe biological changes over time, and support the efficacy of this protocol for experiments requiring long observation time such as clonogenic survival assay used to test cell sensitivity to drug treatments.

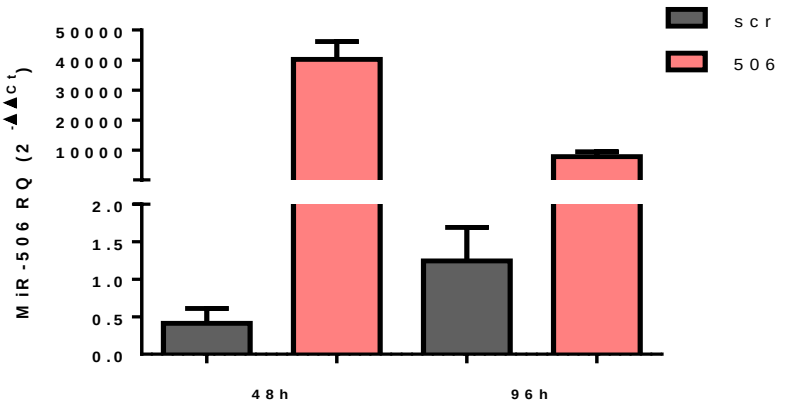

Figure 13: Expression of miR-506 is maintained over time

qRT-PCR experiment reporting that miR-506 expression is stable, with no substantial changes, for up to 96h following miR-506 mimic transfection. RNU48 and RNU44 were used for normalization. Values are relative quantifications (RQ, $2^{-\Delta\Delta Ct}$). scr: scramble miR; 506: miR-506 mimic. Data are mean ± SD of a representative experiment out of two performed.

4.4 MiR-506 overexpression enhances sensitivity to platinum

Upon miR-506 overexpression, we previously described an increased response to platinum (DDP) treatment in the p53wt DDP sensitive OAW42 cell line[144]. In order to check miR-506 contribution in response to platinum treatment also in resistant EOC cells, I transiently transfected miR-506 mimic or scramble control miR in the EOC cell lines SKOV3 and A2774, carrying null and mutated p53 respectively. The day after transfection I exposed cells to serial dilution of DDP (from 0.1 to 100 µM) and percentage of growth was assessed 72 hours later. MiR-506 transfection efficiency was evaluated 48h after transfection by qRT-PCR in both cell lines (Figure 14D). MiR-506 expression was able to significantly re-sensitise A2774 cell line with a drop of IC50 of 3 fold as compared to scr control (Figure 14A, left panel), while no induced sensitivity to DDP was observed in SKOV3 cell line (Figure 14A, right panel). Since miR-506 reintroduction was not able to induce a DDP sensitisation in the SKOV3 resistant cell model, I then performed on this cell line a clonogenic assay as alternative approach to assess response to DDP at longer time points adjusting drug concentration according to literature data. MiR-506 and scr transfected SKOV3 cells seeded in six-well plates, were exposed to different doses of DDP ranging from 0.3 to 1 µM and the ability of a single cell to grow into a colony was evaluated after 10-14 days. In this experimental conditions, miR-506 forced expression significantly enhanced SKOV3 cells sensitivity to DDP treatment compared with control cells (Figure 14B). As expected similar results of increased sensitisation to DDP treatment following miR-506 forced expression was observed in the sensitive OAW42 cell line (Figure 14C). MiR-506 transfection efficiency was evaluated 48h after transfection

by qRT-PCR (Figure 14D). Taking into account that SKOV3 is considered a particular resistant cell line, these results further highlights the role of miR-506 as chemo-sensitising miRNA.

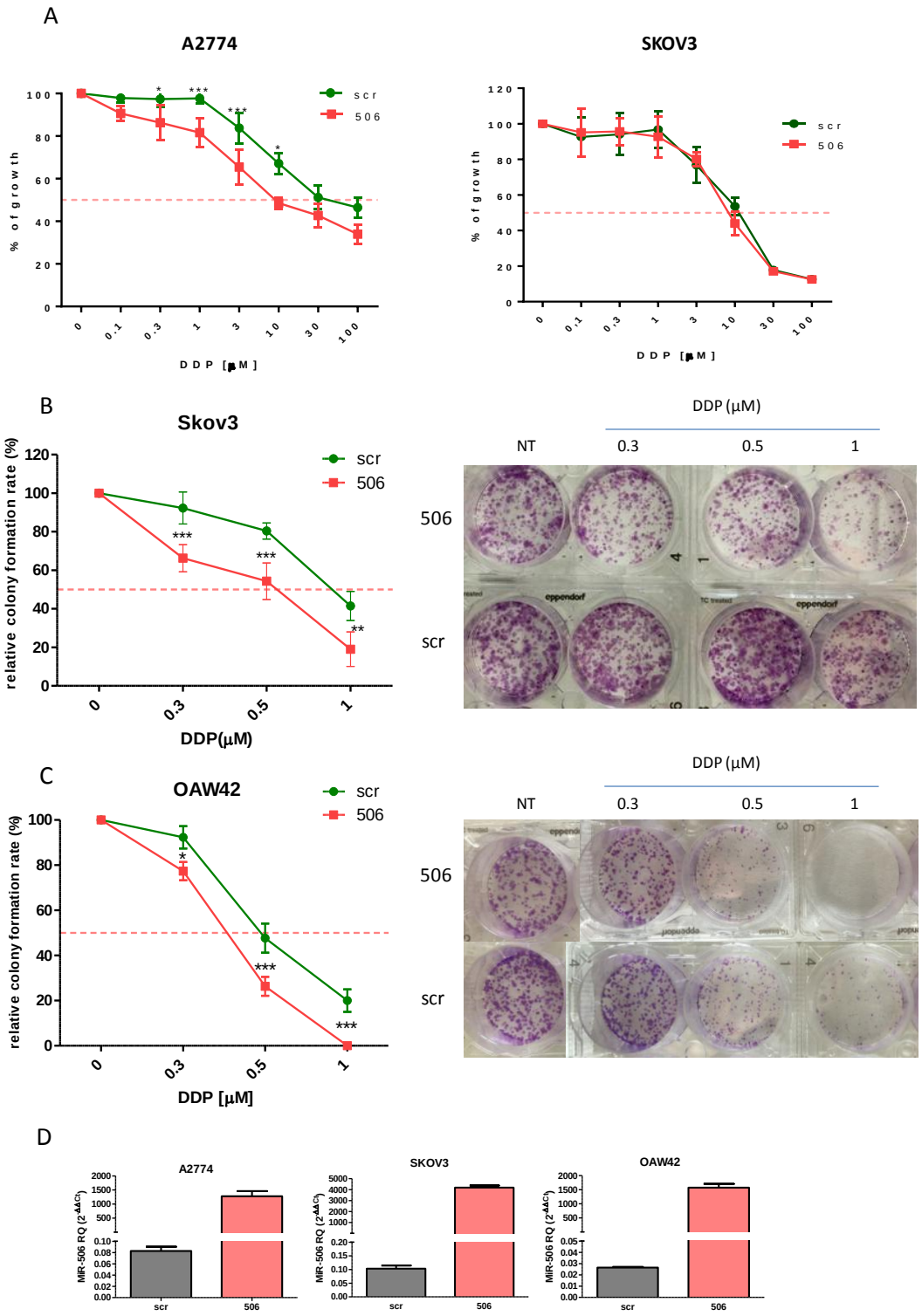

Figure 14: Forced expression of miR-506 increased platinum sensitivity in EOC cell lines
A) A2774 and SKOV3 cell lines were transfected with miR-506 (506) and scramble control (scr), seeded in 96 well plates, treated with DDP at at the indicated µM concentrations and evaluated by CellTiter-Glo® assay 72h after DDP treatment. B) and C) Clonogenic assay on SKOV3 (B) and OAW42 (C) cell lines. Percentage of relative colony formation rate of miR-506 vs scr transfected cells (left panels). Clonogenic assay performed in SKOV3 and OAW42 cell lines (right panels) treated or not (NT) with DDP at the indicated µM concentrations. For each experimental condition a representative well of three independent experiments, each one performed in triplicates, is reported. Colonies were counted using optical microscope. D) qRT-PCR experiments performed 48h following miR-506 mimic transfection in order to evaluate miR-506 transfection efficiency. RNU48 and RNU44 were used for normalization. Values are relative quantifications (RQ, $2^{-\Delta\Delta Ct}$). scr: scramble miR; 506: miR-506 mimic. Data are mean ± SD of at least three experiments. Two way ANOVA and Bonferroni's post test was used to compare miR-506 transfected cells vs scr transfected cells (*p<0.05; ** p<0.01; ***p<0.001).

4.5 Identification of miR-506 target genes and functional analysis of miRNAs targets by Ingenuity Pathway analysis (IPA)

In order to identify the molecular mechanisms by which miR-506 sensitise EOC cells to platinum treatments, I looked at genes potentially targeted by miR-506. I took advantage of the use of publicly available software programs such as TargetScan6.2, Diana-microT, PITA, based on different algorithms/computational methods which apply as determinants: perfect base pairing with the miRNA seed region (the 2-7 nucleotides on the 5' end of a miRNA), accessibility of binding sites, thermodynamic stability of binding sites, target-site abundance, evolutionary conservation of the seed and binding position in the 3' UTR. Since none of the software used consider all the aspects of miRNA-mRNA interactions I intersected the target lists obtained from the different prediction algorithms using VENNY 2.0 software. As reported in the Venn diagram in Figure 15A, around 500 entries were found to be common genes in the three data sets and therefore considered as reliable targets to be validated. Among top score predicted genes I identified: *RAD17* and *RAD51* both related to DNA repair, *CHK1*, *WEE1* and *CHK2* related to cell cycle and *CDH2*, *VIM*, *SNAI2* and *VCAN* related to epithelial mesenchymal transition (EMT) and extracellular matrix.

The list of common predicted genes targeted by miR-506 was challenged with IPA tool, which help to understand how genes in a given dataset appear to work together at the molecular level. Deregulated pathways were derived with top score functions listed in Figure 15B. The most significant molecular networks (pathway's score>20), were associated with DNA replication, recombination and repair, cell cycle and cellular assembly and organization, related to EMT process. These results

are consistent with the role of miR-506 both in the regulation of genes involved in alteration of the normal organization of the extracellular matrix and with EMT and in the process of DNA damage repair (DDR).

A

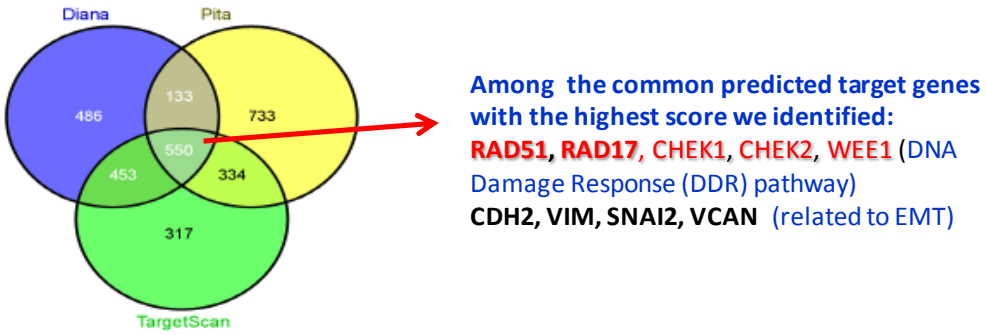

B

ID	Associated Network Functions	Score
1	Cell Cycle, Cellular Assembly and Organization, DNA Replication, Recombination, and Repair	43
2	Cancer, Endocrine System Disorders, Organismal Injury and Abnormalities	36
3	Cellular Assembly and Organization, DNA Replication, Recombination, and Repair, Gene Expression	36
4	Cell Cycle, Cellular Assembly and Organization, Cellular Function and Maintenance	32
5	Cell Cycle, DNA Replication, Recombination, and Repair, Cellular Assembly and Organization	32

Figure 15: Identification of miR-506 target genes and related deregulated cell functions
A) Venn diagram of the target genes of miR-506 predicted by the three algorithms Diana, Pita and TargetScan. B) The first 5 networks identified by IPA on the bases of the 500 commonly predicted mi-506 target genes, with their p-score are shown. The score takes into account the number of genes in the network and the size of the network to approximate how relevant this network is to the original list of genes and allows the networks to be prioritized for further studies.

4.6 RAD51 and RAD17 are regulated by miR-506

To decipher the role of miR-506 in modulating EOC sensitivity to drug treatment, among genes found to be potentially targets of miR-506, I focused on *RAD51* and *RAD17* genes, both involved in DNA damage repair pathway. Acting as damage sensors (*RAD17*) or damage signal mediators (*RAD51*), these genes are important for the recruitment of BRCA1 and BRCA2 to the DNA damage sites activating repair processes. In this perspective, EOC is an intriguing challenge, indeed it has been shown that in these tumours both germline and somatic mutational inactivation of genes related to DNA repair pathway (i.e. *BRCA1* and *BRCA2*) is associated with a more favorable outcome, causing sensitisation to DNA damaging drugs [34, 35]. I hypothesized that if miR-506 consistently regulates the above mentioned genes related to DNA repair, its expression could confer a BRCAness phenotype characterised by increased platinum sensitivity without *BRCA1/2* mutations and might contribute in determining the overall cell sensitivity to DNA damaging agents. To determine whether miR-506 modulation could affect RAD51 and RAD17 expression in my *in vitro* models I ectopically expressed miR-506 in a panel of EOC cell lines: SKOV3, OAW42, A2774 and IGROV1. I performed western blot analysis 48/72 hours after transfection and I was able to detect an evident reduction of both RAD51 and RAD17 protein expression levels, compared to scramble transfected control cells (Figure 16A). MiR-506 overexpression significantly decreased also RAD51 and RAD17 mRNA levels as confirmed by qRT-PCR (Figure 16B). The miR-506-RAD51 axis was investigated in the framework of a collaborative study between my group and Dr Wei Zhang at the MD Anderson Cancer Center[147]. However, RAD17

involvement in EOC biology has never been investigated and it could possibly give new insights about mechanisms of drug resistance. I therefore decided to focus my attention on miR-506 direct modulation on RAD17 and performed functional analysis to better characterize its role in EOC progression.

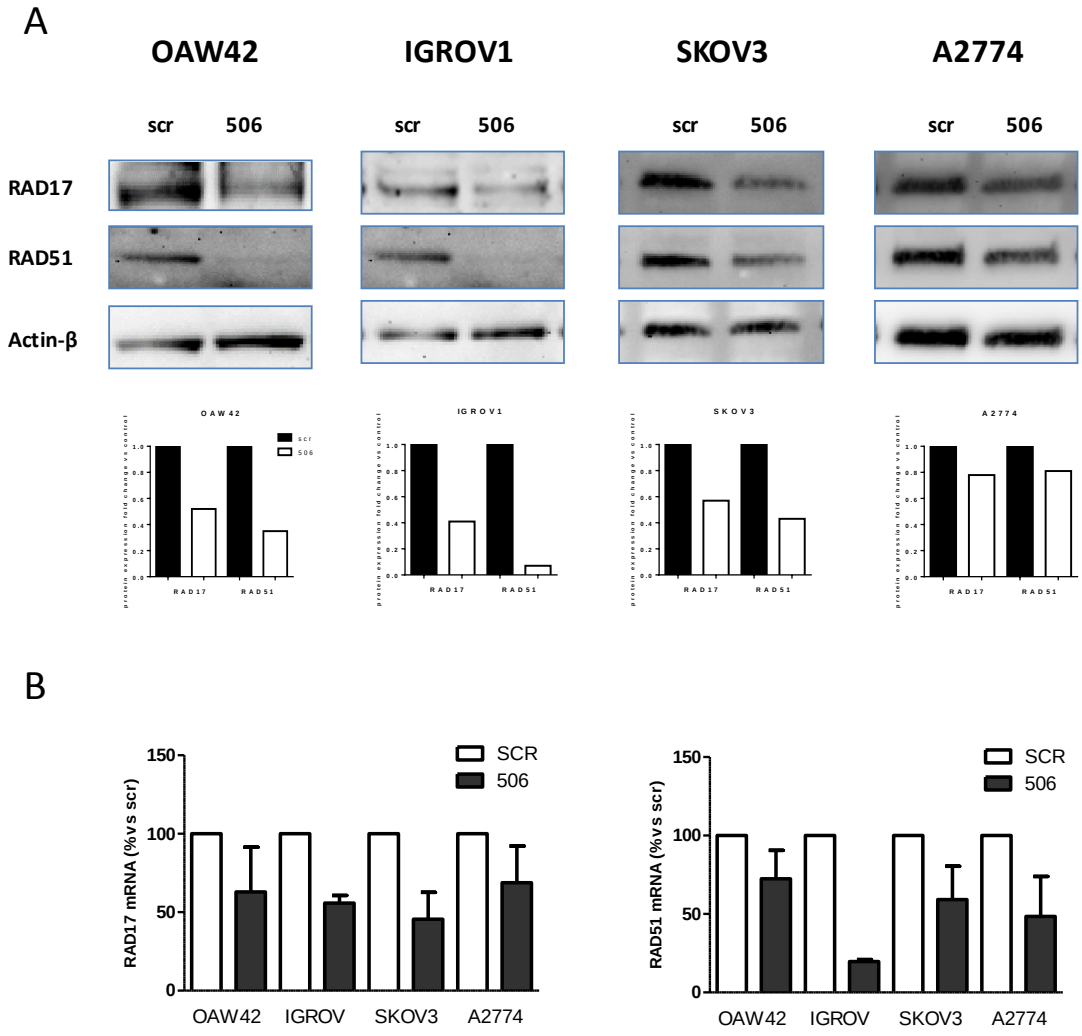

Figure 16: miR-506 regulates expression of RAD17 and RAD51

Four EOC cell lines (OAW42, IGROV1, SKOV3, A2774) were transfected with miR-506 mimic (506) or scr-miR (scr). Proteins and mRNA levels were evaluated at 48 hours after transfection. A) Western blot analysis was carried out in order to check RAD17 and RAD51 protein levels. β-actin was used as loading control. Quantification of protein expression by QuantityOne software was performed and bar chart representing protein expression fold change of miR-506 transfected cells versus controls for both RAD17 and RAD51 is reported below each western blot panel. A representative experiment out of three performed is shown. B) qRT-PCR analysis of RAD17 (left panel) and RAD51 (right panel) mRNA expression levels in the same EOC cell lines. GAPDH was used for normalization. Values are percentage of down-regulation of RAD17 and RAD51 in miR-506 reconstituted cells versus scr transfected cells. Data are mean ± SD of at least three experiments.

4.7 RAD17 is a direct target of miR-506

The RAD17 mRNA contains one miR-506 binding site in its 3'UTR as detected by different prediction algorithms (Figure 17, upper panels). I therefore hypothesized that RAD17 was regulated by miR-506 through direct targeting to its 3'UTR. To test this hypothesis, I performed a Dual-Luciferase® Reporter assay. A 40 base pair region of the RAD17-3'UTR containing the miR-506 seed sequence was firstly cloned into the pmirGLO vector downstream of Firefly luciferase gene, under the control of the human phosphoglycerate kinase (PGK) promoter and the sequence of the insert was confirmed by sequencing. HEK293T cells were co-transfected with pmirGLO empty vector, as control, and with pmirGLO vector containing the miR-506 seed region alone or in combination with miR-506 or scr-miR.

Dual Luciferase activity was assayed 24 hours post transfection and Firefly luciferase activity normalized (firefly luciferase activity/Renilla luciferase activity). Expression of miR-506 significantly reduced the normalized luciferase activity in HEK293T cells compared to the empty vector transfected control cells (Figure 17, lower panel). To confirm that miR-506 specifically regulated this gene, I transfected cells also with another miRNA (miR-unrelated) whose sequence does not have complementary seed in the 3' UTR of RAD17. I observed a luciferase activity comparable to the scr transfected cells and significantly higher than the luciferase activity detected in miR-506 transfected cells (Figure 17 lower panel). Overall these results demonstrate that the overexpression of miR-506 causes a decrease in RAD17 mRNA and protein expression through direct binding on the RAD17 3'UTR.

microRNA.org

hsa-miR-506/RAD17 Alignment

```
    3' agaugagucuuCCCACGGAAu 5' hsa-miR-506
                  | |||||||
369:5' gaguguaaacuGUGUGCCUUa 3' RAD17
```

TargetScan

Position 382-389 of RAD17 3' UTR	5' ...ACGAGUGUAAACUGUGUGCCUUA...
hsa-miR-506	3' AGAUGAGUCUUCCCACGGAAU

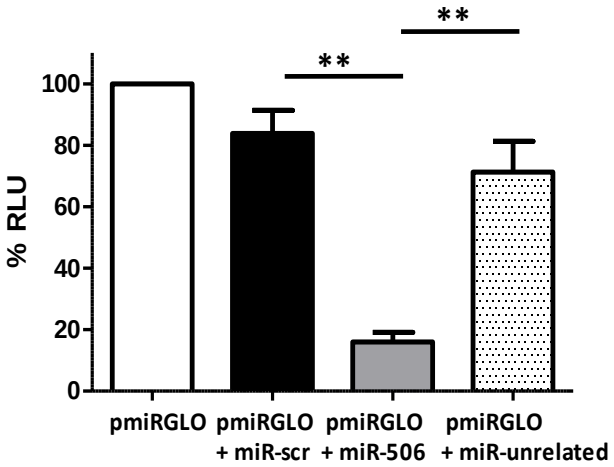

Figure 17: RAD17 is a direct target of miR-506

Images from microRNA.org and TargetScan prediction tools showing the alignment of miR-506 within the predicted binding site in the RAD17 3'UTR (upper panels). Dual-Luciferase® Reporter assay confirming RAD17 as a direct target of miR-506 (lower panel). HEK293T cells were transfected with pmiRGLO empty vector (pmiRGLO, white bar), or pmiRGLO containing the putative binding site of miR-506 in the RAD17 3'UTR in combination with a scrambled miRNA (scr) (pmiRGLO+miR-scr, black bar), miR-506 (pmiRGLO+miR-506, gray bar) and an unrelated miRNA (pmiRGLO+miR-unrelated, dotted bar). Results are percentage of Relative Luminometer Units (RLU) of the ratio Firefly/Renilla. Data are mean ± SD of at least three experiments. Student's t-test was used to compare miR-506 transfected cells versus scr transfected cells (** $p<0.01$).

4.8 Clinical relevance of RAD17 in EOC patients

In order to confirm my *in vitro* data on the correlation between RAD17 and miR-506, I analysed their expression on EOC patients from OC72 case material for whom both miRNA and mRNA profiles were available. As reported in Figure 18A, RAD17 expression was significantly anti-correlated with miR-506 expression (p=0.039) further supporting the importance of this direct regulation. With the aim to correlate RAD17 gene expression levels with patients' clinical outcome I interrogated the online tool OvMark, that integrate gene expression profiles data from up to 2129 EOC samples (around 17000 genes; 14 datasets), and in particular I selected patients for whom information about a platinum therapy was annotated. The RAD17 high expression levels identified patients with worse prognosis; Figure 18B left panel reports the Kaplan-Meier (KM) curves for Disease Free survival (DFS), HR= 1.48, 95% CI=1.22–1.79, log-rank *P*=0.000053; Figure 18B right panel reports KM curves for overall survival (OS), HR=1.61, 95% CI=1.26–2.05, log-rank *P*=0.000092, using median cut off to determine high and low expressing patients. These results suggest a prognostic role for RAD17 expression. Concordantly, high expression of miR-506 has been associated with a favorable prognosis[147].

A

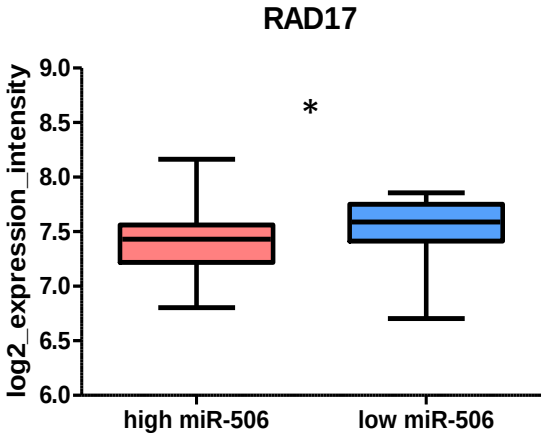

B

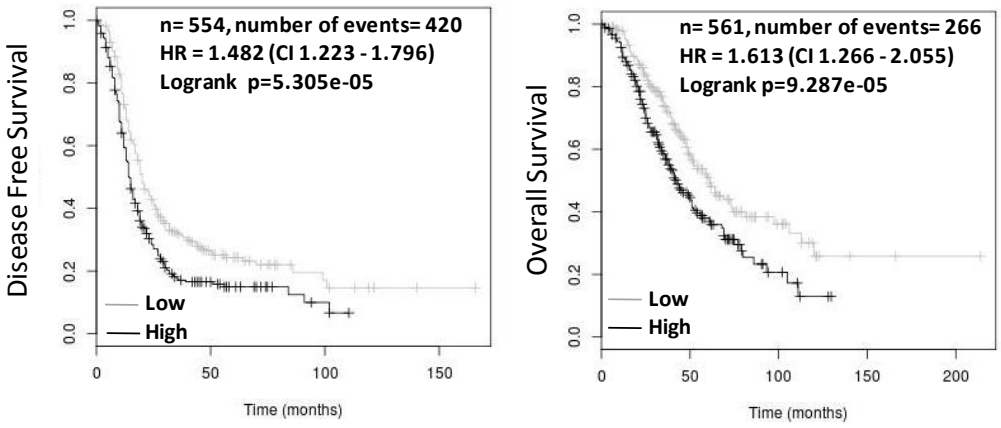

Figure 18: RAD17 is anticorrelated with miR-506 and associates with poor prognosis in EOC samples

A) RAD17 expression by gene expression analysis in EOC patients from OC72 case material. RAD17 expression resulted to be anti-correlated with miR-506 expression. Data are log2 RAD17 expression intensity. Student's t-test was used to compare miR-506 high expressor patients versus miR-506 low expressor patients (* p=0.039).

B) Prognostic significance of RAD17 expression levels evaluated with the online tool OvMark (http://glados.ucd.ie/OvMark/index.html) generating DFS (left panel) and OS (right panel) curves in patients for whom information about platinum treatment was specified in the datasets (GSE30161, GSE9899 and GSE32062). KM curves were generated using a median cut off. Black and Grey lines indicate OC patients with high and low RAD17 expression, respectively. The total number (n) of patients in the two categories is shown. Hazard ratios (HR) with CI (confidence interval) and p values (log rank p, for evaluation of significance) are shown at the top of each panel.

4.9 RAD17 silencing sensitises EOC cells to platinum

According to its role in DDR acting as a sensor of DNA damage, I hypothesized that RAD17 activity could be involved in response to DNA damaging drugs. In order to evaluate whether RAD17 reduction could be critical for platinum sensitivity in EOC cells, I performed CellTiter-Glo® assays in SKOV3 and OAW42 EOC cell lines. Specific inhibition of RAD17 gene expression was obtained by RNA interference method. In particular I transiently transfected cells with a pool of 4 siRNAs against RAD17 (siRAD17) or with a siRNA control sequence (siCTRL). Silencing efficacy was evaluated 72 hours after transfection at protein level, obtaining an almost totally reduction of protein expression in both cell lines as compared to their controls (Figure 19A-B). RAD17 silenced SKOV3 cells resulted more sensitive to platinum treatment across the dose range as compared to siCTRL transfected cells with a drop in the IC50 of 3 fold (Figure 19C). A significant effect of sensitisation upon platinum treatment was observed also in the OAW42 cell line with a drop in the IC50 of 2.5 fold (Figure 19D). Effect of RAD17 silencing in inducing sensitisation to DDP treatment was similar to miR-506 reconstitution effect as shown previously in Figure 14B and 14C. Overall these data are suggestive of the important role of RAD17 expression in modulating platinum sensitivity in EOC cell lines.

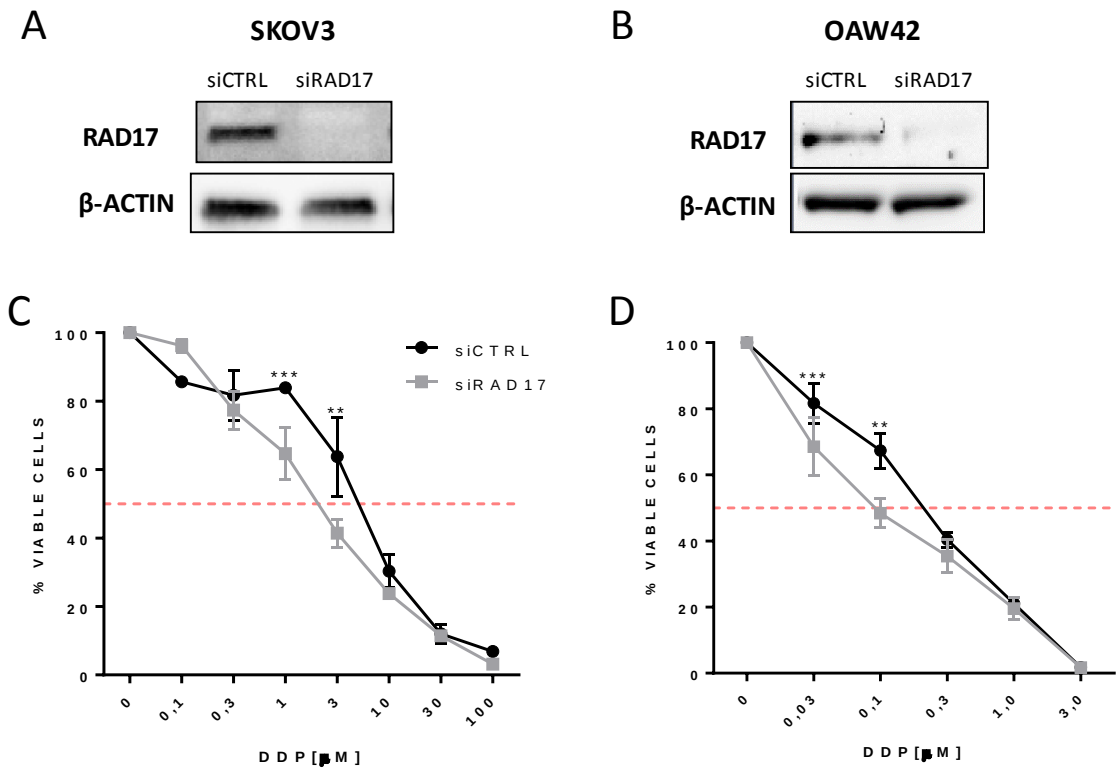

Figure 19 Effect of RAD17 silencing on sensitivity to platinum

SKOV3 and OAW42 cell lines were transfected with RAD17 (siRAD17) and ctrl (siCTRL) siRNAs and seeded in 96 well plates for CellTiter-Glo® assays. The day after transfection cells were treated with serial dilution of DDP as indicated in the graphs. A-B) Western blot analysis of RAD17 silencing efficacy in SKOV3 and OAW42 cell lines. C) SKOV3 and D) OAW42 cell lines treated with DDP. Percentage of viability of siRAD17 and siCTRL transfected SKOV3 (C) and OAW42 (D) cells was evaluated by CellTiter-Glo® assay 72h after DDP treatments. Data are mean ± SD of at least three experiments. Two way ANOVA and Bonferroni's post test was used to compare siRAD17 transfected cells versus siCTRL transfected cells (*p<0.05; ** p<0.01; ***p<0.001).

4.10 RAD17 is directly involved in miR-506-induced drug sensitisation

To verify that RAD17 is a key factor in determining sensitisation induced by miR-506 expression, I employed single-stranded modified RNAs, named target protectors (TP) that are designed to specifically interfere with the interaction of a given miRNA with its specific target gene (Figure 20A). By complementary binding to the seed sequence in the 3'UTR of the targeted gene, TP compete with the miRNA for binding to the target and block miRNA-mediated repression of a specific mRNA without affecting other targets. To this aim I co-transfected miR-506 reconstituted SKOV3 cells with or without two different concentrations (40 nM and 60 nM) of a TP designed to be fully complementary to miR-506 binding site within the RAD17 3'UTR (RAD17-TP), thus preventing the interaction of miR-506 with RAD17 mRNA. I found that RAD17-TP was able to significantly recover RAD17 expression at both mRNA and protein level in miR-506 reconstituted SKOV3 cells compared to miR-scr transfected cells in a dose dependent way (Figure 20B and 20C, respectively). As shown in Figure 20C, RAD51 protein downregulation mediated by miR-506 was not affected by RAD17-TP, further supporting the specificity of the system. The same transfected cells were plated to perform a clonogenic assay following platinum treatment. Interestingly the co-transfection with TP-RAD17 was able to almost completely abrogate the platinum-sensitisation effect induced by miR-506 reconstitution in a dose dependent way (Figure 20D). These results indicate that despite the large number of miR-506 targets, the rescue in sensitisation to platinum treatment is at least in part a result of RAD17 regulation by miR-506 thus confirming a central role of this direct regulation in chemoresponse.

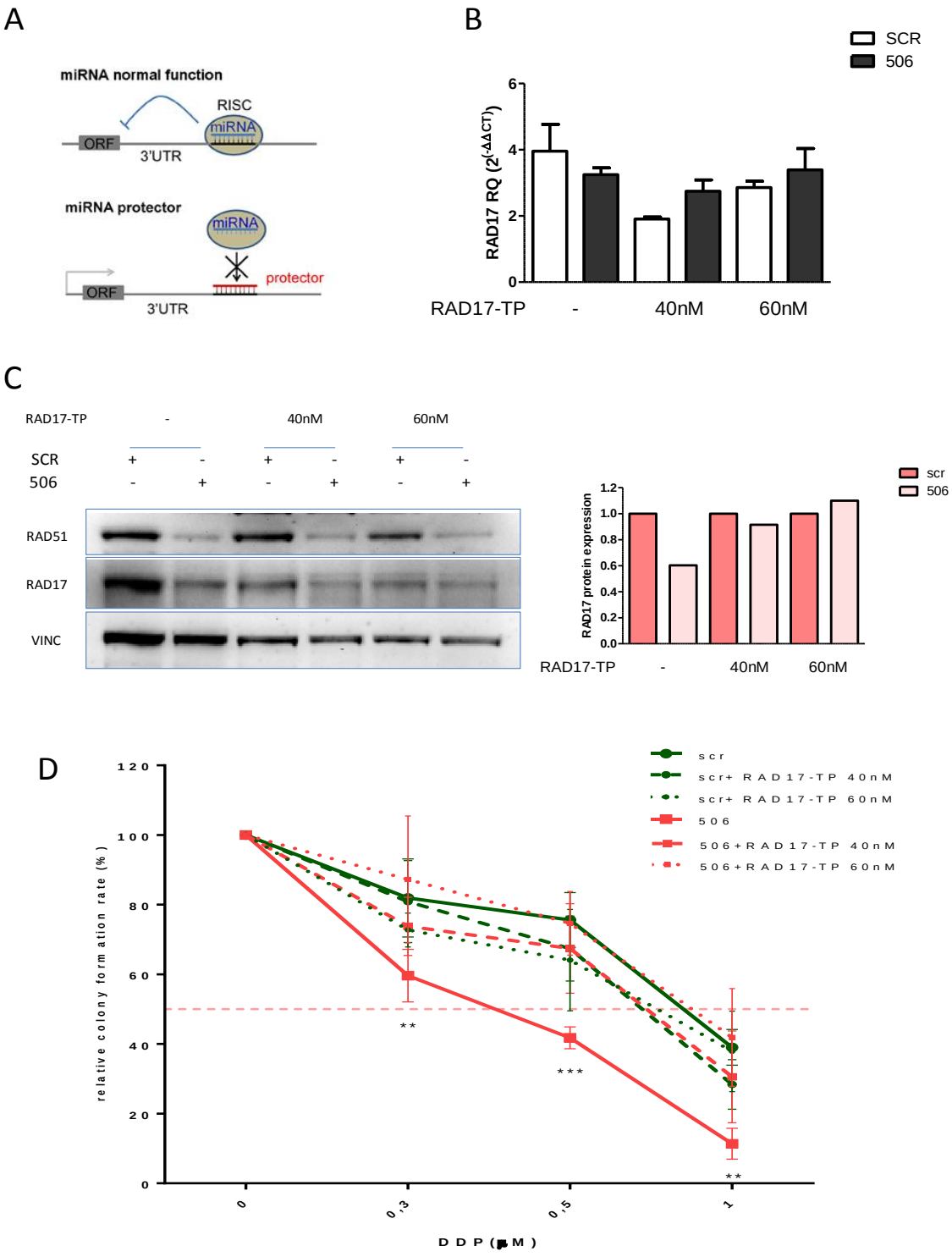

Figure 20: RAD17 contributes to mediate miR-506 induced chemosensitisation

A) Mechanism of action of miScript target-protector (TP) adapted from Zhang et al[163]. SKOV3 cells were transfected with miR-506 (506) or scramble (scr) in presence or absence of RAD17 target protector (RAD17-TP) at two different concentrations. B) qRT-PCR showing RAD17 expression level reconstitution after RAD17-TP co-transfection in miR-506 or scr

transfected cells. GAPDH and RPL13A were used for normalization C) Western blot analysis showing RAD17 protein level after RAD17-TP co-transfection. RAD51 protein expression level was used as positive control of miR-506 efficacy (left panel). Relative protein quantification of RAD17 normalized against vinculin (VINC) performed by Quantity One software and represented as ratio of RAD17 band intensity of miR-506 vs scr for each couple. VINC was used as loading control (right panel). D) Percentage of relative colony formation rate following treatment with platinum (DDP) at indicated doses of miR-506/scr SKOV3 reconstituted cells alone or co-transfected with RAD17-TP (two different doses, 40 nM dashed lines, 60 nM dotted lines). Data are mean ± SD of at least three experiments. Two way ANOVA and Bonferroni's post test was used to compare miR-506 transfected cells versus miR-506+RAD17-TP 60 nM transfected cells (** $p<0.01$; ***$p<0.001$).

AIM 2: Define the miR-506-driven molecular mechanisms at the basis of chemo-response.

4.11 Effect of miR-506-RAD17 regulatory axis on sensitivity to PARP inhibitors

I showed that miR-506 reintroduction was able to sensitise EOC cells to platinum treatment. Since cells with defects in DNA repair pathway has been shown to be sensitive to DNA-damaging drugs and to PARP inhibitors[164], and since miR-506 targets and regulates important components of the DNA damage response (such as RAD17 and RAD51), I hypothesized that this miRNA could modulate also response to PARP inhibitors. I therefore tested my hypothesis on EOC cells treating them with olaparib, a commercially available PARP inhibitor. To this end I selected the p53null SKOV3 and the p53wt OAW42 cell lines and transfected them with miR-506 mimic or a scramble control miR. Cells were seeded in 6 well plates in order to perform a clonogenic assay. The day after cells were exposed to different doses of olaparib ranging from 1 to 10 μM and the ability of a single cell to grow into a colony was evaluated after 10-14 days. MiR-506 forced expression significantly enhanced SKOV3 and OAW42 cells sensitivity to olaparib treatment as compared with control cells (Figure 21A) with drop in the IC50 of 2 fold for both cell lines. Importantly, I obtained the same sensitisation to PARP inhibitor olaparib in both cell lines when I performed a phecocopy experiment by silencing of RAD17 expression with siRNAs, as shown in Figure 21B with drop in the IC50 of 2 fold for SKOV3 and 1.5 fold for OAW42. These results further suggest that miR-506 induced olaparib sensitisation is also a result of RAD17 direct targeting and are supportive of the importance of this new regulatory axis in interfering with DNA repair machinery thus modulating drug

response. Furthermore they suggest the possible use of miR-506 expression level to assess EOC BRCAness phenotype and therefore sensitivity to PARP inhibitors.

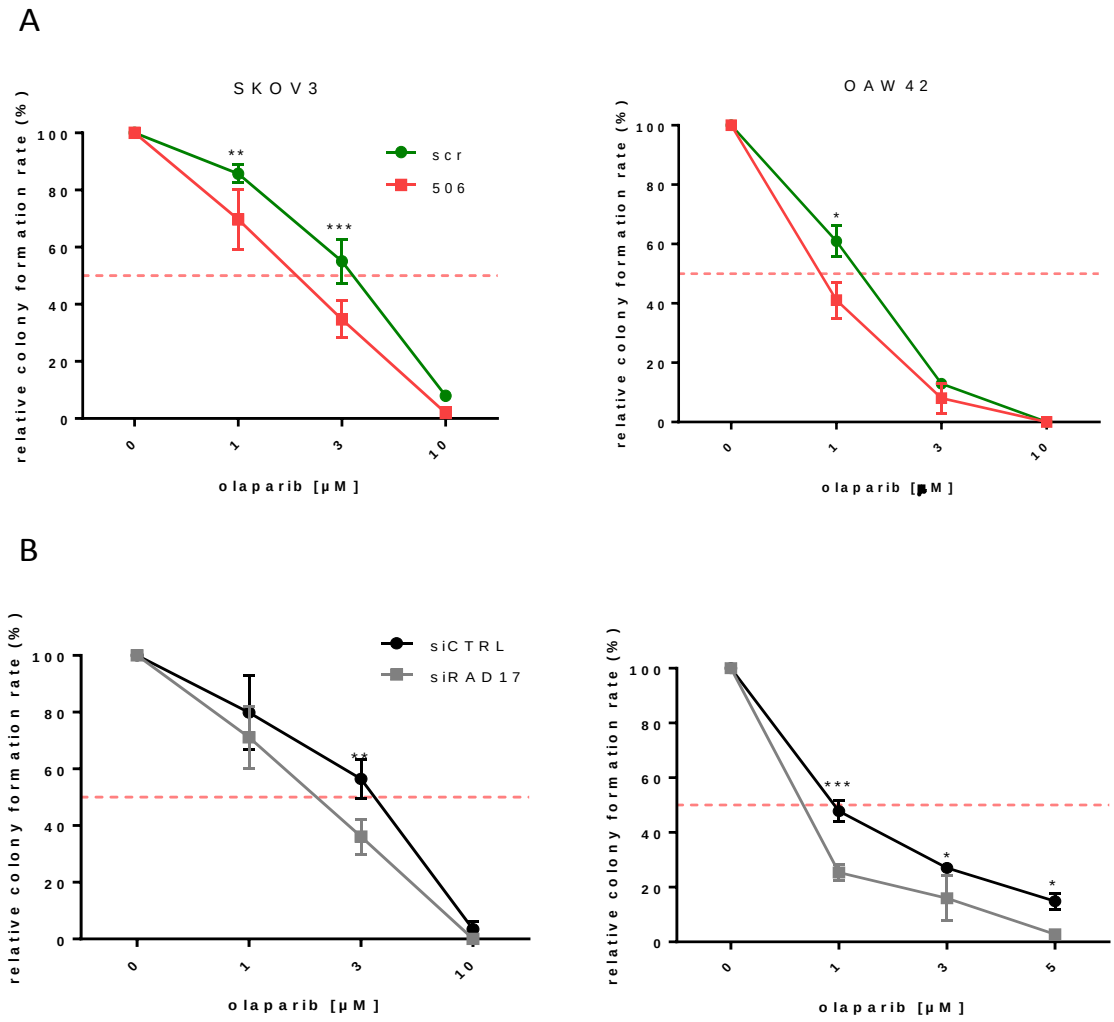

Figure 21: Forced expression of miR-506 induce sensitivity to PARP inhibitors and the effect is phenocopied by RAD17 silencing

SKOV3 and OAW42 cell lines were transfected with miR-506 (506) and control scramble-miR (scr) or silenced with siRNA against RAD17 (siRAD17) or with a control siRNA (siCTRL) and seeded in 6 well plates for clonogenic assays. Percentage of relative colony formation rate of A) miR-506 versus scr transfected cells and of B) siRAD17 versus siCTRL transfected cells are reported. Colonies were counted using optical microscope. Data are mean ± SD of at least three experiments. Two way ANOVA and Bonferroni's post test was used to compare miR-506 transfected cells versus scr transfected cells (*p<0.05; ** p<0.01; ***p<0.001).

4.12 MiR-506 increases frequency of chromosomes breaks and causes abnormalities in mitotic progression in platinum treated cells

It has been recently reported that *RAD17* deletion trigger genomic instability and led to DNA fragmentation and mitotic catastrophe in gemcitabine-treated pancreatic cancer cells[80, 165]. I tested whether miR-506 reintroduction could be responsible of such instability, mimicking the effects of RAD17 depletion. To this purpose I selected SKOV3 cells as most representative of the majority of EOC and I transfected cells with miR-506 mimic or scr and, 48 hours after DDP treatment, I performed an immunofluorescence analysis to evaluate its role in inducing mitotic defects. Immunostaining of acetylated alpha-tubulin to visualize the mitotic spindle, phosphorylated histone H3 (ser10) as marker of mitotic cells, and DAPI to counterstained nuclei, revealed in miR-506 reconstituted cells the presence of aberrant mitotic figures, such as monopolar and multipolar spindles or lagging chromosomes, resulting from asynchronous chromosomes movements at mitosis anaphase (Figure 22B, 22C, 22D), while normal mitosis were observed in scr control transfected cells (Figure 22A). Moreover, I assessed the effect of miR-506 on the appearance of micronuclei, small extra-nuclear chromatin-containing bodies which result from unrepaired chromosome breaks or lagging chromosomes. In response to DDP treatment, miR-506 reconstituted SKOV3 cells displayed higher number of micronuclei compared to scr control cells (Figure 22E), which reflected elevated genomic instability of platinum treated cells induced by miR-506 transfection. Overall these results suggest that sensitisation to drug treatments induced by miR-506 reintroduction may be also a consequence of failure of cell division processes.

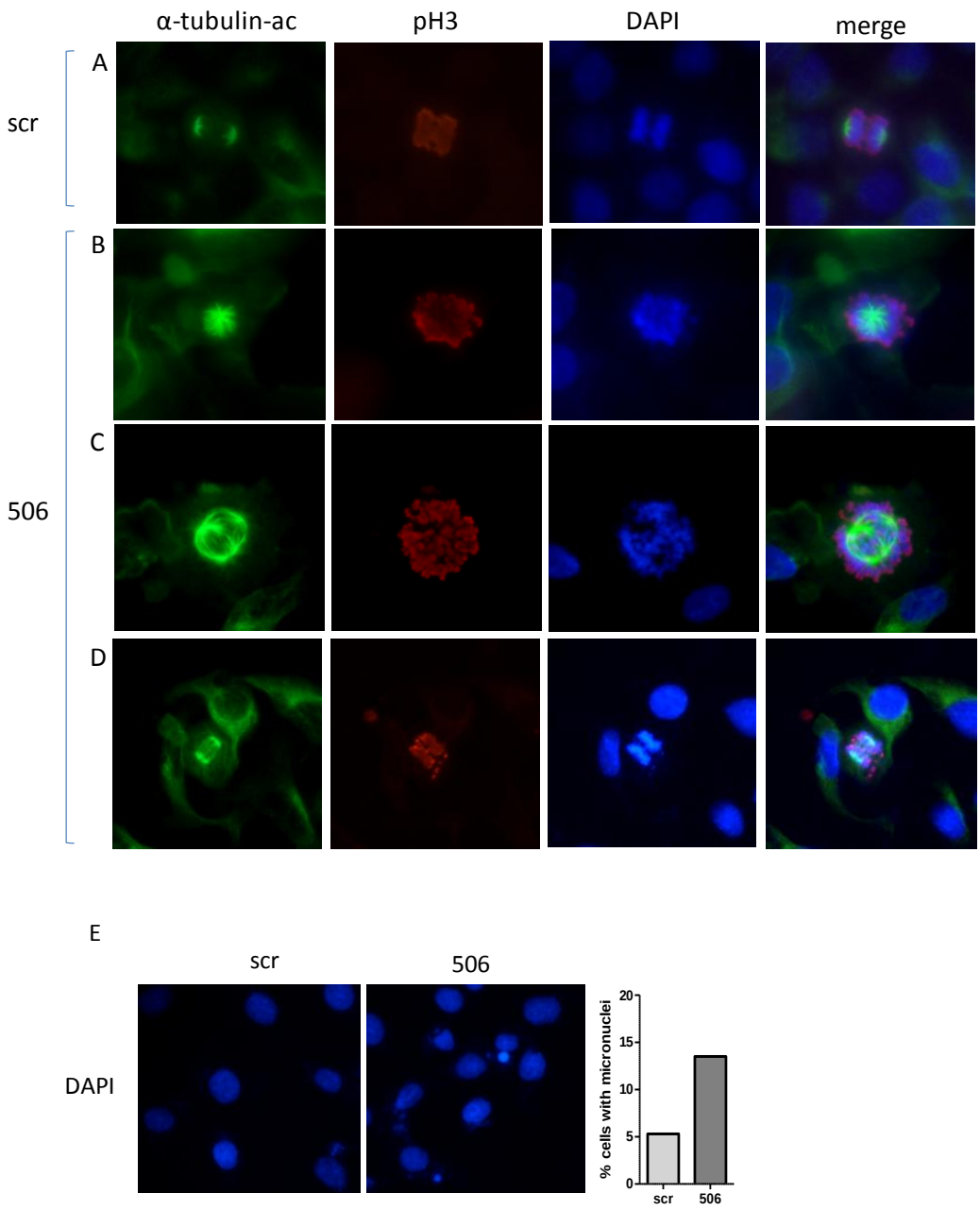

Figure22: MiR-506 reintroduction causes abnormal mitotic figures following drug treatment

MiR-506 reconstituted SKOV3 cells were treated with 3 µM of DDP. 48 h after transfection cells were fixed and immunofluorescence analysis was carried out for Acetylated alpha-tubulin (α-tubulin-ac, green), phosphorylated histone H3 (pH3, red) and DAPI (nuclei, blue). A) Normal mitosis occurring in scr cells, B) monopolar mitosis, C) multipolar mitosis, D) lagging chromosomes. E) Micronuclei in miR-506 transfected cells and scr control. Magnification 40X.

4.13 MiR-506 impacts on DNA Damage

Given the effects of miR-506 reconstitution in inducing aberrant mitotic figures upon DDP treatment, together with the evidence that miR-506 directly targets and regulates different molecules involved in DDR, I further investigated the impact of miR-506 reintroduction on DNA damage. To this end I analysed the expression level of γH2AX (phosphorylated in serine 139), a recognized marker of DNA DSBs. SKOV3 cells were transfected with miR-506 and scr control. The day after, cells were treated with DDP at the concentration of 3 μM for 24 hours to induce DNA damage and western blot analysis was performed. I observed a decrease in γH2AX expression level in miR-506 treated cells compared to scr control treated cells (Figure 23A). I also performed immunofluorescence analysis in order to visualize γH2AX localization at DSBs sites upon platinum treatment. Figure 23B shows a reduced number of γH2AX positive cells, containing more than 15 foci, in miR-506 reconstituted cells, with a mean percentage reduction of 30% in miR-506 transfected cells compared to scr control cells (Figure 23C). Similar to miR-506 reconstitution effects, RAD17 silencing was responsible of the reduction of γH2AX expression level in DDP treated cells, (Figure 23D). These results suggest that miR-506 reduces γH2AX recruitment at DSBs sites thus impairing DNA damage response.

RAD17 is a DNA damage sensor protein important for ATR checkpoint signalling in response to DNA damage insults, such as platinum treatments. It has been recently shown that RAD17 play a role also in the early recruitment and maintenance at damage sites of the MRN (MRE11-RAD50-NBS1) complex, promoting ATM checkpoint response and homologous recombination repair[71]. Since miR-506

negatively regulate RAD17, I hypothesized that miR-506 reintroduction could impair also ATM signalling activation occurring upon DNA damage recognition. In order to validate RAD17 new proposed role in my model of EOC I firstly silenced SKOV3 cells with siRAD17 and siCTRL siRNAs and upon DDP treatment I observed in RAD17 silenced cells a reduced phosphorylation, thus activation, of ATM (Figure 23E, left panel). More importantly, when I ectopically expressed miR-506 in the same cell line, I obtained a reduced activation of ATM after DDP treatment (Figure 23E, right panel), similar to RAD17 silencing effect. These observations further support the important role of miR-506 and its regulation on RAD17 gene expression in DNA damage response and in promoting early ATM checkpoint response. Overall these results suggest that miR-506 may lead to a delayed recruitment of DNA damage proteins at damage sites and a delayed activation of signal cascade upon treatment.

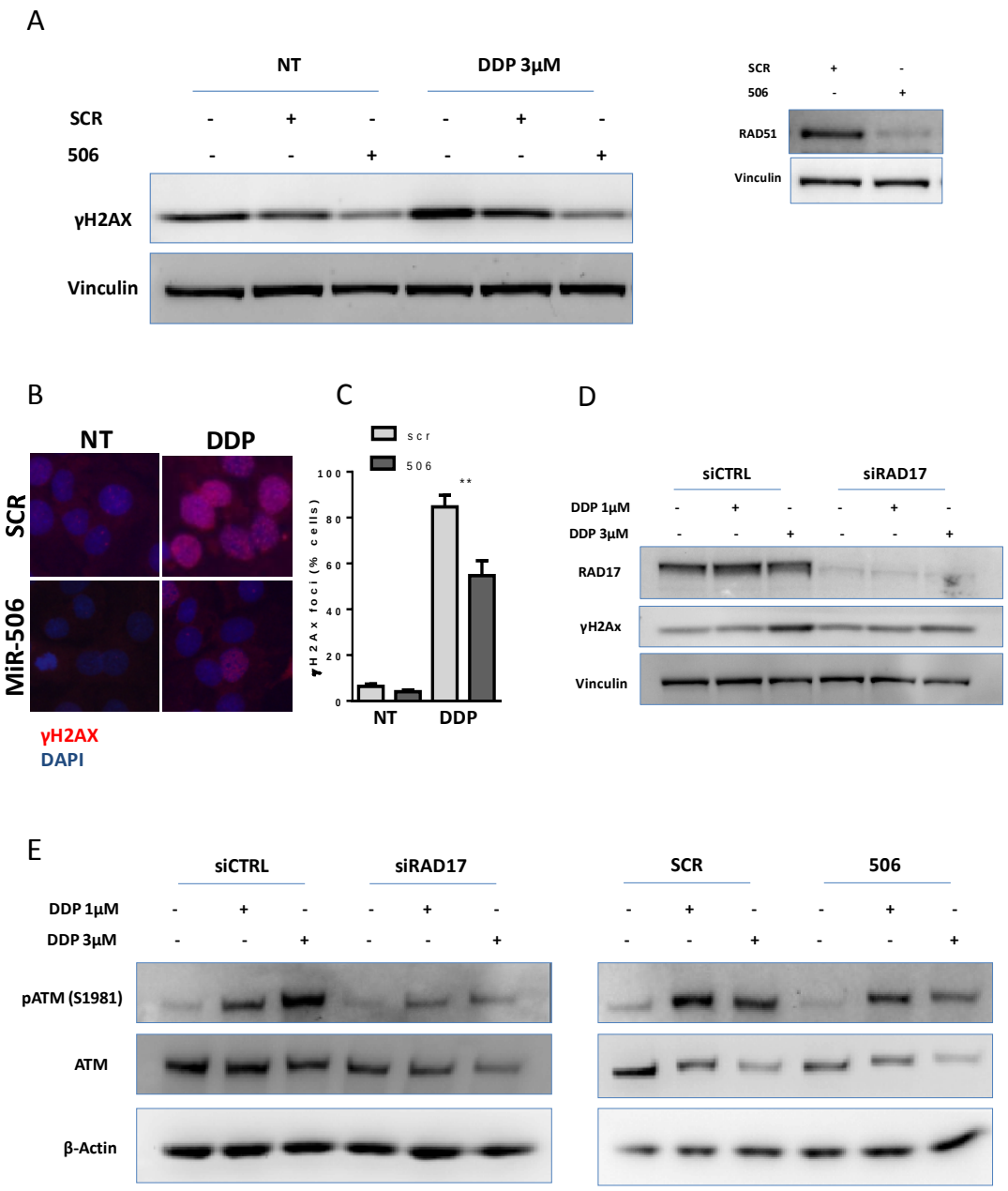

Figure 23: miR-506 reintroduction impairs response to DNA damage

A) Western blot analysis of γH2AX expression in SKOV3 cells transfected with miR-506 mimic or scr control miR and treated with platinum (DDP). Lysates collected at 24 hours after treatment. Vinculin was used as loading control. Inset in the right panel representing RAD51 downregulation used as positive control of miR-506 transfection. B) Representative images of the immunofluorescence staining of γH2AX in SKOV3 transfected with miR-506 or scr control and treated with or without platinum at the concentration of 3 µM for 24h. Magnification 40X. C) Percentage of γH2AX-positive cells following DDP treatment at 3 µM. Cells with more then 15 foci were considered as γH2AX-positive. Data are mean ± SD of two experiments (** $p<0.01$). D) Western blot analysis of γH2AX expression in SKOV3 cells silenced for RAD17 and treated with platinum (DDP) at 1 and 3 µM. Vinculin was used as loading control. E) Western blot analysis of pATM expression upon DDP treatment in both miR-506 and scr transfected and siRAD17 and siCTRL silenced SKOV3 cells. β-actin was used as loading control.

4.14 MiR-506 causes a delay in platinum-induced G2 cell cycle arrest

Sensing and repair of DNA damage are finely regulated events during cell cycle progression. G2/M cell cycle checkpoint is an important surveillance mechanism used by cells in response to DNA damage. Its function is to prevent entry into mitosis of damaged cells. Since miR-506 reintroduction was able to induce a possible delay in sensing DNA damage I decided to investigate the potential role of miR-506 in regulating progression of cell cycle in response to platinum treatment. SKOV3 cells were transfected with miR-506 mimic or scramble control miR and treated with DDP at the concentration of 1 μM and 3 μM. Cells were collected at different time points (24h, 48h and 72h) after treatment and their cell cycle analysed by FACS. As expected, gradual accumulation of cells blocked in S and G2/M phase of the cell cycle was evident over time in scr treated cells (Figure 24A, upper panels). MiR-506 reconstituted cells showed instead a marked delay in accumulation of cells in G2/M phase of the cell cycle particularly evident at 48 hours from DDP treatment compared to scr control cells (Figure 24A, lower panels) (25% versus 53% cells at G2/M phase for miR-506 and scr cells respectively, Figure 24B). After 72 hours of treatment however, both miR-506 and scr cells showed the same extent of block in G2/M phase (Figure 24B). These data suggested that miR-506 reconstitution induced a delay in G2/M cell cycle arrest upon platinum treatment. This delay could allow cells to propagate into the cell cycle with an unrepaired extensive DNA damage with premature entry into mitosis which will cause cell death.

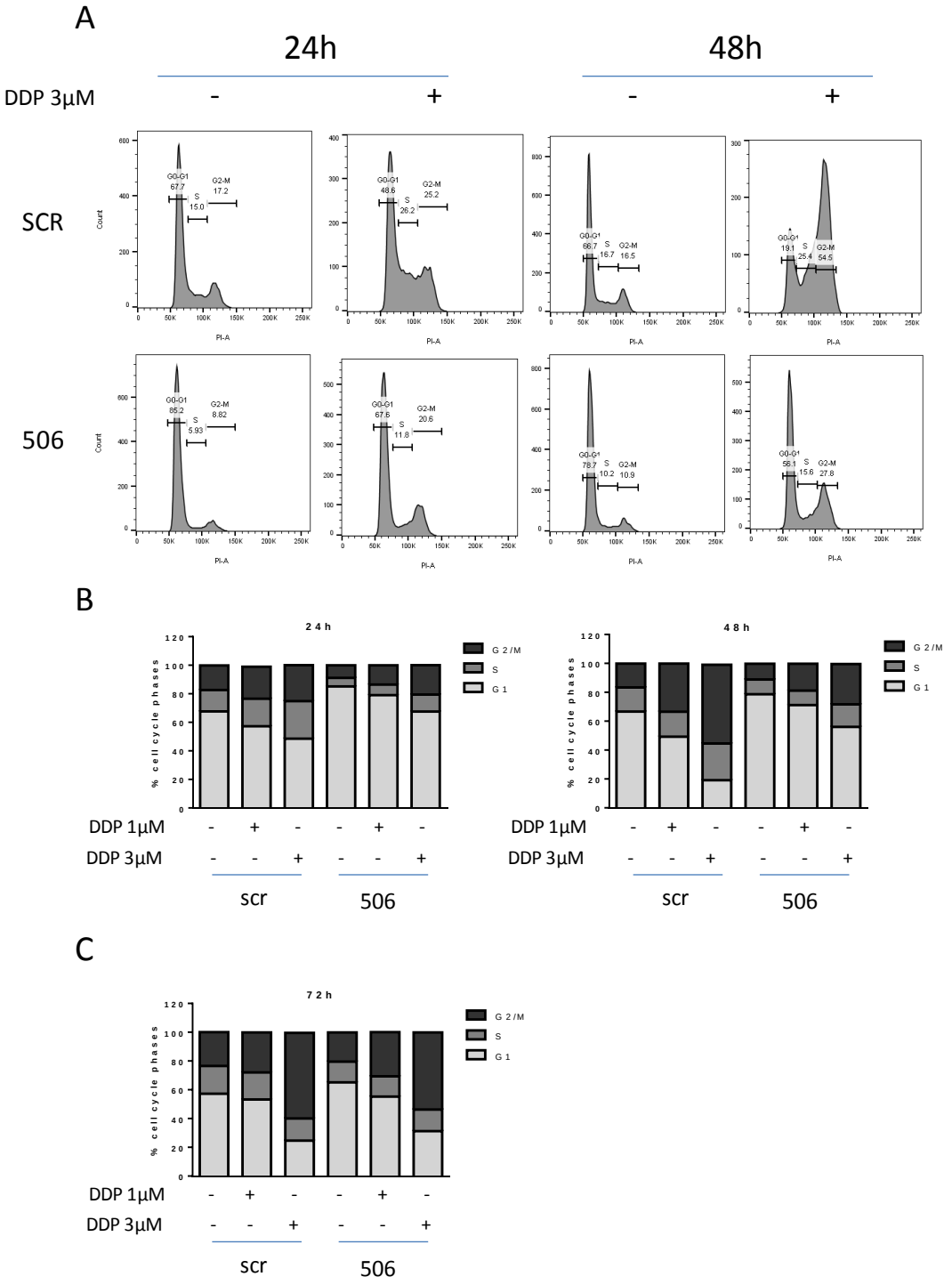

Figure 24: MiR-506 reconstitution affects cell cycle progression

Flow cytometry analysis of the cell cycle distribution after DDP treatment in miR-506 and scr control transfected SKOV3 cells using propidium iodide staining. A) Representative images showing delayed accumulation of cells in phase G2/M of the cell cycle after 3 µM DDP treatment in miR-506 reconstituted cells (lower panels) compared to scr tranfected cells (upper panels). B) Quantification of cell cycle distribution in percentage during time (24h and 48h) upon 1 and 3 µM DDP treatment, with the percentage of cells in G1 phase (light grey), S phase (grey), and G2/M phase (dark gray). C) Quantification of cell cycle distribution following 72h of DDP treatment.

Since the observed effect in impairing the G2/M block of cells upon DDP treatment, I decided to assess if miR-506 reconstitution may cause major alterations in the signal transduction pathway activated upon DNA damage and related to cell cycle G2/M checkpoint activation. Western blot analysis revealed that in SKOV3 cells the ectopic expression of miR-506 drastically abrogated G2/M checkpoint activation signal cascade consistent with its role in delaying block of cells in G2/M phase of the cell cycle upon DDP treatment (Figure 25B). More in detail, I observed a reduction in phosphorylated Chk1 kinase in Serine 296, one of the DNA damage induced phosphorylation sites, which in turn abolished cyclin-B1-CDK1 complex activation, a key event that initiates mitotic entry. Indeed, upon miR-506 reconstitution, a reduction of cyclin-B1 levels was observed in treated cells and abrupt dephosphorylation of the inhibitory phosphorylation site of CDK1 (tyrosine 15, Y15). Moreover CDK1 remained dephosphorylated, thus active, also by the lack of the inhibitory phosphorylation exerted by Wee1 kinase. Indeed I observed a decreased expression and a proportional decreased activation (phosphorylation) of Wee1 protein, which as well as Chk1 resulted impaired following miR-506 transfection. These results further support the role of miR-506 in abrogating G2/M checkpoint in response to DNA damage allowing the entry of damaged cells into mitosis.

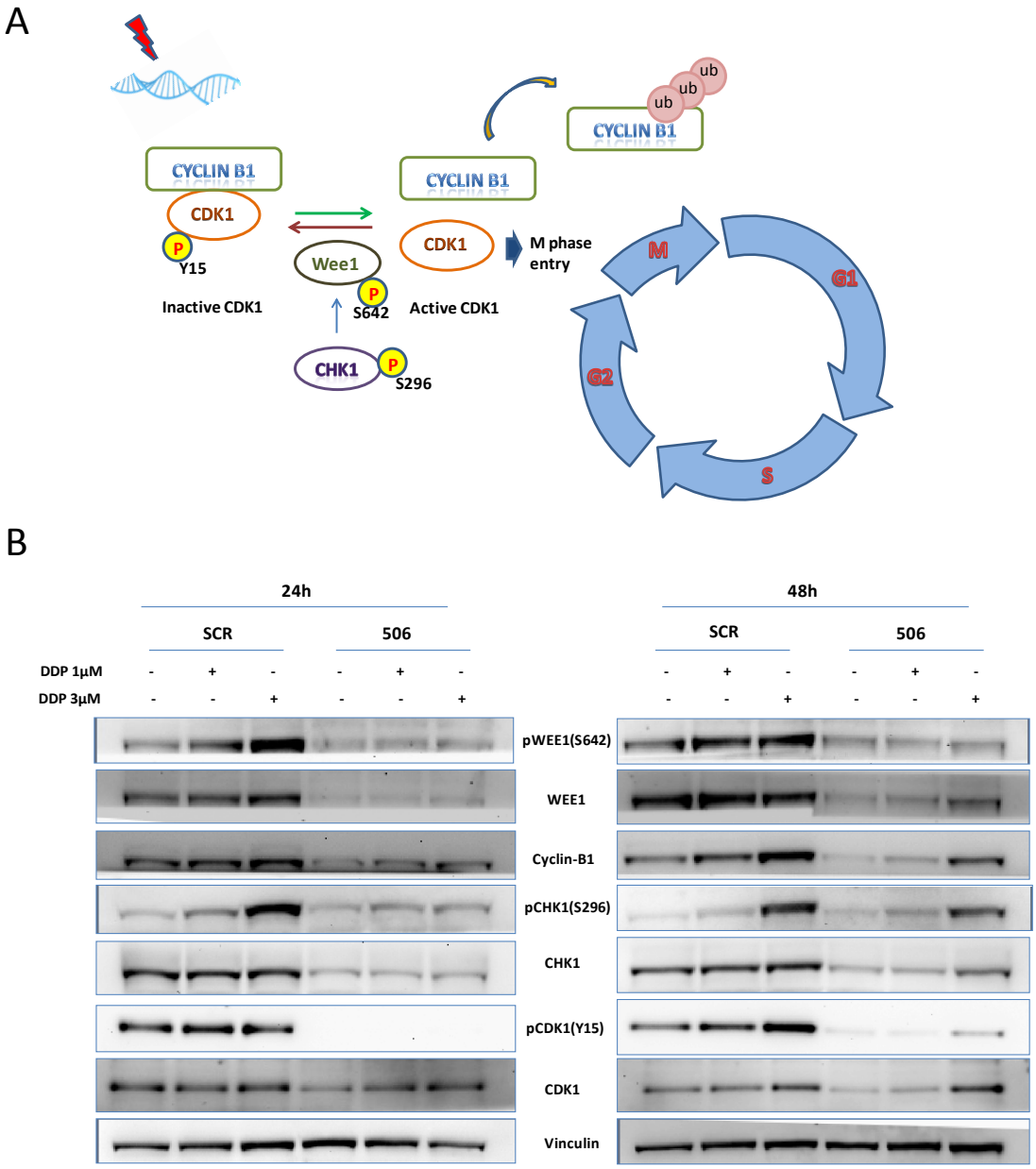

Figure 25: Abrogation of G2/M cell cycle checkpoint in miR-506 reconstituted cells

A) Schematic illustration of the main molecular actors involved in G2/M checkpoint activation. Upon DNA damage, Cyclin-B1-CDK1 complex is activated leading to activation of G2 checkpoint in order to block cell cycle before to give time to cells for repair their damage before enter in mitosis (M). Among key events, CDK1 is phosphorylated in its inhibitory phosphorylation site (Y15) mediated by Chk1 and Wee1 kinases. On the contrary, when Cyclin-B1 is degraded by ubiquitination (ub) and CDK1 dephosphorylated, the Cyclin-B1-CDK1 complex is inactive and cells enter into M phase of the cell cycle. B) SKOV3 cells were transfected with miR-506 (506) or scr-miR (scr) and treated or not with 1 and 3 µM of platinum (DDP) for 24 and 48 hours, time points at which lysates were collected and western blot analysis was performed. Images are representatives of at least three experiments. Vinculin was used as loading control.

4.15 RAD17 is synthetically lethal with Chk1 and Wee1 inhibitors in EOC models *in vitro*

In recent years many efforts are being made to map synthetic-lethal interactions in cancer for the design of targeted therapies in human cancers[166]. It has been shown by Shen and co-authors[81] that RAD17 loss of function was synthetically lethal with Chk1 and Wee1 Inhibitors. In light of this evidence obtained in Hela and LN428 cellular models displaying inactive p53, I wanted to verify if RAD17 suppression could reproduce the same effect in EOC model. For this purpose I silenced RAD17 expression with siRNAs in SKOV3 p53null and OAW42 p53wt cell lines and I evaluated by clonogenic assays the effects of treatment with AZD1775, an inhibitor of Wee1 and with LY2603618, an inhibitor of Chk1 at different doses. Silencing efficacy was evaluated 72h after each transfection at protein level in both cell lines. The Wee1 Inhibitor AZD1775 was significantly more toxic in RAD17 depleted cells compared to control cells in both cell lines with a drop in the IC50 of 3.5 fold for SKOV3 and 2 fold for OAW42 (Figure 26 upper panels). RAD17 silencing induced the same significant effect of enhanced toxicity also upon treatment with the Chk1 inhibitor LY2603618 in the same cell lines with a drop in the IC50 of 1.5 fold for SKOV3 and 3.5 fold for OAW42 (Figure 26 lower panels). These results suggest that depletion of RAD17 is involved in inducing synthetic lethal effect with checkpoint kinases inhibitors also in EOC model further supporting the concept that checkpoint kinases inhibitors could be most active in tumours with defects in DNA damage repair such as RAD17 loss of function.

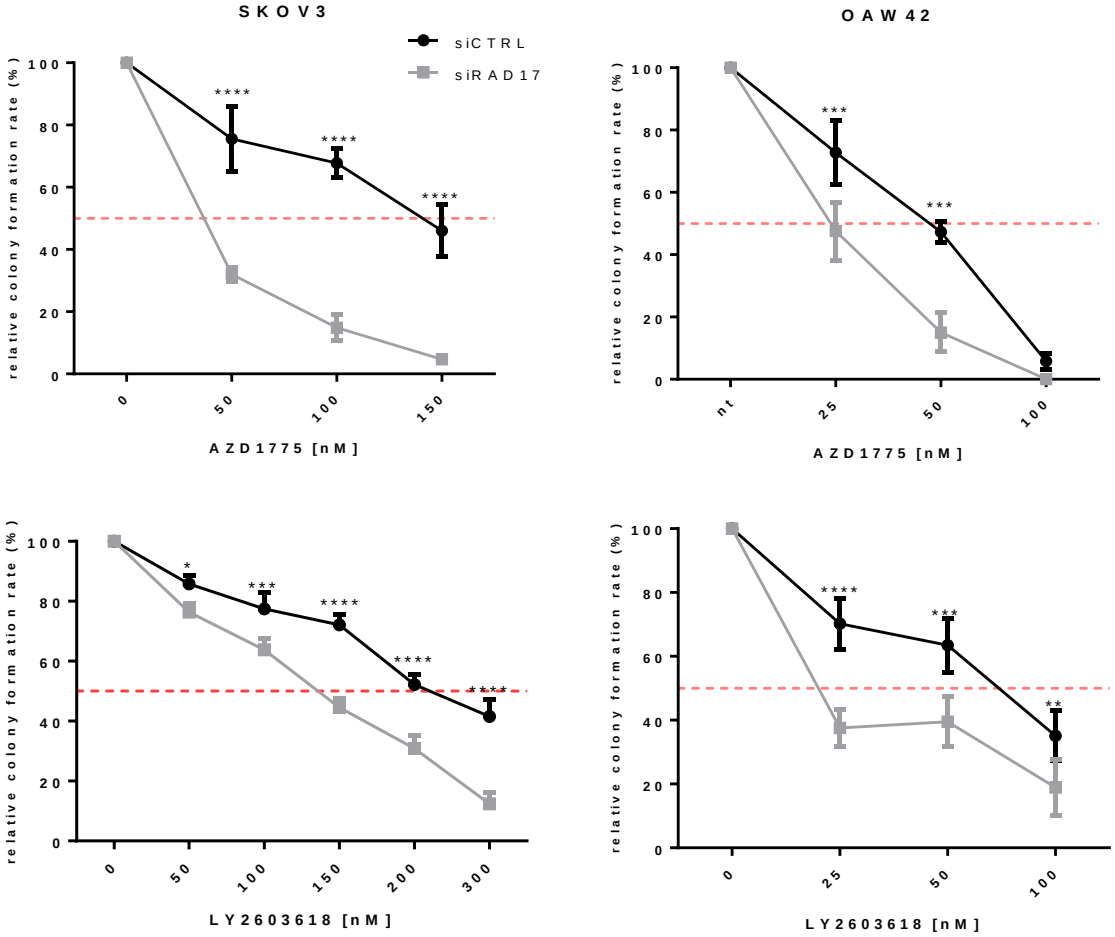

Figure 26: Synthetic lethal effect of RAD17 depletion with checkpoint kinases inhibitors
SKOV3 and OAW42 cell lines were silenced or not for RAD17 using siRNAs (siRAD17 or siCTRL) and seeded in 6 well plates for clonogenic assays. The day after transfection cells were treated with serial dilution of Wee1 inhibitor AZD1775 (upper panels) or the Chk1 inhibitor LY2603618 (lower panels) at indicated concentrations. Percentage of relative colony formation rate of siRAD17 versus siCTRL transfected and treated cells were evaluated. Colonies were counted under optical microscope. Data are mean ± SD of at least three experiments. Two way ANOVA and Bonferroni's post test was used to compare siRAD17 transfected cells versus siCTRL transfected cells (*p<0.05; ** p<0.01; ***p<0.001, ****p<0.0001).

4.16 MiR-506 reintroduction causes synthetic lethality with Chk1 and Wee1 Inhibitors resembling RAD17 silencing.

Since RAD17 silencing was able to sensitise EOC cells to Chk1 and Wee1 inhibitors, I wanted to evaluate if reintroduction of miR-506, through modulation of RAD17 expression, could reproduce the same effect of sensitiveness to these checkpoint kinases inhibitors. For this purpose SKOV3 and OAW42 cells transfected with miR-506 mimic or the miR-scramble control were treated with the Wee1 inhibitor AZD1775, or with the Chk1 inhibitor LY2603618, at different doses and the treatment effects were evaluated by clonogenic assay. MiRNA transfection efficiency was evaluated 48h after transfection by qRT-PCR in both cell lines. Interestingly upon miR-506 reconstitution I was able to obtain a significant sensitisation to both Wee1 and Chk1 inhibitors in SKOV3 cell line (Figure 27, left panels) similar to what obtained following RAD17 depletion, with drop in the IC50 of 1.6 fold for AZD1775 and 2 fold for LY2603618 compared to scr cells. MiR-506 reconstitution in OAW42 cell line was synthetically lethal with the Wee1 inhibitor, with a drop in the IC50 of 1.5 fold compared to scr transfected cells, while no significant effect was observed upon treatment with the Chk1 inhibitor (Figure 27, right panels). These results indicate that miR-506 is able to sensitise EOC cells to Chk1 and Wee1 checkpoint kinases inhibitors resembling the effects induced by RAD17 silencing. Taken together these data highlight the important role of miR-506 in regulating RAD17 expression and function, sustain a synthetic lethal approach based on RAD17 function and checkpoint kinases activity and also support the possibility of using miR-506 expression as a marker of response to checkpoint kinases inhibitors.

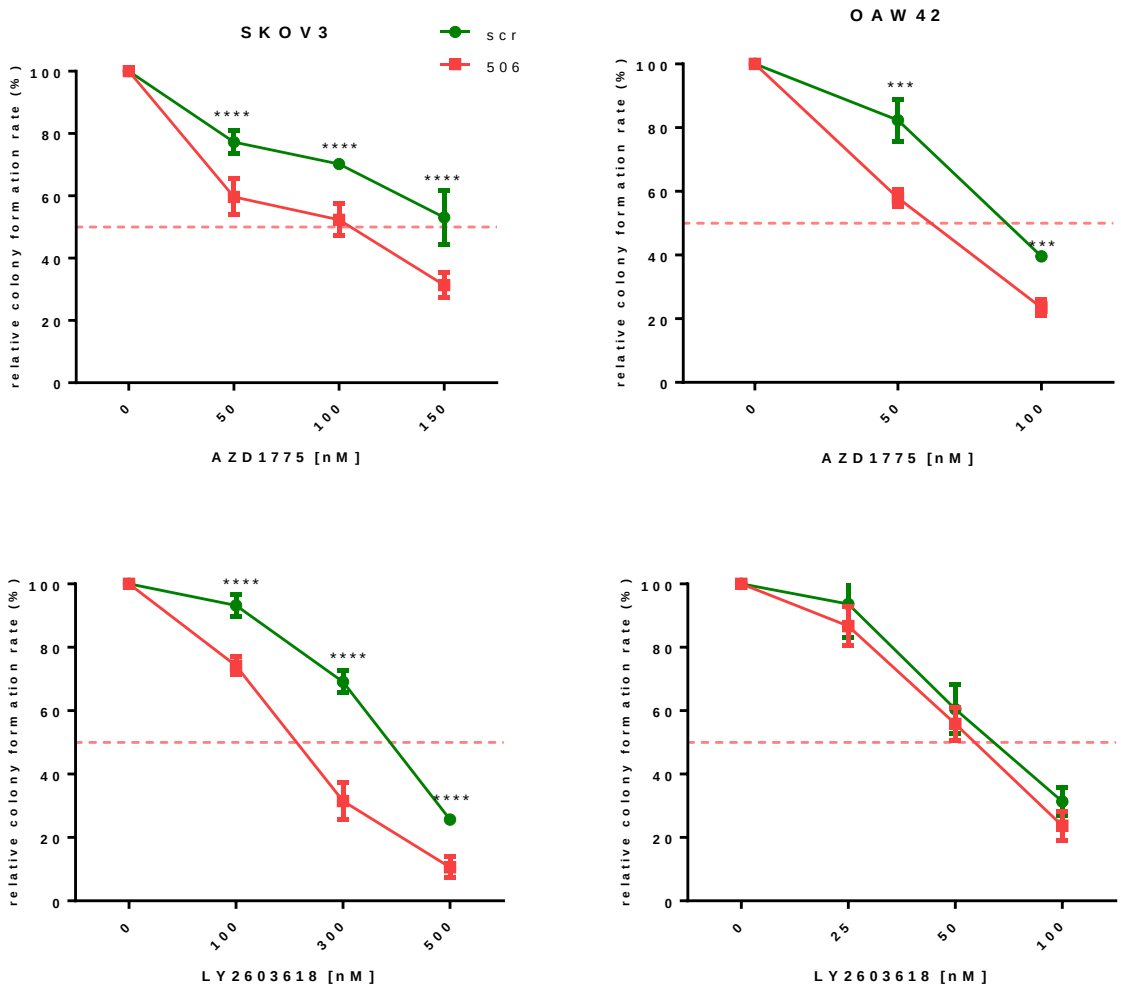

Figure 27: Synthetic lethality effects of miR-506 reconstitution with checkpoint kinases inhibitors

SKOV3 and OAW42 cell lines were ectopically reconstituted with miR-506 mimic (506) or scramble miR (scr) and seeded in 6 well plates for clonogenic assays. The day after transfection, cells were treated with serial dilution of AZD1775, the Wee1 inhibitor (upper panels), or LY2603618, the Chk1 inhibitor (lower panels), at the indicated concentrations. Percentage of relative colony formation rate of miR-506 versus scr transfected cells were evaluated. Colonies were counted under optical microscope. Data are mean ± SD of at least three experiments. Two way ANOVA and Bonferroni's post test was used to compare miR-506 transfected cells versus scr transfected cells (*p<0.05; **p<0.01; ***p<0.001, ****p<0.0001).

4.17 Combination of Chk1 or Wee1 inhibitors with platinum showed a synergistic effect in miR-506-reconstituted SKOV3 cells

Platinum represents the standard of care for EOC patients but development of platinum resistance remains a major problem in the treatment of these patients. I then wanted to evaluate whether combination treatment strategies, combining platinum and checkpoint kinases inhibitors, could sensitise platinum-resistant cells. To this end I ectopically expressed miR-506 in the platinum resistant SKOV3 cell line and then I treated cells with the inhibitor of Wee1 AZD1775, or with the inhibitor of Chk1 LY2603618, alone or in combination with 0.5 μM of platinum (DDP) corresponding to the IC50. The data indicated that the combination of platinum and AZD1775, as well as platinum and LY2603618 were substantially more effective than mono-treatments in reducing colony formation rate. The reduction on IC50 due to treatment combination was evident in scr transfected cells from 200 nM to 135 nM for AZD1775 and from 450 nM to 300 nM for LY2603618. More important when miR-506 reconstituted cells were treated with combination therapy a dramatic effect was observed with an IC50 reduction of 60% (2 fold decrease) for both AZD1775/DDP and LY2603618/DDP combinations (Figure 28, left panels). Moreover the two combination treatments induced synergistic effect in miR-506 reconstituted cells compared with scr control cells as determined by combination index (CI) analysis (Figure 28, right panels). These results suggest that DDP-AZD1775/DDP-LY2603618 combination treatments have an important effect on chemosensitisation in the setting of miR-506 expression compared to individual drugs and induced synergistic effects in miR-506 reconstituted SKOV3 resistant

cells. This could minimize drug concentrations and therefore reduce non-specific effects and general toxicity upon treatment.

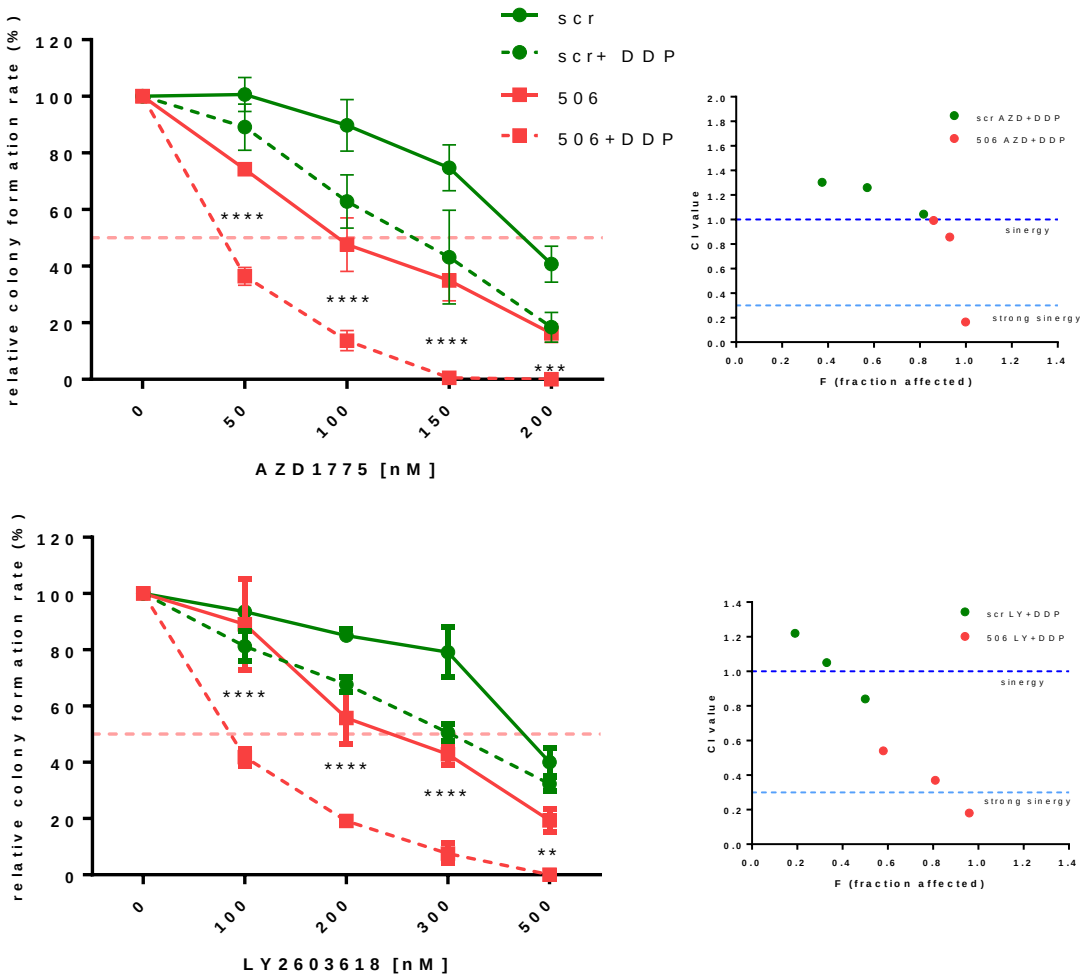

Figure 28: Inhibition on Wee1 or Chek1 in mR-506 reconstituted cells results in synergistic effect with platinum treatment.

SKOV3 cell line was treated with platinum (DDP) (held constant at 0.5 µM) and AZD1775 or LY2603618 at different concentrations as reported in the graphs. Left panels: percentage colony formation rates of miR-506 reconstituted cells treated with AZD1775 and LY2603618 alone or in combination with DDP (dashed lines). Data are mean ± SD of at least three experiments. Two way ANOVA and Bonferroni's post test was used to compare miR-506 transfected cells treated with AZD1775 or LY2603618 versus combinations with DDP (*p<0.05; **p<0.01; ***p<0.001, ****p<0.0001). Right panels: combination Index (CI) analysis was performed using the CompuSyn system. SKOV3 percentage colony formation rate were converted to growth inhibition (Fraction Affected, F) and plotted against CI. The first three doses for each checkpoint kinase inhibitor were plotted. Dotted blue lines on the graph designates a CI equal to 1 (dark blue line) and equal to 0.3 (light blue line). Combination Index indicates additivity when CI value is 1, antagonism when CI>1, synergism when CI<1 and strong synergism when CI<0.3.

5 Discussion

The general aim of this thesis was to identify and better characterize the miRNA-driven role in response to chemotherapy in EOC. EOC patients are usually diagnosed at advanced stages of the disease and often experience disease relapse with instauration of a chemotherapy resistant condition with a consequent poor prognosis[1-3]. One of the major challenges remains the identification of patients with increased risk of disease recurrence for the design of new therapeutic strategies to overcome resistance to treatment. To address these questions, genomic based approaches are needed to deeply characterize this highly heterogeneous disease at the molecular level. Molecular-driven approaches for EOC are recently becoming real therapeutic options in combination to platinum agents as in the case of the addition of the anti-angiogenic drug Bevacizumab[167] or the use of PARP inhibitors in specific molecular subsets[44, 168]. MiRNAs, small non-coding RNAs that regulate gene expression at the post-transcriptional level, represent an important layer of information that could help to explain the behaviour of EOC tumour cells in different processes including chemoresponse[124]. In recent years my laboratory analysed the miRNA expression profiles in EOC patients identifying a cluster of eight miRNAs (ChrXq27.3 cluster) found to be downregulated in high grade advanced stage early relapsing patients[144] and included in a miRNA-based predictor of early relapse[143], suggesting a role of this cluster in disease progression and chemoresponse. I decided to focus on miR-506, belonging to the cluster, the most characterised miRNA and probably the driver of the cluster. I knew by previous works of my group that miR-506 was able to sensitise EOC cells to platinum

treatment in p53wt setting supporting its role in chemoresponse and in disease relapse[144]. In this thesis I have confirmed in two new EOC case cohorts previous observations. Searching for the appropriated cellular models I found that all the EOC cell lines tested presented very low levels of miR-506 expression, a characteristic shared with cell lines of histotypes different from ovary[160-162]. The low expression of miR-506 is a common feature also in EOC patients. Indeed previous analysis of my research group of the microRNA expression profiles in independent cohorts of EOC patients including the TCGA dataset showed that miR-506 was expressed at detectable levels only in 30% of patients[143, 144]. The association of low expression of miR-506 and of the entire cluster with patients' early relapse supports its role as oncosuppressor miRNA.

MiRNAs expression can be regulated by different mechanisms such as major genomic rearrangement, epigenetic events[169-171] or transcription factor deregulations[172]. It is likely that such regulations are responsible for the low expression level I found in my cellular models and in patients. Interestingly ChrXq27.3 miRNAs cluster maps near to an X fragile site region, however no copy number variations of this region were detected in TCGA study[148], and no studies on evaluation of presence of micro-deletion such as LOH have been performed so far. The most studied aspect is epigenetic regulation. Indeed, by analyzing EOC cell lines, in the promoter region of miR-506 Yang and co-workers identified five CpG sites, regions rich in cytosine that can be highly methylated, thus silenced, therefore changing gene expression levels. Treatment with demethylating agents such as 5-aza-2'-deoxycytidine (5-Aza-dC) significantly restored miR-506 levels suggesting that

epigenetic silencing can be responsible for the low expression of miR-506 [148]. They were not able to evaluate the methylation status of the miR-506 promoter in the cohort of patients of the TCGA study due to the lack of the coverage of the ChrXq27.3 in the methylome platform used. However, by pyrosequencing analysis performed on an independent cohort of patients they identified a negative correlation between methylation and miR-506 expression although it was not statistically significant. Similar results were obtained by Li j and collaborators in the context of pancreatic cancer further indicating that DNA methylation contributes to miR-506 gene silencing[153]. Moreover binding sites of putative transcriptional factors have been identified in the promoter region of miR-506 family. In breast and lung cancer, a crosstalk between NF-kB and p53 was shown to regulate miR-506 expression. However, the final effect (inhibitory or promoting) was dependent on the tumour type[173 174]. The causes of miR-506 deregulation in EOC have to be yet investigated. Indeed, given the peculiar way of growth and dissemination of EOC and the well known bidirectional communication between cancer cells and the tumour microenvironment[175], it cannot be excluded also that paracrine signal from tumour microenvironment could play a role in regulation of miR-506 expression[176]. The improving in generation of organotypic tridimentional culture system that mimic the *in vivo* situation could help in elucidating the mechanisms responsible for miR-506 deregulation that need to be further investigated.

Once defined that I could only rely on cellular models allowing gain of function experiments, I explored and confirmed the ability of miR-506 to re-sensitise to platinum treatment EOC cells with p53 mutational status. To investigate the role of

miR-506 in chemotherapy response and identify miR-506 target genes potentially involved in this process, I performed an *in silico* identification of putative miR-506 target genes and related functions, using publicly available softwares. Besides genes involved in EMT such as SNAI2, VIM and N-CADH[145, 148], I identified genes regulating DNA repair pathway such as *RAD51*, involved in homologous recombination repair, and *RAD17* an early sensor of DNA damage. The mechanism of miR-506-RAD51 has already been explored[147] while no data are available concerning *RAD17* in EOC. I therefore concentrated on this miR-506-RAD17 regulatory axis, supposing its involvement in EOC response to therapy. After confirming that *RAD17* was a direct target of miR-506, I showed that the platinum sensitisation induced by miR-506 expression was related to RAD17 regulation. Indeed by performing *RAD17* target protector experiments, I demonstrated that the miR-506 induced sensitisation to platinum treatment was directly depending on the possibility of miR-506 to regulate RAD17 expression. The effect, indeed, was lost when targeting of miR-506 was impaired by the target protection sequence. Moreover, being an early event in DDR and therefore acting upstream of many DDR molecules RAD17 could orchestrate the entire response. Importantly, I found RAD17 to be anti-correlated with miR-506 expression in EOC patients, validating my *in vitro* results. As expected RAD17 expression was associated with poor prognosis when I interrogated online available datasets suggesting its prognostic role and clinical relevance in EOC. Strongly in accordance with my finding, miR-506 expression was associated with EOC good prognosis[147, 148].

DDR dependency in cancer is currently being exploited to generate new cancer therapeutic strategies. Recent findings demonstrated that PARP inhibitors, which act in the BER pathway by inhibiting PARP activity to sense and repair ssDNA breaks, which in turn can lead to dsDNA breaks[177], are particularly effective in patients harbouring *BRCA1/2* mutations. Indeed these patients display defects in HRR, a mechanism required for dsDNA repair. The contemporaneous blocking of both repair pathways lead to cell death by synthetic lethality. The use of PARP inhibitors represents one of the best examples of synthetic lethal approach in cancer for the management of significant subset of tumours including EOC[57-59]. It has to be taken into consideration that HRR deficiency has been observed also in EOC patients with loss of function of genes other than *BRCA1/2* such as *RAD51*, *ATM*, *ATR*[178, 179]. These patients display a 'BRCAness' phenotype, characterised by the ability to respond to multiple platinum treatments, similar to that of *BRCA1/2* mutated patients. Given the complexity of the DDR pathway and the crosstalk between the different DNA repair components involved in such pathway, it is likely that a single biomarker may not be sufficient to predict the benefit of PARP inhibitor therapies[44]. In this thesis I demonstrated that also miR-506-RAD17 axis was able to sensitise EOC cells to the PARP inhibitor olaparib. The involvement of RAD17 in inducing sensitisation to PARP inhibitors could be explained by recent findings on the new role proposed for RAD17 as necessary for activation of the ATM signalling pathway[71], which promote HRR. Accordingly I found that miR-506 expression was able to impair ATM activation similar to RAD17 silencing. Thus miR-506, impairing HRR by acting on both RAD17 and RAD51, could represent a possible new biomarker for the selection of patients

that can benefit from PARP inhibitors treatment. Indeed it would be very interesting to evaluate the expression of miR-506 in *BRCA1/2* proficient EOC patients responding to PARP inhibitors. Accordingly also the loss of function of RAD17 could confer a BRCAness phenotype and therefore being considered a useful biomarker.

The RAD17 mediated activation of MRN/ATM signalling cascade has been recently shown to contribute in maintaining genomic integrity[71] and its depletion has been associated with genome instability in head and neck cancer[73] and associated with DNA fragmentation and mitotic catastrophe[180] in gemcitabine treated pancreatic cancer cells[80, 165]. In my cellular model I observed that sensitisation to platinum treatments induced by miR-506 expression was associated with aberrant mitotic figures and micronuclei formation resulting from asyncronous chromosomes segregation, which are correlated with mitotic catastrophe[180]. The actual contribution of miR-506 in this phenomenon is currently under investigation. I also found that miR-506 reintroduction caused an impairment and overall attenuation of DDR signalling in EOC cells following platinum treatment. This reduction could be due to a decreased RAD17 expression that in turn causes a delay in the recruitment of DDR proteins at damaged sites. I hypothesized that miR-506 expression, by regulating different molecules of the DDR involved in the correct propagation of the signal upon DNA damage, could deceive the tumour cell reducing its ability to properly sense the damage entity. Then, the cells would go ahead into the cycle in spite of their accumulating damages and will be finally committed to death. Indeed I demonstrated that miR-506 expression induced impairment in G2/M checkpoint activation with reduced accumulation of cells in G2 phase of the cell cycle following

platinum treatment by impairing the signalling pathway at the basis of the G2/M block. However the effects on G2 block was transitory, sustaining the hypothesis of a delay in activation of DNA repair mechanisms that may contribute to an increase of genomic instability with a subsequent sensitisation to DNA damaging drugs.

The central role of RAD17 in DDR is highlighted also by recent studies on networks of synthetic-lethal interactions that identified RAD17 knockdown to be synthetically lethal with different tumour suppressor and druggable genes[81, 166]. In this thesis I demonstrated that RAD17 silencing, besides being synthetically lethal with PARP inhibitors, exerted the same effects with Chk1 and Wee1 Checkpoint kinases inhibitors and, accordingly, miR-506 expression induced the same synthetic lethal effect. As expected the synthetic lethality observed in the context of p53null cell line was more efficient than in a p53wt context[181]. This could be explained by the fact that cancer cells which retain p53 function can activate a series of mechanisms in response to DNA damage insults, like cell cycle arrest in G1 phase. p53 mutated cells loose this ability therefore targeting G2/M checkpoint in p53 mutated setting can be a valid therapeutic alternative strategy particularly in HGSOCs patients which display a near universal p53 aberration. The two checkpoint kinases inhibitors that I used in this thesis are selective for the proteins they targets with reduced possibility of off-target effects. This characteristic makes these drugs particularly attractive for cancer therapy. In particular the Wee1 inhibitor is currently in clinical development in combination with chemotherapy in patients with platinum-resistant EOC (NCT02272790).

Of note I identified also *WEE1* and *CHEK1* among the putative miR-506 predicted target genes. Therefore, it cannot be exclude that the miR-506 induced sensitivity to Chk1 and Wee1 checkpoint kinases inhibitors could be a results of the combinatorial effect of miR-506 targeting on different molecules that regulate DNA damage repair pathway at different levels. All together these findings suggest miR-506 to be a key node in the regulation of DDR in response to drug treatments.

Reduce the general toxicity and over treatment of EOC patients still remain a problem. I demonstrated that the combination treatment of platinum with Chk1 and Wee1 checkpoint kinases inhibitors resulted to be more effective than mono treatments in EOC cells and synergistic in the context of miR-506 expression. This combinatorial effect may potentiate drug clinical efficacy with the consequent reduction in general toxicity[182, 183].

MiR-506 pleiotropic effects on DDR pathway need to be better clarified and lay the ground to future studies aimed to identify all the possible synthetic lethal pairs that can be therapeutically targeted.

6 Conclusions and Future perspectives

The work presented in this thesis highlighted the importance of miR-506 as a chemosensitizing miRNA in EOC acting as a key node in the regulation of DNA damage response pathway. The identification of a new miR-506-RAD17 axis could represent a new biomarker to be proposed as selection criteria for patients susceptible to DNA damaging drugs in combination with different new small molecules that target DDR.

Since I have observed that expression of miR-506 in platinum treated cells caused mitotic defects and micronuclei appearance, the occurrence of mitotic cell death by mitotic catastrophe, as final outcome, remain to be assessed. Time lapse microscopy analysis (live imaging) on EOC cells will be performed in order to monitor cell division and cell fate in the setting of miR-506 expression and drug treatment.

To assess the important role of the miR-506-RAD17 axis in EOC, the effects of its modulation will be assessed in additional cell lines representative of high grade serous ovarian cancer and in patients' derived cells as more appropriated model.

Since its pleiotropic role in modulating different molecules of the DDR pathway, I will better define the miR-506-driven molecular mechanisms related to sensitisation to drug treatments on different target genes. In particular the assessment of the direct targeting of miR-506 on WEE1 and CHEK1 by luciferase assay will be tested.

RAD17 expression at protein level will be assessed by IHC analysis in EOC tissues from datasets already profiled for miRNA expression in order to correlate miR-506 and RAD17 expression

List of publications during PhD

Bagnoli M, Granata A, **Nicoletti R**, Krishnamachary B, Bhujwalla ZM, Canese R, Podo F, Canevari S, Iorio E, Mezzanzanica D. Choline Metabolism Alteration: A Focus on Ovarian Cancer Front Oncol. 2016 Jun 22

- Cocco E, Shapiro EM, Gasparrini S, Lopez S, Schwab CL, Bellone S, Bortolomai I, Sumi NJ, Bonazzoli E, **Nicoletti R**, Deng Y, Saltzman WM, Zeiss CJ, Centritto F, Black JD, Silasi DA, Ratner E, Azodi M, Rutherford TJ, Schwartz PE, Pecorelli S, Santin AD. Clostridium Perfringens Enterotoxin C-terminal domain labeled to fluorescent Dyes for in vivo visualization of micro-metastatic chemotherapy-resistant ovarian cancer. Int J Cancer. 2015 Jun 9.

- Granata A**, Nicoletti R**, Perego P, Iorio E, Krishnamachary B, Benigni F, Ricci A, Podo F, Bhujwalla ZM, Canevari S, Bagnoli M and Mezzanzanica D. Global metabolic profile identifies choline kinase alpha as a key regulator of glutathione-dependent antioxidant cell defense in ovarian carcinoma. Oncotarget. 2015 Mar 14.

- **Nicoletti R**, Lopez S, Bellone S, Cocco E, Schwab CL, Black JD, Centritto F, Zhu L, Bonazzoli E, Buza N, Hui P, Mezzanzanica D, Canevari S, Schwartz PE, Rutherford TJ, Santin AD. T-DM1, a novel antibody-drug conjugate, is highly effective against uterine and ovarian carcinosarcomas overexpressing HER2. Clin Exp Metastasis. 2015 Jan.

- Schwab CL, Bellone S, English DP, Roque DM, Lopez S, Cocco E, **Nicoletti R**, Bortolomai I, Ratner E, Silasi DA, Azodi M, Schwartz PE, Rutherford TJ, Santin AD. Afatinib demonstrates remarkable activity against HER2-amplified uterine serous endometrial cancer in vitro and in vivo. Br J Cancer. 2014 Oct 28

- Schwab CL, English DP, Roque DM, Bellone S, Lopez S, Cocco E, **Nicoletti R**, Rutherford TJ, Schwartz PE, Santin AD. Neratinib shows efficacy in the treatment of HER2/neu amplified uterine serous carcinoma in vitro and in vivo. Gynecol Oncol. 2014 Oct

Acknowledgements

I would like to express my deepest appreciation to all who have provided me the support and invaluable guidance through the years of this PhD program. A special gratitude I give particularly to my Director of Study, Dr. Delia Mezzanzanica, for all the advice and constant financial support in my scientific work. She has been a very good advisor who brings out the optimism in me. My most sincere thanks to my supervisor Dr Marina Bagnoli and Prof Iain McNeish for their support and guidance while carrying out my work.

I thank my old and new fellow labmates, in particular Barbara, Katia, Francesca, Anna, Alessandro and Francesco for their support and for all the fun we have had in the last years. I would like to thanks to my friends, near and far, who have supported me throughout the process.

Last, but definitely not the least, a big thank you to my family: my parents and my sister for supporting me spiritually throughout these years and my life in general. A huge thank you goes to my boyfriend. He supported me with love and patience and helped me to keep things in perspective. I deeply appreciate his belief in me. I dedicate this thesis to him.

Bibliography

References

1. Jayson, G. C., Kohn, E. C., Kitchener, H. C. & Ledermann, J. A. Ovarian cancer *Lancet* **384**, 1376-1388 (2014).

2. Siegel, R. L., Miller, K. D. & Jemal, A. Cancer Statistics, 2017 *CA Cancer. J. Clin.* **67**, 7-30 (2017).

3. Buys, S. S. *et al*. Effect of screening on ovarian cancer mortality: the Prostate, Lung, Colorectal and Ovarian (PLCO) Cancer Screening Randomized Controlled Trial *JAMA* **305**, 2295-2303 (2011).

4. Markman, M. & Bookman, M. A. Second-line treatment of ovarian cancer *Oncologist* **5**, 26-35 (2000).

5. Chen, V. W. *et al*. Pathology and classification of ovarian tumors *Cancer* **97**, 2631-2642 (2003).

6. Ledermann, J. A. *et al*. Newly diagnosed and relapsed epithelial ovarian carcinoma: ESMO Clinical Practice Guidelines for diagnosis, treatment and follow-up *Ann. Oncol.* **24 Suppl 6**, vi24-32 (2013).

7. Nik, N. N., Vang, R., Shih, I. & Kurman, R. J. Origin and pathogenesis of pelvic (ovarian, tubal, and primary peritoneal) serous carcinoma *Annu. Rev. Pathol.* **9**, 27-45 (2014).

8. Shih, I. & Kurman, R. J. Ovarian tumorigenesis: a proposed model based on morphological and molecular genetic analysis *Am. J. Pathol.* **164**, 1511-1518 (2004).

9. Kurman, R. J. & Shih, I. Molecular pathogenesis and extraovarian origin of epithelial ovarian cancer--shifting the paradigm *Hum. Pathol.* **42**, 918-931 (2011).

10. Tothill, R. W. *et al*. Novel molecular subtypes of serous and endometrioid ovarian cancer linked to clinical outcome *Clin. Cancer Res.* **14**, 5198-5208 (2008).

11. Kurman, R. J. & Shih, I. The Dualistic Model of Ovarian Carcinogenesis: Revisited, Revised, and Expanded *Am. J. Pathol.* **186**, 733-747 (2016).

12. Cancer Genome Atlas Research Network. Integrated genomic analyses of ovarian carcinoma *Nature* **474**, 609-615 (2011).

13. Ahmed, A. A. *et al*. Driver mutations in TP53 are ubiquitous in high grade serous carcinoma of the ovary *J. Pathol.* **221**, 49-56 (2010).

14. Karst, A. M. & Drapkin, R. Ovarian cancer pathogenesis: a model in evolution *J. Oncol.* **2010**, 932371 (2010).

15. Labidi-Galy, S. I. *et al*. High grade serous ovarian carcinomas originate in the fallopian tube *Nat. Commun.* **8**, 1093-017-00962-1 (2017).

16. Hao, D. *et al*. Integrated Analysis Reveals Tubal- and Ovarian-Originated Serous Ovarian Cancer and Predicts Differential Therapeutic Responses *Clin. Cancer Res.* **23**, 7400-7411 (2017).

17. Ayhan, A. *et al*. Defining the cut point between low-grade and high-grade ovarian serous carcinomas: a clinicopathologic and molecular genetic analysis *Am. J. Surg. Pathol.* **33**, 1220-1224 (2009).

18. Vaughan, S. *et al*. Rethinking ovarian cancer: recommendations for improving outcomes *Nat. Rev. Cancer.* **11**, 719-725 (2011).

19. Kobel, M., Huntsman, D. & Gilks, C. B. Critical molecular abnormalities in high-grade serous carcinoma of the ovary *Expert Rev. Mol. Med.* **10**, e22 (2008).

20. du Bois, A. *et al*. Role of surgical outcome as prognostic factor in advanced epithelial ovarian cancer: A combined exploratory analysis of 3 prospectively randomized phase 3 multicenter trials. *Cancer* **115**, 1234-1244 (2009).

21. Kelland, L. R. *et al*. Preclinical antitumor evaluation of bis-acetato-ammine-dichloro-cyclohexylamine platinum(IV): an orally active platinum drug *Cancer Res.* **53**, 2581-2586 (1993).

22. Cohen, S. M. & Lippard, S. J. Cisplatin: from DNA damage to cancer chemotherapy *Prog. Nucleic Acid Res. Mol. Biol.* **67**, 93-130 (2001).

23. Bellon, S. F., Coleman, J. H. & Lippard, S. J. DNA unwinding produced by site-specific intrastrand cross-links of the antitumor drug cis-diamminedichloroplatinum(II) *Biochemistry* **30**, 8026-8035 (1991).

24. Shuck, S. C., Short, E. A. & Turchi, J. J. Eukaryotic nucleotide excision repair: from understanding mechanisms to influencing biology *Cell Res.* **18**, 64-72 (2008).

25. Vaisman, A. *et al*. The role of hMLH1, hMSH3, and hMSH6 defects in cisplatin and oxaliplatin resistance: correlation with replicative bypass of platinum-DNA adducts *Cancer Res.* **58**, 3579-3585 (1998).

26. Jackson, S. P. & Bartek, J. The DNA-damage response in human biology and disease *Nature* **461**, 1071-1078 (2009).

27. Galluzzi, L. *et al*. Molecular mechanisms of cisplatin resistance. *Oncogene* **31**, 1869 (2011).

28. Dabholkar, M. *et al*. ERCC1 and ERCC2 expression in malignant tissues from ovarian cancer patients *J. Natl. Cancer Inst.* **84**, 1512-1517 (1992).

29. Weberpals, J. *et al*. The DNA repair proteins BRCA1 and ERCC1 as predictive markers in sporadic ovarian cancer *Int. J. Cancer* **124**, 806-815 (2009).

30. Aebi, S. *et al*. Loss of DNA mismatch repair in acquired resistance to cisplatin *Cancer Res.* **56**, 3087-3090 (1996).

31. Brown, R. *et al*. hMLH1 expression and cellular responses of ovarian tumour cells to treatment with cytotoxic anticancer agents *Oncogene* **15**, 45-52 (1997).

32. Drummond, J. T., Anthoney, A., Brown, R. & Modrich, P. Cisplatin and adriamycin resistance are associated with MutLalpha and mismatch repair deficiency in an ovarian tumor cell line *J. Biol. Chem.* **271**, 19645-19648 (1996).

33. Gifford, G., Paul, J., Vasey, P. A., Kaye, S. B. & Brown, R. The acquisition of hMLH1 methylation in plasma DNA after chemotherapy predicts poor survival for ovarian cancer patients *Clin. Cancer Res.* **10**, 4420-4426 (2004).

34. Alsop, K. *et al*. BRCA Mutation Frequency and Patterns of Treatment Response in BRCA Mutation–Positive Women With Ovarian Cancer: A Report From the Australian Ovarian Cancer Study Group. *JCO* **30**, 2654-2663 (2012).

35. Yang, D. *et al*. Association of BRCA1 and BRCA2 mutations with survival, chemotherapy sensitivity, and gene mutator phenotype in patients with ovarian cancer *JAMA* **306**, 1557-1565 (2011).

36. Edwards, S. L. *et al*. Resistance to therapy caused by intragenic deletion in BRCA2 *Nature* **451**, 1111-1115 (2008).

37. Dhillon, K. K., Swisher, E. M. & Taniguchi, T. Secondary mutations of BRCA1/2 and drug resistance *Cancer. Sci.* **102**, 663-669 (2011).

38. Sakai, W. *et al*. Secondary mutations as a mechanism of cisplatin resistance in BRCA2-mutated cancers *Nature* **451**, 1116-1120 (2008).

39. Holzer, A. K. & Howell, S. B. The internalization and degradation of human copper transporter 1 following cisplatin exposure *Cancer Res.* **66**, 10944-10952 (2006).

40. Kilari, D., Guancial, E. & Kim, E. S. Role of copper transporters in platinum resistance *World J. Clin. Oncol.* **7**, 106-113 (2016).

41. Samimi, G. *et al*. Increased expression of the copper efflux transporter ATP7A mediates resistance to cisplatin, carboplatin, and oxaliplatin in ovarian cancer cells *Clin. Cancer Res.* **10**, 4661-4669 (2004).

42. Safaei, R. *et al*. Cross-resistance to cisplatin in cells with acquired resistance to copper *Cancer Chemother. Pharmacol.* **53**, 239-246 (2004).

43. Patch, A. M. *et al*. Whole-genome characterization of chemoresistant ovarian cancer *Nature* **521**, 489-494 (2015).

44. Mirza, M. R. *et al*. Niraparib Maintenance Therapy in Platinum-Sensitive, Recurrent Ovarian Cancer *N. Engl. J. Med.* **375**, 2154-2164 (2016).

45. Ledermann, J. *et al*. Olaparib maintenance therapy in patients with platinum-sensitive relapsed serous ovarian cancer: a preplanned retrospective analysis of outcomes by *BRCA* status in a randomised phase 2 trial. *The Lancet Oncology* **15**, 852-861.

46. Swisher, E. M. *et al*. Rucaparib in relapsed, platinum-sensitive high-grade ovarian carcinoma (ARIEL2 Part 1): an international, multicentre, open-label, phase 2 trial *Lancet Oncol.* **18**, 75-87 (2017).

47. Coleman, R. L. *et al*. Rucaparib maintenance treatment for recurrent ovarian carcinoma after response to platinum therapy (ARIEL3): a randomised, double-blind, placebo-controlled, phase 3 trial. *The Lancet* **390**, 1949-1961.

48. Lord, C. J. & Ashworth, A. BRCAness revisited *Nat. Rev. Cancer.* **16**, 110-120 (2016).

49. Turner, N., Tutt, A. & Ashworth, A. Hallmarks of 'BRCAness' in sporadic cancers *Nat. Rev. Cancer.* **4**, 814-819 (2004).

50. Walsh, T. *et al*. Mutations in 12 genes for inherited ovarian, fallopian tube, and peritoneal carcinoma identified by massively parallel sequencing *Proc. Natl. Acad. Sci. U. S. A.* **108**, 18032-18037 (2011).

51. Tung, N. *et al*. Counselling framework for moderate-penetrance cancer-susceptibility mutations *Nat. Rev. Clin. Oncol.* **13**, 581-588 (2016).

52. Carmeliet, P. & Jain, R. K. Principles and mechanisms of vessel normalization for cancer and other angiogenic diseases *Nat. Rev. Drug Discov.* **10**, 417-427 (2011).

53. Jain, R. K. Normalizing tumor microenvironment to treat cancer: bench to bedside to biomarkers *J. Clin. Oncol.* **31**, 2205-2218 (2013).

54. Kasparek, T. R. & Humphrey, T. C. DNA double-strand break repair pathways, chromosomal rearrangements and cancer *Semin. Cell Dev. Biol.* **22**, 886-897 (2011).

55. Ciccia, A. & Elledge, S. J. The DNA damage response: making it safe to play with knives *Mol. Cell* **40**, 179-204 (2010).

56. Polo, S. E. & Jackson, S. P. Dynamics of DNA damage response proteins at DNA breaks: a focus on protein modifications *Genes Dev.* **25**, 409-433 (2011).

57. Uziel, T. *et al*. Requirement of the MRN complex for ATM activation by DNA damage *EMBO J.* **22**, 5612-5621 (2003).

58. Flynn, R. L. & Zou, L. ATR: a master conductor of cellular responses to DNA replication stress *Trends Biochem. Sci.* **36**, 133-140 (2011).

59. Chapman, J. R., Taylor, M. R. & Boulton, S. J. Playing the end game: DNA double-strand break repair pathway choice *Mol. Cell* **47**, 497-510 (2012).

60. Schwartz, G. K. & Shah, M. A. Targeting the cell cycle: a new approach to cancer therapy *J. Clin. Oncol.* **23**, 9408-9421 (2005).

61. Bartek, J. & Lukas, J. Mammalian G1- and S-phase checkpoints in response to DNA damage *Curr. Opin. Cell Biol.* **13**, 738-747 (2001).

62. Smits, V. A. & Medema, R. H. Checking out the G(2)/M transition *Biochim. Biophys. Acta* **1519**, 1-12 (2001).

63. Ishikawa, K., Ishii, H. & Saito, T. DNA damage-dependent cell cycle checkpoints and genomic stability *DNA Cell Biol.* **25**, 406-411 (2006).

64. Lin, A. B., McNeely, S. C. & Beckmann, R. P. Achieving Precision Death with Cell-Cycle Inhibitors that Target DNA Replication and Repair *Clin. Cancer Res.* **23**, 3232-3240 (2017).

65. Benada, J. & Macurek, L. Targeting the Checkpoint to Kill Cancer Cells *Biomolecules* **5**, 1912-1937 (2015).

66. von Deimling, F. *et al*. Human and mouse RAD17 genes: identification, localization, genomic structure and histological expression pattern in normal testis and seminoma *Hum. Genet.* **105**, 17-27 (1999).

67. Bluyssen, H. A. *et al*. Human and mouse homologs of the Schizosaccharomyces pombe rad17+ cell cycle checkpoint control gene *Genomics* **55**, 219-228 (1999).

68. Zou, L., Cortez, D. & Elledge, S. J. Regulation of ATR substrate selection by Rad17-dependent loading of Rad9 complexes onto chromatin *Genes Dev.* **16**, 198-208 (2002).

69. Navadgi-Patil, V. M. & Burgers, P. M. A tale of two tails: activation of DNA damage checkpoint kinase Mec1/ATR by the 9-1-1 clamp and by Dpb11/TopBP1 *DNA Repair (Amst)* **8**, 996-1003 (2009).

70. Mohni, K. N., Smith, S., Dee, A. R., Schumacher, A. J. & Weller, S. K. Herpes simplex virus type 1 single strand DNA binding protein and helicase/primase complex disable cellular ATR signaling *PLoS Pathog.* **9**, e1003652 (2013).

71. Wang, Q. *et al*. Rad17 recruits the MRE11-RAD50-NBS1 complex to regulate the cellular response to DNA double-strand breaks *EMBO J.* **33**, 862-877 (2014).

72. Paull, T. T. & Lee, J. H. Rad17, the clamp loader that loads more than clamps *EMBO J.* **33**, 783-785 (2014).

73. Zhao, M., Begum, S., Ha, P. K., Westra, W. & Califano, J. Downregulation of RAD17 in head and neck cancer *Head Neck* **30**, 35-42 (2008).

74. Bao, S. *et al*. ATR/ATM-mediated phosphorylation of human Rad17 is required for genotoxic stress responses *Nature* **411**, 969-974 (2001).

75. Kataoka, A. *et al*. Overexpression of HRad17 mRNA in human breast cancer: correlation with lymph node metastasis *Clin. Cancer Res.* **7**, 2815-2820 (2001).

76. Sasaki, H. *et al*. Overexpression of Hrad17 gene in non-small cell lung cancers correlated with lymph node metastasis *Lung Cancer* **34**, 47-52 (2001).

77. Zhang, S. *et al*. Clinically relevant microRNAs in ovarian cancer *Mol. Cancer. Res.* **13**, 393-401 (2015).

78. Johannsdottir, H. K. *et al*. Chromosome 5 imbalance mapping in breast tumors from BRCA1 and BRCA2 mutation carriers and sporadic breast tumors *Int. J. Cancer* **119**, 1052-1060 (2006).

79. Peng, H. Q., Liu, L., Goss, P. E., Bailey, D. & Hogg, D. Chromosomal deletions occur in restricted regions of 5q in testicular germ cell cancer *Oncogene* **18**, 3277-3283 (1999).

80. Fredebohm, J., Wolf, J., Hoheisel, J. D. & Boettcher, M. Depletion of RAD17 sensitizes pancreatic cancer cells to gemcitabine *J. Cell. Sci.* **126**, 3380-3389 (2013).

81. Shen, J. P. *et al*. Chemogenetic profiling identifies RAD17 as synthetically lethal with checkpoint kinase inhibition *Oncotarget* **6**, 35755-35769 (2015).

82. Hanahan, D. & Weinberg, R. A. Hallmarks of cancer: the next generation *Cell* **144**, 646-674 (2011).

83. Curtin, N. J. DNA repair dysregulation from cancer driver to therapeutic target *Nat. Rev. Cancer.* **12**, 801-817 (2012).

84. Kobel, M. *et al*. The biological and clinical value of p53 expression in pelvic high-grade serous carcinomas *J. Pathol.* **222**, 191-198 (2010).

85. Hosoya, N. & Miyagawa, K. Targeting DNA damage response in cancer therapy *Cancer. Sci.* **105**, 370-388 (2014).

86. Thorstenson, Y. R. *et al*. Contributions of ATM mutations to familial breast and ovarian cancer *Cancer Res.* **63**, 3325-3333 (2003).

87. Song, H. *et al*. Contribution of Germline Mutations in the RAD51B, RAD51C, and RAD51D Genes to Ovarian Cancer in the Population *J. Clin. Oncol.* **33**, 2901-2907 (2015).

88. Pearl, L. H., Schierz, A. C., Ward, S. E., Al-Lazikani, B. & Pearl, F. M. Therapeutic opportunities within the DNA damage response *Nat. Rev. Cancer.* **15**, 166-180 (2015).

89. Benada, J., Burdova, K., Lidak, T., von Morgen, P. & Macurek, L. Polo-like kinase 1 inhibits DNA damage response during mitosis *Cell. Cycle* **14**, 219-231 (2015).

90. O'Neil, N. J., Bailey, M. L. & Hieter, P. Synthetic lethality and cancer *Nat. Rev. Genet.* **18**, 613-623 (2017).

91. Konecny, G. E. & Kristeleit, R. S. PARP inhibitors for BRCA1/2-mutated and sporadic ovarian cancer: current practice and future directions *Br. J. Cancer* **115**, 1157-1173 (2016).

92. Rottenberg, S. *et al*. High sensitivity of BRCA1-deficient mammary tumors to the PARP inhibitor AZD2281 alone and in combination with platinum drugs *Proc. Natl. Acad. Sci. U. S. A.* **105**, 17079-17084 (2008).

93. Helleday, T., Petermann, E., Lundin, C., Hodgson, B. & Sharma, R. A. DNA repair pathways as targets for cancer therapy *Nat. Rev. Cancer.* **8**, 193-204 (2008).

94. Morales, J. *et al*. Review of poly (ADP-ribose) polymerase (PARP) mechanisms of action and rationale for targeting in cancer and other diseases *Crit. Rev. Eukaryot. Gene Expr.* **24**, 15-28 (2014).

95. Fong, P. C. *et al*. Inhibition of poly(ADP-ribose) polymerase in tumors from BRCA mutation carriers *N. Engl. J. Med.* **361**, 123-134 (2009).

96. Banerjee, S. & Kaye, S. B. New strategies in the treatment of ovarian cancer: current clinical perspectives and future potential *Clin. Cancer Res.* **19**, 961-968 (2013).

97. http://www.ema.europa.eu/ema/index.jsp?curl=pages/news_and_events/news/2014/10/news_detail_002196.jsp&mid=WC0b01ac058004d5c1.

98. Pignata S et al. Carboplatin plus paclitaxel versus carboplatin plus pegylated liposomal doxorubicin as first-line treatment for patients with ovarian cancer: the MITO-2 randomized phase III trial. J Clin Oncol. 29(27):3628-35 (2011)

99. Audeh, M. W. *et al*. Oral poly(ADP-ribose) polymerase inhibitor olaparib in patients with BRCA1 or BRCA2 mutations and recurrent ovarian cancer: a proof-of-concept trial *Lancet* **376**, 245-251 (2010).

100. Wiggans, A. J., Cass, G. K., Bryant, A., Lawrie, T. A. & Morrison, J. Poly(ADP-ribose) polymerase (PARP) inhibitors for the treatment of ovarian cancer *Cochrane Database Syst. Rev.* **(5):CD007929. doi**, CD007929 (2015).

101. Gelmon, K. A. *et al*. Olaparib in patients with recurrent high-grade serous or poorly differentiated ovarian carcinoma or triple-negative breast cancer: a phase 2, multicentre, open-label, non-randomised study. *The Lancet Oncology* **12**, 852-861.

102. Iglehart, J. D. & Silver, D. P. Synthetic lethality--a new direction in cancer-drug development *N. Engl. J. Med.* **361**, 189-191 (2009).

103. Macheret, M. & Halazonetis, T. D. DNA replication stress as a hallmark of cancer *Annu. Rev. Pathol.* **10**, 425-448 (2015).

104. Toledo, L. I. *et al*. ATR prohibits replication catastrophe by preventing global exhaustion of RPA *Cell* **155**, 1088-1103 (2013).

105. Petermann, E., Woodcock, M. & Helleday, T. Chk1 promotes replication fork progression by controlling replication initiation *Proc. Natl. Acad. Sci. U. S. A.* **107**, 16090-16095 (2010).

106. Beck, H. *et al*. Cyclin-dependent kinase suppression by WEE1 kinase protects the genome through control of replication initiation and nucleotide consumption *Mol. Cell. Biol.* **32**, 4226-4236 (2012).

107. O'Connor, M. J. Targeting the DNA Damage Response in Cancer *Mol. Cell* **60**, 547-560 (2015).

108. Jossé, R. *et al*. ATR Inhibitors VE-821 and VX-970 Sensitize Cancer Cells to Topoisomerase I Inhibitors by Disabling DNA Replication Initiation and Fork Elongation Responses. *Cancer Res.* **74**, 6968-6979 (2014).

109. Erice, O. *et al*. MGMT Expression Predicts PARP-Mediated Resistance to Temozolomide *Mol. Cancer. Ther.* **14**, 1236-1246 (2015).

110. Leijen, S. *et al*. Phase I/II study with ruthenium compound NAMI-A and gemcitabine in patients with non-small cell lung cancer after first line therapy. *Invest. New Drugs* **33**, 201-214 (2015).

111. Catalanotto, C., Cogoni, C. & Zardo, G. MicroRNA in Control of Gene Expression: An Overview of Nuclear Functions *Int. J. Mol. Sci.* **17**, 10.3390/ijms17101712 (2016).

112. Kim, V. N. & Nam, J. W. Genomics of microRNA *Trends Genet.* **22**, 165-173 (2006).

113. Bartel, D. P. MicroRNAs: genomics, biogenesis, mechanism, and function *Cell* **116**, 281-297 (2004).

114. Barca-Mayo, O. & Lu, Q. R. Fine-Tuning Oligodendrocyte Development by microRNAs *Front. Neurosci.* **6**, 13 (2012).

115. Croce, C. M. Causes and consequences of microRNA dysregulation in cancer *Nat. Rev. Genet.* **10**, 704-714 (2009).

116. Garzon, R., Calin, G. A. & Croce, C. M. MicroRNAs in Cancer *Annu. Rev. Med.* **60**, 167-179 (2009).

117. Lu, J. *et al*. MicroRNA expression profiles classify human cancers *Nature* **435**, 834-838 (2005).

118. Esquela-Kerscher, A. & Slack, F. J. Oncomirs - microRNAs with a role in cancer *Nat. Rev. Cancer.* **6**, 259-269 (2006).

119. Visone, R. & Croce, C. M. MiRNAs and cancer *Am. J. Pathol.* **174**, 1131-1138 (2009).

120. Calin, G. A. *et al*. Frequent deletions and down-regulation of micro- RNA genes miR15 and miR16 at 13q14 in chronic lymphocytic leukemia *Proc. Natl. Acad. Sci. U. S. A.* **99**, 15524-15529 (2002).

121. Tagawa, H. & Seto, M. A microRNA cluster as a target of genomic amplification in malignant lymphoma *Leukemia* **19**, 2013-2016 (2005).

122. Hayashita, Y. *et al*. A polycistronic microRNA cluster, miR-17-92, is overexpressed in human lung cancers and enhances cell proliferation *Cancer Res.* **65**, 9628-9632 (2005).

123. Svoronos, A. A., Engelman, D. M. & Slack, F. J. OncomiR or Tumor Suppressor? The Duplicity of MicroRNAs in Cancer *Cancer Res.* **76**, 3666-3670 (2016).

124. Mezzanzanica, D., Bagnoli, M., De Cecco, L., Valeri, B. & Canevari, S. Role of microRNAs in ovarian cancer pathogenesis and potential clinical implications *Int. J. Biochem. Cell Biol.* **42**, 1262-1272 (2010).

125. Corney, D. C. & Nikitin, A. Y. MicroRNA and ovarian cancer *Histol. Histopathol.* **23**, 1161-1169 (2008).

126. Dahiya, N. & Morin, P. J. MicroRNAs in ovarian carcinomas *Endocr. Relat. Cancer* **17**, F77-89 (2010).

127. Iorio, M. V. *et al*. MicroRNA signatures in human ovarian cancer *Cancer Res.* **67**, 8699-8707 (2007).

128. Zhang, L. *et al*. Genomic and epigenetic alterations deregulate microRNA expression in human epithelial ovarian cancer *Proc. Natl. Acad. Sci. U. S. A.* **105**, 7004-7009 (2008).

129. Vang, S. *et al*. Identification of ovarian cancer metastatic miRNAs *PLoS One* **8**, e58226 (2013).

130. Turchinovich, A., Samatov, T. R., Tonevitsky, A. G. & Burwinkel, B. Circulating miRNAs: cell-cell communication function? *Front. Genet.* **4**, 119 (2013).

131. Turchinovich, A., Weiz, L. & Burwinkel, B. Extracellular miRNAs: the mystery of their origin and function *Trends Biochem. Sci.* **37**, 460-465 (2012).

132. Lawrie, C. H. *et al*. Detection of elevated levels of tumour-associated microRNAs in serum of patients with diffuse large B-cell lymphoma *Br. J. Haematol.* **141**, 672-675 (2008).

133. Li, H. *et al*. MicroRNA screening identifies circulating microRNAs as potential biomarkers for osteosarcoma *Oncol. Lett.* **10**, 1662-1668 (2015).

134. Le Large, T. Y. *et al*. Circulating microRNAs as diagnostic biomarkers for pancreatic cancer *Expert Rev. Mol. Diagn.* **15**, 1525-1529 (2015).

135. Mitchell, P. S. *et al*. Circulating microRNAs as stable blood-based markers for cancer detection *Proc. Natl. Acad. Sci. U. S. A.* **105**, 10513-10518 (2008).

136. Cortez, M. A., Welsh, J. W. & Calin, G. A. Circulating microRNAs as noninvasive biomarkers in breast cancer *Recent Results Cancer Res.* **195**, 151-161 (2012).

137. Yu, X., Odenthal, M. & Fries, J. W. Exosomes as miRNA Carriers: Formation-Function-Future *Int. J. Mol. Sci.* **17**, 10.3390/ijms17122028 (2016).

138. Elias, K. M. *et al*. Diagnostic potential for a serum miRNA neural network for detection of ovarian cancer *Elife* **6**, 10.7554/eLife.28932 (2017).

139. Nam, E. J. *et al*. MicroRNA expression profiles in serous ovarian carcinoma *Clin. Cancer Res.* **14**, 2690-2695 (2008).

140. Marchini, S. *et al*. Association between miR-200c and the survival of patients with stage I epithelial ovarian cancer: a retrospective study of two independent tumour tissue collections. *The Lancet Oncology* **12**, 273-285.

141. Tang, Z., Ow, G. S., Thiery, J. P., Ivshina, A. V. & Kuznetsov, V. A. Meta-analysis of transcriptome reveals let-7b as an unfavorable prognostic biomarker and predicts molecular and clinical subclasses in high-grade serous ovarian carcinoma. *International Journal of Cancer* **134**, 306-318 (2014).

142. Calura, E. *et al*.
A prognostic regulatory pathway in stage I epithelial ovarian cancer: new hints for the poor prognosis assessment. *Annals of Oncology* **27**, 1511--1519 (2016).

143. Bagnoli, M. *et al*. Development and validation of a microRNA-based signature (MiROvaR) to predict early relapse or progression of epithelial ovarian cancer: a cohort study. *The Lancet Oncology* **17**, 1137-1146 (2016).

144. Bagnoli, M. *et al*. Identification of a chrXq27.3 microRNA cluster associated with early relapse in advanced stage ovarian cancer patients *Oncotarget* **2**, 1265-1278 (2011).

145. Sun, Y. *et al*. MiR-506 inhibits multiple targets in the epithelial-to-mesenchymal transition network and is associated with good prognosis in epithelial ovarian cancer *J. Pathol.* **235**, 25-36 (2015).

146. Liu, G. *et al*. MiR-506 suppresses proliferation and induces senescence by directly targeting the CDK4/6-FOXM1 axis in ovarian cancer *J. Pathol.* **233**, 308-318 (2014).

147. Liu, G. *et al*. Augmentation of response to chemotherapy by microRNA-506 through regulation of RAD51 in serous ovarian cancers *J. Natl. Cancer Inst.* **107**, 10.1093/jnci/djv108. Print 2015 Jul (2015).

148. Yang, D. *et al*. Integrated analyses identify a master microRNA regulatory network for the mesenchymal subtype in serous ovarian cancer *Cancer. Cell.* **23**, 186-199 (2013).

149. Chen, Z. *et al*. miR-124 and miR-506 inhibit colorectal cancer progression by targeting DNMT3B and DNMT1 *Oncotarget* **6**, 38139-38150 (2015).

150. Hua, K. *et al*. Up-regulation of miR-506 inhibits cell growth and disrupt the cell cycle by targeting YAP in breast cancer cells *Int. J. Clin. Exp. Med.* **8**, 12018-12027 (2015).

151. Wen, S. Y. *et al*. miR-506 acts as a tumor suppressor by directly targeting the hedgehog pathway transcription factor Gli3 in human cervical cancer *Oncogene* **34**, 717-725 (2015).

152. Deng, Q., Xie, L. & Li, H. MiR-506 suppresses cell proliferation and tumor growth by targeting Rho-associated protein kinase 1 in hepatocellular carcinoma *Biochem. Biophys. Res. Commun.* **467**, 921-927 (2015).

153. Li, J. *et al*. Downregulated miR-506 expression facilitates pancreatic cancer progression and chemoresistance via SPHK1/Akt/NF-ÎºB signaling. *Oncogene* **35**, 5501 (2016).

154. Marchini, S. *et al*. Resistance to platinum-based chemotherapy is associated with epithelial to mesenchymal transition in epithelial ovarian cancer *Eur. J. Cancer* **49**, 520-530 (2013).

155. Iwatsuki, M. *et al*. Epithelial-mesenchymal transition in cancer development and its clinical significance *Cancer. Sci.* **101**, 293-299 (2010).

156. Helleman, J., Smid, M., Jansen, M. P., van der Burg, M. E. & Berns, E. M. Pathway analysis of gene lists associated with platinum-based chemotherapy resistance in ovarian cancer: the big picture *Gynecol. Oncol.* **117**, 170-176 (2010).

157. Beaufort, C. M. *et al*. Ovarian cancer cell line panel (OCCP): clinical importance of in vitro morphological subtypes *PLoS One* **9**, e103988 (2014).

158. Pignata, S. *et al*. Carboplatin Plus Paclitaxel Versus Carboplatin Plus Pegylated Liposomal Doxorubicin As First-Line Treatment for Patients With Ovarian Cancer: The MITO-2 Randomized Phase III Trial. *JCO* **29**, 3628-3635 (2011).

159. Perrone, F. *et al*. Biomarker analysis of the MITO2 phase III trial of first-line treatment in ovarian cancer: predictive value of DNA-PK and phosphorylated ACC *Oncotarget* **7**, 72654-72661 (2016).

160. Zhang, Y. *et al*. MicroRNA-506 suppresses tumor proliferation and metastasis in colon cancer by directly targeting the oncogene EZH2 *Oncotarget* **6**, 32586-32601 (2015).

161. Sun, G., Liu, Y., Wang, K. & Xu, Z. miR-506 regulates breast cancer cell metastasis by targeting IQGAP1 *Int. J. Oncol.* **47**, 1963-1970 (2015).

162. Li, Z. *et al*. miR-506 Inhibits Epithelial-to-Mesenchymal Transition and Angiogenesis in Gastric Cancer *Am. J. Pathol.* **185**, 2412-2420 (2015).

163. Zhang, H., Shykind, B. & Sun, T. Approaches to manipulating microRNAs in neurogenesis *Front. Neurosci.* **6**, 196 (2013).

164. McCabe, N. *et al*. Deficiency in the repair of DNA damage by homologous recombination and sensitivity to poly(ADP-ribose) polymerase inhibition *Cancer Res.* **66**, 8109-8115 (2006).

165. Wang, X. *et al*. Genomic instability and endoreduplication triggered by RAD17 deletion *Genes Dev.* **17**, 965-970 (2003).

166. Srivas, R. *et al*. A Network of Conserved Synthetic Lethal Interactions for Exploration of Precision Cancer Therapy *Mol. Cell* **63**, 514-525 (2016).

167. Perren, T. J. *et al*. A phase 3 trial of bevacizumab in ovarian cancer *N. Engl. J. Med.* **365**, 2484-2496 (2011).

168. Pujade-Lauraine, E. *et al*. Olaparib tablets as maintenance therapy in patients with platinum-sensitive, relapsed ovarian cancer and a BRCA1/2 mutation (SOLO2/ENGOT-Ov21): a double-blind, randomised, placebo-controlled, phase 3 trial. *The Lancet Oncology* **18**, 1274-1284 (2017).

169. Rouhi, A., Mager, D. L., Humphries, R. K. & Kuchenbauer, F. MiRNAs, epigenetics, and cancer *Mamm. Genome* **19**, 517-525 (2008).

170. Lujambio, A. *et al*. Genetic unmasking of an epigenetically silenced microRNA in human cancer cells *Cancer Res.* **67**, 1424-1429 (2007).

171. Lopez-Serra, P. & Esteller, M. DNA methylation-associated silencing of tumor-suppressor microRNAs in cancer *Oncogene* **31**, 1609-1622 (2012).

172. Iorio, M. V. & Croce, C. M. Causes and consequences of microRNA dysregulation *Cancer J.* **18**, 215-222 (2012).

173. Arora, H., Qureshi, R. & Park, W. Y. miR-506 regulates epithelial mesenchymal transition in breast cancer cell lines *PLoS One* **8**, e64273 (2013).

174. Yin, M. *et al*. Selective killing of lung cancer cells by miRNA-506 molecule through inhibiting NF-ÎºB p65 to evoke reactive oxygen species generation and p53 activation. *Oncogene* **34**, 691 (2014).

175. Hanahan, D. & Coussens, L. M. Accessories to the crime: functions of cells recruited to the tumor microenvironment *Cancer. Cell.* **21**, 309-322 (2012).

176. Mitra, A. K. *et al*. Microenvironment-induced downregulation of miR-193b drives ovarian cancer metastasis *Oncogene* **34**, 5923-5932 (2015).

177. Virag, L. & Szabo, C. The therapeutic potential of poly(ADP-ribose) polymerase inhibitors *Pharmacol. Rev.* **54**, 375-429 (2002).

178. Venkitaraman, A. R. A growing network of cancer-susceptibility genes *N. Engl. J. Med.* **348**, 1917-1919 (2003).

179. Cancer Genome Atlas Research Network. Integrated genomic analyses of ovarian carcinoma *Nature* **474**, 609-615 (2011).

180. Vakifahmetoglu, H., Olsson, M. & Zhivotovsky, B. Death through a tragedy: mitotic catastrophe *Cell Death Differ.* **15**, 1153-1162 (2008).

181. Reinhardt, H. C., Aslanian, A. S., Lees, J. A. & Yaffe, M. B. p53-deficient cells rely on ATM- and ATR-mediated checkpoint signaling through the p38MAPK/MK2 pathway for survival after DNA damage *Cancer. Cell.* **11**, 175-189 (2007).

182. Zabludoff, S. D. *et al*. AZD7762, a novel checkpoint kinase inhibitor, drives checkpoint abrogation and potentiates DNA-targeted therapies *Mol. Cancer. Ther.* **7**, 2955-2966 (2008).

183. Guzi, T. J. *et al*. Targeting the replication checkpoint using SCH 900776, a potent and functionally selective CHK1 inhibitor identified via high content screening *Mol. Cancer. Ther.* **10**, 591-602 (2011).